ISSN
2395-6992

International Journal of Engineering Research & Science

www.ijoer.com
www.adpublications.org

Volume-3! Issue-12 ! December, 2017 www.ijoer.com ! info@ijoer.com

Preface

We would like to present, with great pleasure, the inaugural volume-3, Issue-12, December 2017, of a scholarly journal, *International Journal of Engineering Research & Science*. This journal is part of the AD Publications series *in the field of Engineering, Mathematics, Physics, Chemistry and science Research Development*, and is devoted to the gamut of Engineering and Science issues, from theoretical aspects to application-dependent studies and the validation of emerging technologies.

This journal was envisioned and founded to represent the growing needs of Engineering and Science as an emerging and increasingly vital field, now widely recognized as an integral part of scientific and technical investigations. Its mission is to become a voice of the Engineering and Science community, addressing researchers and practitioners in below areas

Chemical Engineering	
Biomolecular Engineering	Materials Engineering
Molecular Engineering	Process Engineering
Corrosion Engineering	
Civil Engineering	
Environmental Engineering	Geotechnical Engineering
Structural Engineering	Mining Engineering
Transport Engineering	Water resources Engineering
Electrical Engineering	
Power System Engineering	Optical Engineering
Mechanical Engineering	
Acoustical Engineering	Manufacturing Engineering
Optomechanical Engineering	Thermal Engineering
Power plant Engineering	Energy Engineering
Sports Engineering	Vehicle Engineering
Software Engineering	
Computer-aided Engineering	Cryptographic Engineering
Teletraffic Engineering	Web Engineering
System Engineering	
Mathematics	
Arithmetic	Algebra
Number theory	Field theory and polynomials
Analysis	Combinatorics
Geometry and topology	Topology
Probability and Statistics	Computational Science
Physical Science	Operational Research
Physics	
Nuclear and particle physics	Atomic, molecular, and optical physics
Condensed matter physics	Astrophysics
Applied Physics	Modern physics
Philosophy	Core theories

Chemistry	
Analytical chemistry	Biochemistry
Inorganic chemistry	Materials chemistry
Neurochemistry	Nuclear chemistry
Organic chemistry	Physical chemistry
Other Engineering Areas	
Aerospace Engineering	Agricultural Engineering
Applied Engineering	Biomedical Engineering
Biological Engineering	Building services Engineering
Energy Engineering	Railway Engineering
Industrial Engineering	Mechatronics Engineering
Management Engineering	Military Engineering
Petroleum Engineering	Nuclear Engineering
Textile Engineering	Nano Engineering
Algorithm and Computational Complexity	Artificial Intelligence
Electronics & Communication Engineering	Image Processing
Information Retrieval	Low Power VLSI Design
Neural Networks	Plastic Engineering

Each article in this issue provides an example of a concrete industrial application or a case study of the presented methodology to amplify the impact of the contribution. We are very thankful to everybody within that community who supported the idea of creating a new Research with IJOER. We are certain that this issue will be followed by many others, reporting new developments in the Engineering and Science field. This issue would not have been possible without the great support of the Reviewer, Editorial Board members and also with our Advisory Board Members, and we would like to express our sincere thanks to all of them. We would also like to express our gratitude to the editorial staff of AD Publications, who supported us at every stage of the project. It is our hope that this fine collection of articles will be a valuable resource for *IJOER* readers and will stimulate further research into the vibrant area of Engineering and Science Research.

Mukesh Arora

(Chief Editor)

Board Members

Dr. S.R.Boselin Prabhu

Ph.D, Wireless Sensor Networks, M.E. Network Engineering, Excellent Professional Achievement Award Winner from Society of Professional Engineers Biography Included in Marquis Who's Who in the World (Academic Year 2015 and 2016). Currently Serving as Assistant Professor in the department of ECE in SVS College of Engineering, Coimbatore.

Dr. Maheshwar Shrestha

Postdoctoral Research Fellow in DEPT. OF ELE ENGG & COMP SCI, SDSU, Brookings, SD Ph.D, M.Sc. in Electrical Engineering from SOUTH DAKOTA STATE UNIVERSITY, Brookings, SD.

Zairi Ismael Rizman

Senior Lecturer, Faculty of Electrical Engineering, Universiti Teknologi MARA (UiTM) (Terengganu) Malaysia Master (Science) in Microelectronics (2005), Universiti Kebangsaan Malaysia (UKM), Malaysia. Bachelor (Hons.) and Diploma in Electrical Engineering (Communication) (2002), UiTM Shah Alam, Malaysia

Dr. D. Amaranatha Reddy

Ph.D.(Postdocteral Fellow,Pusan National University, South Korea), M.Sc., B.Sc. : Physics.

Dr. Dibya Prakash Rai

Post Doctoral Fellow (PDF), M.Sc.,B.Sc., Working as Assistant Professor in Department of Physics in Pachhuncga University College, Mizoram, India.

Dr. Pankaj Kumar Pal

Ph.D R/S, ECE Deptt., IIT-Roorkee.

Dr. P. Thangam

BE(Computer Hardware & Software), ME(CSE), PhD in Information & Communication Engineering, currently serving as Associate Professor in the Department of Computer Science and Engineering of Coimbatore Institute of Engineering and Technology.

Dr. Pradeep K. Sharma

PhD., M.Phil, M.Sc, B.Sc, in Physics, MBA in System Management, Presently working as Provost and Associate Professor & Head of Department for Physics in University of Engineering & Management, Jaipur.

Dr. R. Devi Priya

Ph.D (CSE),Anna University Chennai in 2013, M.E, B.E (CSE) from Kongu Engineering College, currently working in the Department of Computer Science and Engineering in Kongu Engineering College, Tamil Nadu, India.

Dr. Sandeep

Post-doctoral fellow, Principal Investigator, Young Scientist Scheme Project (DST-SERB), Department of Physics, Mizoram University, Aizawl Mizoram, India- 796001.

Mr. Abilash

MTech in VLSI, BTech in Electronics & Telecommunication engineering through A.M.I.E.T.E from Central Electronics Engineering Research Institute (C.E.E.R.I) Pilani, Industrial Electronics from ATI-EPI Hyderabad, IEEE course in Mechatronics, CSHAM from Birla Institute Of Professional Studies.

Mr. Varun Shukla

M.Tech in ECE from RGPV (Awarded with silver Medal By President of India), Assistant Professor, Dept. of ECE, PSIT, Kanpur.

Mr. Shrikant Harle

Presently working as a Assistant Professor in Civil Engineering field of Prof. Ram Meghe College of Engineering and Management, Amravati. He was Senior Design Engineer (Larsen & Toubro Limited, India).

Table of Contents

Theoretical and Experimental Studies on Piezoelectric Thermal Fire Annunciator

Mammadov R.G.[1], Rahimova E.G.[2]

Azerbaijan State Oil and Industry University, the department of Instrumentation Engineering, AZ 1010, Azadliq avenue, 20, Baku, Az1010, Azerbaijan

Abstract— *The paper presents theoretical and experimental studies on testing the possibility of using piezoelectric converters as a signaling device in fire protection systems. The advantage of this process is the absence of the necessity to connect electrical lines, which in most cases they themselves cause fire.*

Keywords— Piezoelectric converter, transformer mode, depolarization, signaling device, fire security.

I. INTRODUCTION

The systems, designed for remote registration of occurrence moment of fire situation at oil and gas industry facilities, contain a primary converter (located directly at the facility), a communication channel and a signaling device installed in the control room.

Practice shows that, the reliability of such systems is mainly determined by the primary converter, so that their design is presented by very stringent requirements. Therefore, currently, several types of devices have been developed reacting either to an increase in the ambient temperature caused by it [1,2,3]. The converters used in practice are mainly fusible and ferromagnetic fuses and photoelectric signaling devices.

II. STATEMENT OF THE PROBLEM

The disadvantage of the first two types of converters is that their work is connected with the need of using sufficiently powerful electrical circuits, which in case of fault, they themselves can be sources of an explosion or a fire. Photoelectric converters operation is connected with the need of using special power supplies and amplifiers complicating the signaling scheme, thus, reducing its reliability. These shortcomings can be eliminated if a piezoelectric ceramic, having the ability to be depolarized under the effect of temperature is used as a sensitive element [4,5].

III. SOLUTION

Fig 1. presents the diagram of the device, which can be recommended as a signaling device on the occurrence of a fire situation. The device contains a piezoelectric transformer, the first section *1*being connected to the 220 V network, however, the secondary one-2 is loaded onto gas-discharge indicator 4through the communication channel 3.

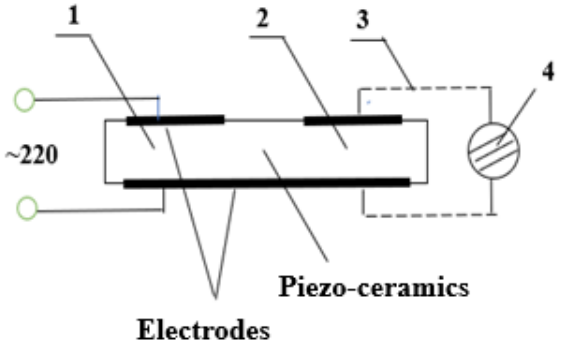

FIG.1: SIGNALING DEVICE ON THE OCCURRENCE OF A FIRE SITUATION

The transformer is installed at the facility; however, the gas-discharge indicator is installed in the control room. Under normal conditions, the transformable voltage in the network maintains luminescence indicator. When the temperature increases on the object, the piezo-ceramics becomes depolarized, the voltage transformation stops to the indicator and it goes down, signaling the occurrence of a fire situation.

Since the problems, related to the design of piezoelectric transformers, have been sufficiently fully illuminated in [6], the results of the studies on thermal depolarization and piezo-ceramics inertia are of practical interest in constructing signaling schemes. This is due to the fact that depolarization rate and heating time of piezo-ceramics to the point of phase transition determine such an important parameter of the system as its speed.

In accordance with the known thermodynamics dependence, the thermal time constant of the converter can be determined by the following formula [7]:

$$\tau = \frac{Cml_3}{\lambda l_1 l_2} \tag{1}$$

where C- is the heat capacity, cal/g·deg.; λ- is thermal conductivity, cal/s·m deg.; *m*- is the transformer mass, *g; l_1, l_2, l_3*- are length, width and thickness of the transformer, *m.*

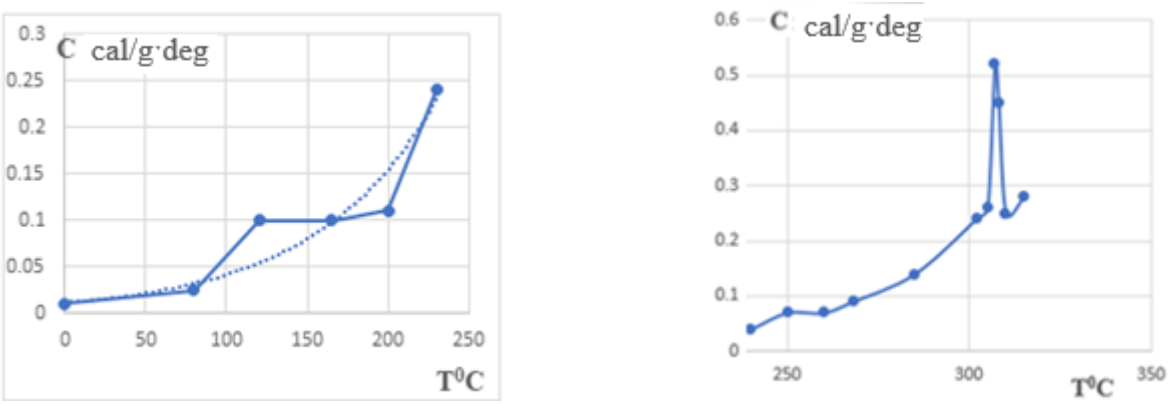

a) **b)**

FIG. 2: RESULT OF EXPERIMENTAL STUDIES

As a result of experimental studies (Fig. 2, a, b), it was discovered that the average heat capacity for piezoceramics ZTL-19 (zirconate-titanate-lead) is (0.2-0.4) cal./g·deg.;, while temperature is close to the point of the base transition, its value increases to (0.8-1) cal./g·deg;.

The study of the heat capacity enabled to determine the temperature at which the piezo-ceramics was completely depolarized. This temperature for ceramics, ZTL-19 is $(305 \div 308)^0$C.

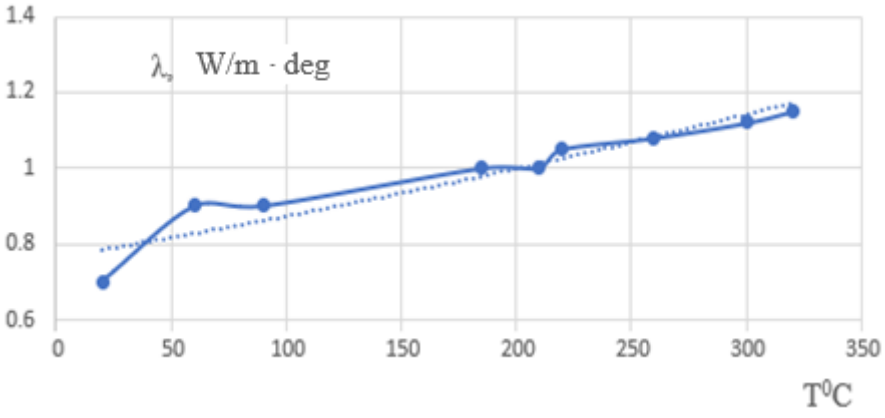

FIG.3: THERMAL CONDUCTIVITY MEASUREMENT OF PIEZO-CERAMICS

The thermal conductivity measurement of piezo-ceramics ZTL-19 (Fig. 3) allows us to conclude that its value, depending on the ambient temperature, varies from 0.7 W/m·deg;. at normal temperature to 1.1 W/m·deg.; at phase transition temperature. The signaling system speed is determined not only by thermal time constant. This is due to the process of depolarization having certain inertia. Currently, there are no sufficiently simple analytical dependencies allowing determining the depolarization inertia, in connection with the fact that this parameter has been determined experimentally.

Fig. 4 defines a curve allowing determining the depolarization degree of ceramics ZTL-19 depending on the exposure time to it of the phase transition temperature.

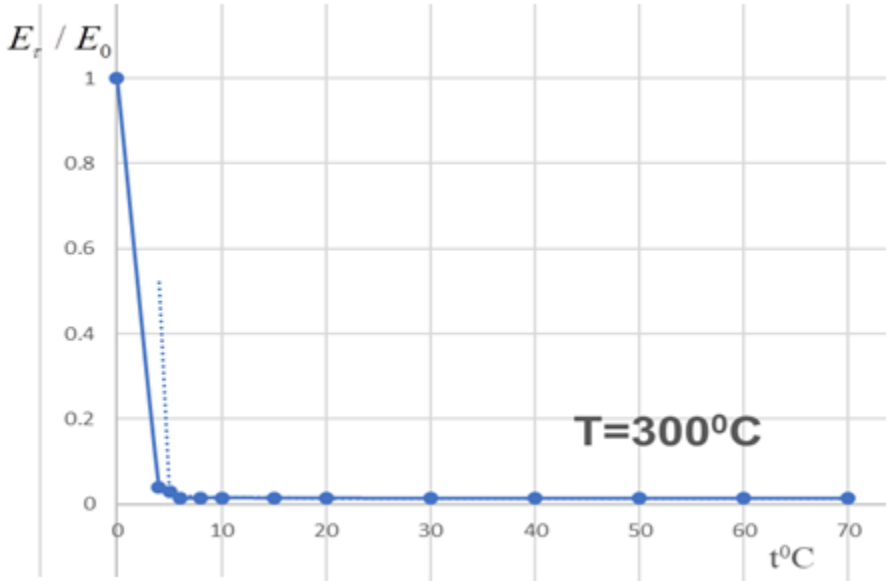

FIG.4: DETERMINE THE DEPOLARIZATION DEGREE OF CERAMICS ZTL-19

In this case it is advisable to use a number of relative values to characterize the depolarization degree [8].

$$K_E = \frac{E_\tau}{E_0} \tag{2}$$

where Eτ- is the current value of permanent polarization in piezoceramics; E_0- is the initial value of permanent polarization. For piezoceramics, ZTL-19 $E_0 = 2 \cdot 106$ V/m.

IV. CONCLUSION

The analysis of the available experimental data allows us to conclude that the duration of depolarization does not exceed 10 c. Thus, taking into account the thermal inertia, the total time required for triggering the signaling system from the occurrence moment of a fire situation does not exceed (10 ÷ 15) s.

REFERENCES

[1] Ilinskaya L.N. Elements of fire-protection automatics. Publish. “Energy”, 1969.

[2] Fomenko A.A.Dotty maximum thermal fire annunciator: construction and applicationfeatures. // Security Systems. 2007. - N. 5. P. 85.

[3] EN 54-5: 2000 Fire alarm systems -Part 5: Heat detectors - Point detectors.

[4] Sharovar F.I. Comparative evaluation of the application effectiveness of thermal maximum, differential and smoke fire annunciators//Groteck security systems. 2003. №1. P. 62.

[5] Bakanov V., Neplokhov I. Thermal fire annunciators. Part 2. Application problems. Security Algorithm, 2011, № 6.

[6] A.N. Members. Modern thermal fire signaling: the main characteristics and features of the application. “Security Systems”, N. 1 (55), 2004.

[7] R.G. Jagupov, A.A. Erofeev - Piezoelectric elements in instrumentation and automation, L., “Mechanical Engineering”, 1988.

[8] V. Sharapov, M. Musienko, E. Sharapova- Piezoelectric sensors, M: “TECHNOSPHERE”, 2006.

Language and Didactic potential of Ukrainian for Specific Purposes Teaching forms in Developing Future Navigators' Text Formation Competency

Tetiana Gulchuk

Teacher of Ukrainian language and literature, Maritime College of technical fleet of National University "Odessa Maritime Academy", Odesa

Abstract— *The article is devoted to determining the peculiarities of the organization of future navigators 'text formation competence development during various forms of training on the basis of the analysis of scientific literature on language teaching methods. On the basis of analysis, generalization and systematization of scientific sources, we elucidated the forms of organization of language teaching (lectures, practical classes, seminars), which enable to improve the future navigators' ability to summarize, review and an notate texts that ensures the development of their textual competency. The conclusions drawn in the article can be used during theoretical justification and practical development of a methodology for developing future navigators' and marine educational institution scadets (students)' text formation competency.*

Keywords— language teaching material, methods of development, teaching methods, text formation competency, lecture, practical class, seminar, speech skills, future navigators.

I. INTRODUCTION

Introduction of competency approach into educational process caused focus shifts of its goals, objectives, and accordingly, the content: from the accumulation of knowledge, skills and capacities in the Ukrainian language for specific purposes to the development of students' ability to use them in practice, to employ individual speaking strategies and experience of successful speech situation in simulated professional activity and social practice.

The analysis of scientific works of the Ukrainian language teaching theorists proves that "text as a basic learning tool enables determining the tasks on all language levels, repeating speech-related information (determining the type, style of speech, ways of sentences connection within the complex syntactic unity, means of sentences connection in the text, finding a topic and comment, etc.). <...> It is the text level where the word semantics, its conceptual relationships are identified, where stylistic differentiation of coherent utterance simulation modelling is realized." [10, p. 61].

Today of great topicality is the problem of developing students' text formation competency. N. Holub, O. Horoshkina, O. Kopus, L. Mamchur, M. Pentyliuk et al. emphasize in their studies that text is a source of information, a product, a tool and object of activity; N. Bondarenko, L. Varzatska, V. Melnychaiko, H. Shelekhova et al. reveal the peculiarities of students' text formation skills developing; O. Hlazova, T. Hruba, I. Drozdova, O. Karaman, L. Kratasiuk, L. Ovsiienko, N. Perkhailo et al. determined the specifics of pupils and students' text formation activity organization. However, these works focus primarily on elaborating productive combinations of methods and techniques of pupils and students' text formation competency development or on elaborating the system of tasks aimed at developing text formation competency.

One of the main directions of higher education development is training competitive specialists capable of professional development, acquiring advanced knowledge based and information technologies. In this context, the problem of students', especially, future navigators' text formation competency development requires comprehensive study, since this competency provides acquiring communication strategies and tactics necessary for solving multiple life tasks in different situations. This justifies the necessity of studying language and didactic potential of Ukrainian for specific purposes teaching forms in developing future navigators' text formation competency.

II. AIM & SCOPE

The goal of the paper is to determine the peculiarities of arranging future navigators' text formation competency development during various forms of teaching based on the analysis of the scientific literature in language teaching.

We agree with T. Symonenko that "despite the large number of methods of implementing forms of learning organization, the commonly recognized is the following system: lecture (lecture-information, problem-based lecture, lecture-visualization, lectures- press conference); self-guided work (under the teacher's guidance, without the teacher's guidance); proseminar,

actual seminar, special seminar, seminar-research; other forms of learning organization (tutorials, clubs, colloquia, consultations, practices, study groups); practical classes, laboratory classes" [15, p. 200]. We will consider some forms of teaching future navigators the Ukrainian language for specific purposes.

One of the time-tested and relevant so far remains the lecture (lecture class) – logically complete, scientifically based and systematized presentation of educational and scientific material; one of the main organizational forms of classes in high school that forms the basis of knowledge in a particular scientific field, determines the direction, the essence and character of all other classes and self-guided work in the relevant discipline [7, p. 247]. This definition is the most reasonable and comprehensively reveals the peculiarities of the lecture as a classical form of learning organization in modern universities. In addition, we support the position of O. Kopus who regards lecture as a secondary scientific and educational professional text. It is important that during the lecture, students perceive a model text of scientific style, mastering in practice the text formation rules and at the same time create their own texts (notes). It seems appropriate to focus on building students' skills of creating secondary academic genres that include the ability to perceive and analyze information, interpret it when taking notes.

We consider correct an opinion of A. Aleksiuk, that unlike other forms of learning organization, lecture has the following advantages: compared to textbooks it has much more opportunities to incorporate the audience's specifics, latest scientific achievements; it does not only provide students with knowledge, but also teaches to critically evaluate the learning material; it facilitates the perception of information through the living word, intonation, teacher's or lecturer's facial expressions and gestures; it opens up the opportunities of direct contact of the lecturer with the audience that enhances their attention; lecturing saves student's time [1, p. 457].

Without going into a detailed analysis of the peculiarities of university lectures we will make use of some generalizations of the Ukrainian language teaching theorists which are acceptable for working out the criteria of the efficiency of educational lecture on the Ukrainian language for specific purposes:

- lecture's subordination to the goal and objectives of modern language education in Ukraine; lecturing focuses on developing future specialist's language and communicative professional competency; motivation of students' learning activity;
- scientific and solid character of the content, accuracy of formulations, clarity and consistency of presentation, arguing in favour of theoretical positions on the Ukrainian language with the examples of linguistic units, citing reliable information sources; providing clarity of presentation with modern electronic learning tools;
- mandatory inclusion in the content of the lecture of those problems which are the subjects of discussion among scientists and have controversial outlining in the scientific and academic literature. Teacher and scholar expresses his view on a particular issue at the same time giving students the right to choose any of the conceptions. But as a rule, students share the lecturer's authoritative opinion;
- the content of the lecture should reflect the interdisciplinary relationships, predominantly those with special disciplines. Herewith, it provides mainstreaming of students' basic knowledge gained in the process of mastering other courses that activates the development of professional competency;
- introduction to lecture plan of questions (with a list of references) required for independent study by students, and the questions recommended for an in-depth study of the lecture theme to students' request beyond the curriculum;
- professional orientation of the lectures' content, subordination of the lecture's structure to specific didactic purpose; taking into consideration the specifics of the lecture theme when choosing methods of lecturing;
- optimal combination of traditional and innovative types of lectures within the modules of the disciplines; interrelationship of the lecture with other organizational forms of students' classroom and extracurricular learning;
- lecturer's consideration of mechanisms of and long-term and random-access memory: memorizing, storing, realizing and reproducing information (I. Zymniaia); use of mnemotechnical tools that facilitate students' memorization of theoretical information on the Ukrainian language for specific purposes;
- teacher's differentiated approach to the content and methods of lecturing, conditioned by the form of students' learning (full-time, evening classes, distance learning), the discipline's specifics, the theme of the lecture, the overall level of students' success in the Ukrainian language for specific purposes;

- clear structure of the lecture, the unity of content and form, ideal verbal design, curiosity and vividness, normal rate of presentation [6, p. 209; 8, p. 151].

III. OBJECTIVE

The main objective of the lecture is to lay the foundations of scientific knowledge, to introduce the scientific research methodology of the discipline and yet provide scientific and educational interaction of the teacher and students [13, p. 3]. And in parallel students improve skills of text compression – "transformation of the source text with an intention to turn it into a more concise form, which is achieved by the omission of redundant elements of the utterance, elements that can be restored from the context and extralinguistic situation, and through the use of more compact constructions" [14, p . 43]. According to the observations, students perceive a lecture by hearing (full-time learning), and this perception causes most difficulties, or visually (distance learning). Therefore, we consider rational preliminary training students for creating a secondary text – outline, since understanding the lecturer's speech speaker but not having the skills of taking notes students can not normally make notes. Thus, to teach students note-taking is one of the main tasks of teaching the Ukrainian language in high school [4, p. 273–274].

Modern theory of language teaching (O. Biliaiev, O. Horoshkina, L. Skurativsky, H. Shelekhova, O. Shunevych et al.) defined the basic types of notes and justified the effectiveness of exercises and tasks. We will only state those skills improvement of which should be continued in high school, particularly, in the perception of the lecture: to apply the techniques of text compression; to represent the sense structure of the text using the logical and structure schemes and tables; to present scientific and educational text in an optimal form for further activity and others.

We consider favorable the conclusions of O. Shunevych that to develop the skills of taking notes the following methods and techniques are optimal: semantic text analysis, observations on the language of the text, producing statements from previous training exercises, transformation, projecting; creative constructing techniques, algorithmization elements, condensing of linguistic units, analysis of their own and others' statements, modelling [17, p. 13]. Some of them can be used during lectures on the Ukrainian language for specific purposes.

We agree with the conclusions of M. Hreb, that the lecture effectiveness depends on objective and subjective factors, including the level of professional competency of the teacher, namely: the possession of the lecturing methods, knowledge of factual material on the subject, a high level of speech culture and oratorical skills, etc. – and students' readiness to perceive the information, development of a special hearing culture [3, p. 186].

Particularly noteworthy are semantic notes to which future navigators are involved when mastering special disciplines. Teachers of the Ukrainian language for specific purposes should rely on the principles of preparing semantic notes: discrete principle, according to which factual knowledge must be represented as separate utterances; the principle of finality, which implies that a set of utterances should reflect the knowledge of the subject in full; the conciseness principle, according to which the utterances should consist of a minimum number of words expressing a complete thought; the principle of the primacy of definitions, requiring introduction of new concepts through definition; the uniqueness principle according to which any utterance must not contain more than one notion; the unambiguity principle – each utterance is a semantic fact and must express only one idea; the consistency principle that leads to the location of the utterances according to the logics of presenting the course; the sufficiency principle, according to which any utterance is given in its full formulation, its sense does not depend on other utterances; the grammatical principle determines the subordination of the utterances' structure to the logics of constructing correct speech [5, p. 105-106].

When developing the future navigators' text-formation competency special attention should be paid to practical classes, whose purpose is to deepen and consolidate the knowledge acquired at lectures or using textbooks, to develop the skills of using knowledge, performing certain actions and operations [9, p. 103]. Modern theory of language teaching revealed the methods of giving practical classes in universities. We consider it necessary to focus on the functions of this form of studies organization: ongoing monitoring of the results of students' self-guided work; students' mastering the skills of independent oral presentations, justifying their position on the issue under discussion; teaching students the rules of discussing and skills of listening to the interlocutor; realization of communicative and activity-based teaching approach [15].

During practical classes students can perform analytical and synthetic text-formation activity: annotate and summarize professionally oriented texts, create their own utterances, review the classmates' answers etc. Clearly, special attention should be given to the choice of professionally oriented texts. O. Roshchupkina considers them as a communicative unit, aimed at developing students' specific skills at a particular stage of training. The text, the scholar argues, is a structural and

semantic functionally conditioned unity of sentences organized with the didactic purpose in semantic and content, linguistic and compositional sense that includes professionally significant for student information. [12, p. 71-72].

Preparing for practical class the teacher must take into account that students' activity on processing (understanding, realizing, assignment, evaluation, etc.) the text serves as a certain tentative basis for other activity and, therefore, is a structural component of other activities. Student's work with the subject content, based usually on a scientific text involves not reproduction, but active productive activity, allowing to translate the essence (semantic core) of original (primary) text to any other form of its reproduction. Obtaining a new product (secondary text) is possible only on condition of the student's permanent communication with the author of the original text, student's staying in a kind of indirect dialogue with him [16, p. 193].

IV. CONCLUSION

The aim of practical training is threefold – educational-developmental-upbringing. As the authors of the manual "Workshop on methods of teaching linguistic subjects in high school" correctly claim, learning objective involves acquiring the theory, elaborating a system of subject and speech skills. Developmental aim is realized when mastering the experience of the search, creative activity, it provides the development of the skills of transferring knowledge and skills into a new situation based on the problem and search activity, linguistic intuition, phonetic and intonation hearing, logical presentation of ideas, intellectual and cognitive abilities (audio and visual, operational and long-term memory, voluntary and involuntary attention, imagination, etc.), psychological readiness to communicate in different situations. The upbringing goal is realized by selection of the educational material (texts, illustrations, pictures, situations, etc.), which reflects universal moral values. Didactic material should be directed to the developing national consciousness, understanding the laws of their native language and society, associated with the leading ideas of philology, which allows students to understand the history of the language development, to master the richness of its expressive means [11, p. 109].

Development of text-formation competency should be continued during the seminars, which is an important form of learning organization in higher educational institutions and provides the development of professional thinking, cognitive motivation and professional use of knowledge in educational conditions [2, p. 179]. If during practical classes analytical and synthetic work with the text dominates, students' speech during seminars is the result of methodically properly organized preparatory work: based on the written notes, abstracts and thematic notes to create their own text – speech in front of the audience or participating in debates and discussions.

During seminars students acquire knowledge about the diversity and variety of academic genres – abstract, theses of article, article summaries, review, article and so on. Analysis of these genres makes it possible to focus future navigators' attention on general genre and stylistic characteristics of texts, to acquaint them with the typical speech clichés, compression, text folding up techniques.

Thus, methodically appropriate selection of learning forms, adequate to the content allows improving future navigators' ability to take notes, review, annotate texts, which provides developing text formation competency.

REFERENCES

[1] Aleksiuk, A. M. (1998). *Pedahohikavyshchoiosvity. Istoriia. Teoriia: pidruch.dliastud., asp. tamolodykhvykl.vuziv[Pedagogy of higher education. History. Theory: Manual for students, post-graduates and young scientists]*. Kyiv: Lybid [in Ukrainian].

[2] Vitvitska, S. O. (2006). *Osnovypedahohikyvyshchoishkoly: pidruch. zamodulno-reitynhovoiusystemoiunavchanniadliastud. mahistratury [Foundations of high school pedagogy: text book on credit and module system of education for master students]*. Kyiv: Tsentrnavch. lit-ry [in Ukrainian].

[3] Hreb, M. M. (2016). Problem yiperspektyvyvykorystannialektsiiyakefektyvnoi for my orhanizatsiinav channialeksykolohiiifrazeolohiimaibutnikhuchytelivpochantkovykhklassiv [Problems and perspectives of using lecture as an effective form of organizing teaching lexicology and phraseology to future primary school teachers]. VisnykDnipropetrovskohouniversytetuimeniAlfredaNobelia. Seriia "Pedahohikaipsykholohiia" – Bulletin of Dnipropetrovsk university named after Alfred Nobel. Series "Pedagogy and Psychology", 2 (12), 182-188.

[4] Drozdova, I. P. (2010). Naukoviosnovy for muvaniiaukrainskohopr of esiinihimovlennia student ivnefilolohichnykhfak *ultetivVNZ[ScientificfoundationsofdevelopingUkrainianprofessionalspeechofthenon-linguistic*university departments]. Kharkiv: KhNAMH [in Ukrainian].

[5] Yevseieva, Ye. G. (2005). Semanticheskiikonspektpolineinoi algebra [Semantic notes on linear algebra]. Didacticsofmathematics: ProblemsandInvestigations, 24, 103-110. Retrieved from: http://ea.donntu.org:8080/handle/123456789/7932

[6] Klimova, K. (2010). *Teoriiaipraktyka for muvanniamovnokommunikatyvnoyipr of esiinoikompetentsii student ivnefilolohichnykhspetsialnosteipedahohicnhykhuniversytetiv [Theory and practice of developing lingual and communicative professional competence of pedagogicaluniversitynon-linguiststudents]*.Zhytomyr: Ruta [in Ukrainian]

[7] Kopus, O. A. (2012). *Teoretychnizasady for muvanniafakhovoilinhvodydaktychnoilompetentnostimaibutnikhmahistriv-filolohivuvyshchomunavchalnomuzakladi [Theoretical foundations of developing lingua-didactic competency of future masters and linguists in higher educational establishment]*.Odesa [in Ukrainian].

[8] Kochan, I. M. &Zakhliupin, N. M. (2005). *Slovnyk-dovidnykizmetodykyvykladanniaukrainskoimovy [Reference dictionary in methods of teaching Ukrainian]*. L.: Vydavnychyitsentr LNU im. IvanaFranka [in Ukrainian].

[9] Malykhin, O. V., Pavlenko, I. H., Lavrentieva, O. O. &Matukova, H. I. (2014). *Metodykavykladannia u vyshchiishkoli: navch. posibnyk [Teaching methods in high school: textbook]*. K.: KNT [in Ukrainian].

[10] Pentyliuk, M. I., Horoshkina, O. M. &Nikitina, A. V. *Osnovykohnityvnoyimetodykynavchanniaukrayinskoyimovy [Foundations of cognitive methods of teaching Ukrainian]*. Retrieved from: http://ps.stateuniversity.ks.ua/file/issue_42/12.pdf.

[11] Horoshkina, O. M., Karaman, S. O., Bakum, Z. P., Karaman, O. V. &Kopus, O. A. (2015). *Praktykum z metodykynavchanniamovoznavchykhdystsyplin u vyshchiishkoli: navch. posib. [Workshop on methods of teaching linguistic subjects in high school]*. K.: "AkmeHrup" [in Ukrainian].

[12] Roshchupkina, O. A. (2014). Profesiinooriientovanyitekstyakzasibnavchanniainozemnykhstudentiv [Professionally oriented textasa tool of teaching foreign students]. *Vykladanniamov u vyshchykhnavchalnykhzakladakhosvitynasuchasnouetapi. Mizhpredmetnizviazky. Naukovidoslidzhennia. Dosvid. Poshuky – Teaching language in higher educational establishments at modern stage. Intersubject relationships. Scientific studies. Experience. Search, 24, 70-79.* Retrieved from:http://nbuv.gov.ua/UJRN/vmvn_2014_24_11. [in Ukrainian].

[13] Semenoh, O. (2011). Akademichnalektsiiayakprofesiinyikomunikatyvnyifenomen [Academiclectureasprefosseional communicative phenomenon]. *Estetykaietykapedahohichnoyi dii – Aesthetics and ethics of pedagogical action, 2, 91-101*. Retrieved from: http://nbuv.gov.ua/UJRN/eepd_2011_2_11 [in Ukrainian].

[14] Semenoh, O. M., Rud, O. M. (2014). *Kulturafakhovoimovy: navch. posib. [Culture of special language: textbook]*. Sumy: RVV SOIPPO [in Ukrainian].

[15] Symonenko, T. V. (2006). *Teoriiaipraktykaprofesiinoimovnokommunikatyvnoikompetentsiistudentivfilolohichnykhfakultetiv [Theory and practice of lingual and communicativ ecompetence of philology departments' students]*.Cherkasy: Vyd. Vovchok O. Yu. [in Ukrainian].

[16] Tsepkalo, O. V. (2013). Tekstova diialnist studentiv tekhnichny khspetsialnosteiusytuatsiiakhnaukovo-doslidnytskoirobotyvpreotsesnavchanniaanhliiskoimovy [Text activity of technical specialities' students insituations of research and development work when teaching English]. *Naukovizapysky [Natsionalnohopedahohichnohouniversytetuim. M. P. Drahomanova]. Seriia: Pedahohichni ta istorychninauky – Scientific Bulletin [of National pedagogical university named after M. P. Drahomanov]. Series: Pedagogical and historic sciences,* 112, 190-198 [in Ukrainian]. Retrieved from: http://nbuv.gov.ua/UJRN/Nzped_2013_112_30.

[17] Shunevych, O. M. (2009). Formuvanniaustarshoklasnykivuminniakonspektuvatynavchalnitekstynaurokakhridnoimovy [Developinghighschoolstudents' skillsoftakingnotesoneducationaltextsatthelessonsofmothertongue].*Extended abstract of candidate's thesis*. K. [in Ukrainian].

Research of image registration algorithm based on template matching

Zirui Fu

Beijing Institute of Graphic Communication, Beijing, 102600, China

Abstract**—***In order to provide support for image registration, the application of template matching in image registration is studied. This paper sums up four types, introduces the principle of each algorithm, and compares their advantages and disadvantages through simulation experiments: Based on the gray information of the algorithm is simple and real-time, but for complex image and low gray contrast images, cross matching results; mathematical transform based on the complex, large amount of calculation; mutual information does not require preprocessing, registration effect is good, is the research hotspot at present, but ignores the spatial relationship between pixels*.

Keywords—Image registration, Image matching, Template matching.

I. INTRODUCTION

Image matching is one of the traditional research directions in image processing. In practical application, It is often required by different sensors at different time, register the images of the same scene in the space position under different imaging conditions, or find the corresponding target in another picture according to the known template. Therefore, image matching [1-2] is the basis of image processing techniques such as image rectification and image fusion. In recent years, image registration [3-5] research has sprung up, especially in medical image [6-9] research. From the theoretical and conceptual point of view, it is the development of image matching technology, and some of the methods and ideas in image matching still play a special role. From this point of view, this paper sorts out the related research of image registration from the perspective of template matching, and analyzes their respective characteristics in combination with simulation.

II. METHODOLOGY

2.1 The method based on image gray information

2.1.1. MAD algorithm and its derivative algorithm

LeeSe proposed the Mean absolute difference algorithm in 1971, and its mathematical model is:

$$D(i,j)=\frac{1}{M\times N}\sum_{s=1}^{M}\sum_{t=1}^{N}\left|S(i+s-1,j+t-1)-T(s,t)\right| \tag{1}$$

where: $1\le i\le m-M+1$, $1\le j\le n-N+1$

S (x, y) is the detection image, and T (x, y) is the template. The algorithm calculates the average of L1 distance between the subgraph and the template, and the sub-graph with the lowest average absolute difference is the best matching object. In graph S, select the MxN size of the subgraph, at a certain point (i, j) for the upper left corner,. And calculate its similarity with the template and traverse the entire search map. The subgraph which is most similar with the template is the final result of the match, in all the sub-graphs which can be found.

The mean absolute difference algorithm [10-11] is a simple and stable algorithm with high matching degree. Different algorithms are derived along this line of thought. Sum of Absolute Differences algorithm is referred to SAD algorithm, and MAD algorithm is basically similar to the idea. But it is only simplified, which calculates the distance between the subgraph and the template.

$$D(i,j)=\sum_{s=1}^{M}\sum_{t=1}^{N}\left|S(i+s-1,j+t-1)-T(s,t)\right| \tag{2}$$

The Sum of Squared Differences algorithm (SSD), is also known as the error square sum algorithm, which calculates the L2 distance between the subgraph and the template.

$$D(i,j)=\sum_{s=1}^{M}\sum_{t=1}^{N}\left[S(i+s-1,j+t-1)-T(s,t)\right]^2 \tag{3}$$

The Mean Square Difference algorithm(MSD), is known as the mean square error algorithm, which calculates the average of the distance between the subgraph and the template.

$$D(i,j)=\frac{1}{M\times N}\sum_{s=1}^{M}\sum_{t=1}^{N}\left[S(i+s-1,j+t-1)-T(s,t)\right]^2 \tag{4}$$

2.2 NCC algorithm

Normalized Cross Correlation algorithm is mainly through the normalized formula to calculate the local part of the image and the gray value of the template. The following correlation measure to calculate the relationship of match between the two.

$$R(i,j)=\frac{\sum_{s=1}^{M}\sum_{t=1}^{N}\left|S^{i,j}(s,t)-E\left(S^{i,j}\right)\right|\bullet\left|T(s,t)-E(T)\right|}{\sqrt{\sum_{s=1}^{M}\sum_{t=1}^{N}\left[S^{i,j}(s,t)-E\left(S^{i,j}\right)\right]^2\bullet\sum_{s=1}^{M}\sum_{t=1}^{N}\left[T(s,t)-E(T)\right]^2}} \tag{5}$$

Where $E\left(S^{i,j}\right)$ and $E(T)$ denote the gray scale mean of subgraph and template graphs respectively in (i, j).

2.3 SSDA algorithm

Sequential Similarity Detection Algorithm is put forward by Barnea and Sliverman in 1972. The algorithm is mainly through the error to determine the pros and cons, to find the best match. The specific process is as follows:

Define the absolute error, which actually describes the pixel value of a certain pixel value minus the pixel mean value of the image, and The absolute value of sub-map minus template map corresponding to the location of the pixel poin:

$$\begin{cases} e(i,j,s,t)=\left|S_{i,j}(s,t)-\overline{S}-T(s,t)+\overline{T}\right| \\ 1\le i\le m-M-1, 1\le j\le n-N-1 \end{cases} \tag{6}$$

Where, the ones with the crossed lines represent the mean of the subgraph and template respectively:

$$\overline{S_{i,j}}=E\left(S_{i,j}\right)=\frac{1}{M\times N}\sum_{s=1}^{M}\sum_{t=1}^{N}S_{i,j}(s,t) \tag{7}$$

$$\overline{T}=E(T)=\frac{1}{M\times N}\sum_{s=1}^{M}\sum_{t=1}^{N}T(s,t) \tag{8}$$

In the template map, randomly selecte non-repetitive pixels, and calculate the absolute error with the current subgraph. With the error accumulation, write down the cumulative number of times H, when the error accumulated value exceeds the threshold. The cumulative times of all subgraphs H is represented by a table R (I, j). SSDA detection is defined as:

$$R(i,j)=\left(H\left|\min_{1\le H\le M\times N}\left[\sum_{h=1}^{H}e(i,j,s,t)\ge Th\right]\right.\right\} \tag{9}$$

The threshold of the valve is the interruption condition of the program. It is also a measure, which increases slowly by comparing the cumulative growth rate of the error, which is likely to be the matching point.

2.4 PIU algorithm

In 1992, Woods found that in the medical image, the same tissue structure was different in different modes of gray values, thus suggesting an image registration based on the uniform intensity of MR PET. The basic idea of PIU measurement is that the pixel of a certain grayscale value in a mode is the distribution of a different grayscale value in the other mode. The expression of PIU measure is defined as:

$$PIU(R,F)=\sum_{r}\frac{n_r\sigma_{F_\tau}(r)}{N\mu_{F_\tau}(r)}+\sum_{f}\frac{n_f\sigma_R(f)}{N\mu_R(f)} \tag{10}$$

Among them, N is the total number of pixels in the template, which is the product of the number of template rows. n_r and n_f respectively represent the number of pixels in the template and the subgraph with the grayscale of r and f, and it should be noted that although the gray values of the two are different, there is a certain corresponding relationship. F_τ represents a subgraph in the search diagram. Where:

$$\begin{cases} \mu_{F_\tau}(r)=\dfrac{1}{n_r}\sum\limits_{\omega_r}F_\tau(X_R) \\ \mu_R(f)=\dfrac{1}{n_f}\sum\limits_{\omega_f}R(X_{F_\tau}) \\ \sigma_{F_\tau}(r)=\dfrac{1}{n_r}\sum\limits_{\omega_r}\left[F_\tau(X_R)-\mu_{F_\tau}(r)\right]^2 \\ \sigma_R(r)=\dfrac{1}{n_f}\sum\limits_{\omega_f}\left[R(X_{F_\tau})-\mu_R(f)\right]^2 \end{cases} \tag{11}$$

$\sum\limits_{\omega_r}F_\tau(X_R)$ indicates that the gray value of r pixels in template R is the sum of pixel gray values in the corresponding position in subgraph F_τ.

III. THE METHOD OF MATHEMATICAL TRANSFORMATION

3.1 Fourier-Mellin invariant

Reddy et al. proposed the Fourier-Mellin invariant based on the translational property of Fourier transform.

Given two images $f_1(x,y)$ and $f_2(x,y)$, the following geometric transformations are met:

$$f_2(x,y)=f_1(\alpha(x\cos\theta_0+y\sin\theta_0)-dx,\alpha(-x\sin\theta_0+y\cos\theta_0)-dy) \tag{12}$$

Where dx and dy are the translations, α 3 represents the scale factor for the two image sizes, and θ_0 is the rotation angle. The Fourier transform can be used to obtain their relationship in the frequency domain:

$$F_2(x,y)=\alpha^{-2}\left|F_1\left[\alpha^{-1}(\mu\cos\theta_0+\nu\sin\theta_0),\alpha^{-1}(\nu\cos\theta_0-\mu\sin\theta_0)\right]\right|\exp\{-j\phi_{f2}(\mu,\nu)\} \tag{13}$$

Where, $\phi_{f2}(\mu,\nu)$ is the spectral phase of image $f_2(x,y)$, and the shift property of Fourier transform can have its power spectrum relation as:

$$\left|F_2(\mu,\nu)\right|=\alpha^{-2}\left|F_1\left[\alpha^{-1}(\mu\cos\theta_0+\nu\sin\theta_0),\alpha^{-1}(\nu\cos\theta_0-\mu\sin\theta_0)\right]\right| \tag{14}$$

Let's rewrite this in terms of polar coordinates:

$$\begin{cases} \alpha^{-1}(-\mu\cos\theta_0+\nu\sin\theta_0)=\dfrac{\rho}{\alpha}\cos(\theta-\theta_0) \\ \alpha^{-1}(-\mu\sin\theta_0+\nu\cos\theta_0)=\dfrac{\rho}{\alpha}\sin(\theta-\theta_0) \end{cases} \tag{15}$$

$$\text{then}\begin{cases} S(\rho,\theta)=\left|F_2(\rho\cos\theta,\rho\sin\theta)\right| \\ R(\rho,\theta)=\left|F_1(\rho\cos\theta,\rho\sin\theta)\right| \end{cases} \tag{16}$$

Thus, the above power spectrum relation can be rewritten as

$$S(\rho,\theta)=\alpha^{-2}R\left(\theta-\theta_0,\rho/\alpha\right) \tag{17}$$

The logarithm $\begin{cases}\lambda=\log\rho \\ k=\log\alpha\end{cases}$ is introduced to further rewrite.

$$S(\rho,\theta)=\alpha^{-2}R(\theta-\theta_0,\lambda-k) \tag{18}$$

By Fourier transform:

$$S(\mu,\nu)=\alpha^{-2}R(\mu,\nu)\exp\{-j2\pi(\mu\theta_0+\nu k)\} \tag{19}$$

$S(\mu,\nu)$ and $R(\mu,\nu)$ are pairs of matching images pairs, and the upper formula transforms the rotation and scaling of the two into the translational change of the Fourier domain.

3.2 SATD algorithm

The Sum of Absolute transformation Difference (SATD algorithm) is a summation algorithm of the Absolute value of adama transformation. The Hadamard transform, or the walshe-adama transformation, is a generalized Fourier transform, which is an orthogonal square matrix composed of the +1 and -1 elements. The so-called orthogonal square matrix means that any two rows (or two columns) of it are orthogonal. The hadamard transform is equivalent to multiplying the original image S matrix by one hadamard transformation matrix, H, which is HQH. The sum of the absolute value of the elements obtained after transformation is the value of SATD, which is the basis for the discrimination of similarity. Go through all of the subgraphs above and find the smallest subgraph of the SATD value, which is the best match.

3. Methods based on mutual information

The registration of mutual information is a hot topic in the field of medical image registration in recent years. In 1995, collignon and viola were first used for medical image registration. Mutual Information (MI) describes the correlation between the two systems. In the registration of two images, the mutual information is to reflect the degree of mutual information between them through their entropy and combined entropy. For an image, its entropy represents the information contained in the image. Its mathematical form is as follows:

$$\begin{cases} p_i=\dfrac{h_i}{\sum_{i=1}^{N-1}h_i} \\ H(R)=-\sum_{i=0}^{N-1}p_i\log p_i \end{cases} \tag{20}$$

p_i represents the probability of grey degree i. h_i represents the total number of pixels of i pixels in image R, and N represents the grayscale series of image R.The combined entropy reflects the correlation between the two images, R and S. The joint information entropy of R and S is expressed as:

$$H(R,S)=-\sum_{r,s}P_{RS}(r,s)\log P_{RS}(r,s) \tag{21}$$

For images R and S, the mutual information is expressed as:

$$MI(R,S)=H(R)+H(S)-H(R,S) \tag{22}$$

According to the definition of MI, when the similarity of two images is higher or the greater the overlap, the mutual information between them is larger, but the overlap part of the meeting causes misregistration. Subsequent researchers point out that the reduction of overlapped areas means less sampling points, thereby reducing the statistical index of probability distributions; At the same time, with MI as the correlation measure, the overlap between the two images decreases, which can lead to misregistration. Mismatch usually occurs when the gray value gap between image and background is smaller, while the increase in marginal entropy is much faster than that of combined entropy. To this end, Studholme et al introduced the concept of NMI (normalized Mutual Information). Maes et al. introduced the concept of ECC (Entropy Correlation Coefficient,). The formula is as follows

$$NMI(R,S)=\frac{H(R)+H(S)}{H(R,S)} \qquad ECC(R,S)=\frac{2MI(R,S)}{H(R)+H(S)} \tag{23}$$

The greater the similarity between the two images, the greater the correlation and the smaller the joint entropy, the greater the mutual information.

IV. EXPERIMENTAL RESULTS

Several representative algorithms are selected from the three methods. For the Fourier-Mellin method, it was tested in four cases, such as rotary translation, and found that its registration effect was good.

Template **SAD search figure** **SAD registration**

FIG. 1. SAD REGISTRATION

Template **SATD search figure** **SATD registration**

FIG. 2. SATD REGISTRATION

Template (crop) **Template (rotation)** **Template ((rotation +translation)** **Template (translation)**


Fourier-Mellin search figure **Fourier-Mellin registration figure**

FIG. 3. FOURIER-MELLIN REGISTRATION RESULTS

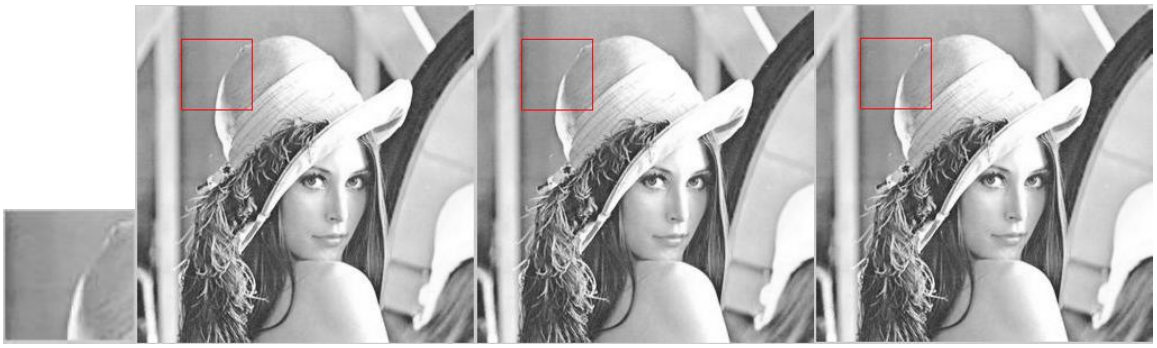

Template MI registration figure NMI registration figure ECC registration figure

FIG. 4. MUTUAL INFORMATION REGISTRATION RESULTS

V. CONCLUSION

The results show that the algorithm based on gray-level information is simple and real-time, and it is sensitive to noise. The calculated amount is proportional to the size of the input image. For the image with complex image and low gray contrast, the matching result is cross- The Fourier-Mellin method is still correct for the picture after the rotation translation. The mutual information does not need to be preprocessed and the registration effect is good. It is the current research hotspot, but ignores the spatial position between the pixels relationship.

REFERENCES

[1] zhu qiguang, zhang peng zhen, li haoli, zhan xianjiao, Chen ying. Research on image matching algorithm based on global and local feature fusion [J]. Journal of instrumentation, 2016,(01):170-176.

[2] hu min, he xiaojia, wang xiaohua. Fast regional center image matching algorithm [J]. Journal of electronic measurement and instrumentation, 2011,(05):455-462.

[3] xu jiajia, zhang ye, zhang he.based on improved image registration algorithm of Harris-SIFT operator [J]. Journal of electronic measurement and instrumentation, 2015,(01):48-54.

[4] Yang sa, Yang chunling. Image registration algorithm based on compression sensing and scale invariant feature transformation [J]. Optical journal, 2014,(11):106-110.

[5] don't be in the forest. Research on medical image registration algorithm based on mutual information [D]. Beijing: Beijing jiaotong university, 2014.

[6] wang wei. Research on non-rigid registration of medical images [D]. Dalian: dalian university of technology, 2012.

[7] zhang qian. Research on medical image registration algorithm based on mutual information [D]. Jinan: shandong university, 2008.

[8] liao xiuxiu. Research on image registration algorithm based on implicit shape representation and edge information fusion. Hangzhou: zhejiang university, 2007.

[9] wang hainan, hao chong Yang, lei fang yuan, zhang xianyong. Review of non-rigid medical image registration [J]. Computer engineering and application, 2005,(11):180-184.

[10] Chen hao, ma caiwen, Chen yue-cheng, sun xiaolin, tang self-reliance. Rapid template matching algorithm based on grayscale statistics [J]. Journal of photonics, 2009,(06):1586-1590.

[11] ding huizhen. Study on the method of matching gray scale image matching at any Angle [D]. Nanjing: hohai university, 2006.

[12] liu baijiang, jiang mingxin. Image matching algorithm based on sift characteristics [J]. Information systems engineering, 2011,(05):34-36+41.

[13] liu jian, zhang guohua, huang linlin. Based on improving the image registration algorithm of SIFT [J]. Journal of Beijing university of aeronautics and astronautics, 2010,(09):1121-1124+1130.

[14] zheng yongbin, huang xinsheng, feng songjiang. SIFT and rotation invariable LBP image matching algorithm [J]. Journal of computer aided design and graphics, 2010,(02):286-292.

[15] su koxin, han guangliang, sun haijiang. Based on SURF's anti-view transform image matching algorithm [J]. LCD and display, 2013,(04):626-632.

[16] qu tianwei, anbo, Chen guilan. An improved RANSAC algorithm for image registration [J]. Computer application, 2010, (07):1849-1851+1872.

Experimental study on treatment of municipal sludge by electro-osmotic method

Xiaoyu Fan[1], Jihui Ding[2], Yaxing Wei[3], Qi Zhao[4]

College of Civil Engineering, Hebei University, Baoding, Hebei 071002, China

Abstract*— *The main purpose of the electro-osmosis method in engineering is to reinforce the foundation. The electro-osmosis method has a lot of research on the foundation reinforcement. The most application is the experiment of electro-osmotic combined loading. The experiment on treatment of heavy metals in municipal sludge by electro-osmotic method is still in a blank state. In this paper, the changes of basic physical properties of sludge before and after electro-osmosis and the changes of heavy metals in sludge before and after electro-osmosis were analyzed. The feasibility of electro-osmotic treatment of heavy metals in sludge was verified by comparing the content of heavy metals in the sludge with the standard value of soil environmental quality after electro-osmotic treatment.

Keywords*— *Electro-osmotic method, Physical properties of sludge, Heavy metal, Experimental research.

I. INTRODUCTION

The field test proves that it is feasible to reinforce the beach land in Bohai Bay by electro-osmotic method (Cheng et al., 2001).In the contrast test of electrode arrangement in electro-osmotic method, 3 kinds of electrodes are arranged with rectangle, plum blossom shape and parallel dislocation. Comparing the experimental results, it is found that the parallel arrangement electrode is reasonable(Tao et al., 2013).In the theoretical and experimental study of reducing the energy consumption of electro-osmotic energy, it is found that the gradual increase of voltage can delay the occurrence of cracks in the process of electro-osmosis and the extent of the crack development. This method effectively reduces the energy loss at the crack during the electro-osmotic process(Pan et al., 2014).In the experimental study of the effect of electro-osmotic reinforcement of soft soil, the effectiveness of electrode inversion has been proved. The concrete calculation method of the parameters of the drainage volume and the electrical permeability coefficient is given through the experimental data. According to the existing engineering examples, the range of empirical values is given for the parameters that can not be determined(Zhuo Chen., 2015).In the experimental study on Influence Factors of electro-osmotic coefficient of soft clay and improvement method, the electro-osmosis heap loading combined air pressure splitting test is carried out aiming at the problem of the poor effect of the electro-osmosis method on the deep soil. The experimental results show that the shear strength of the combined pressure splitting test of electro-osmotic loading is higher than that of the deep soil under the electro-osmotic loading test. This discovery has certain reference significance for some projects which have high requirements for the reinforcement effect of deep soil soil (Hu et al., 2015).An experimental study of the effect of electrode spacing on electro-osmosis under the equal potential gradient using an indoor 1:5 model. The effects of two electrode spacing of 2m x 1m and 1m x 0.5m on the electro-osmotic properties of soft clay under the equal potential gradient were also studied. The results show that keeping the electric potential gradient unchanged and reducing the electrode spacing by half can speed up the electro-osmotic drainage, reduce the soil moisture content, reduce the energy consumption and electrode interface resistance, but also cause the change of pH value and the amount of anode corrosion. It is also found that the smaller the electrode spacing, the lower the potential loss on the electrode and the soil interface, but the loss potential increases the proportion of the supply voltage (Li et al., 2015).

There are few experiments in many literatures on the treatment of heavy metals in municipal sludge by electro-osmotic method. At present, if the basic physical indicators of sludge are improved and the content of heavy metals can be effectively reduced, the basic situation of urban land stress can be alleviated. In this paper, the basic physical properties of the treatment of sludge by electro-osmotic method and the content of heavy metals in sludge are described in this paper.

II. RESEARCH CONTENT METHODS AND BASIC PARAMETERS

2.1 Research Content

Through electro-osmotic real treatment of municipal sludge in laboratory experiments, we measured and calculated the moisture content, density, dry density; void ratio, porosity, saturation, shear strength and heavy metal (copper and zinc) content in the sludge section. Real-time monitoring of the settlement of A, B, C, and recording of current voltage are used to

Notes: Post-graduate's Innovation Fund Project of Hebei University

calculate the energy consumption, and finally summarize the data.

2.2 Experimental Scheme

1) An organic glass box with 50*30*40 (CM) size used in the experiment. A small hole with a diameter of 1cm at the bottom of the box and a soft rubber hose prepared for electro-osmotic drainage. The bottom of the box has 5cm thick sand in the coarse sand with a catheter to provide drainage layer for drainage.
2) The sludge is taken from the artificial landscape lake in a city in Hebei. The trees are dense around the lake, and there are many sewage and industrial sewage in the lake.
3) Using three iron bar （d=1.5cm） as electro-osmosis anode, using three carbon bar （d=1.5cm） as cathode electro-osmosis. A wide (2cm) draining belt wrapped in a permeable cloth is inserted near each electrode. Insert three groups of electrodes into the device(the two sets of output voltage are 30V, arranged on both sides. Another set of output voltage is 5V, arranged in the middle.)
4) The YBD displacement sensor is used to detect the real time settlement. The results are introduced into the computer for processing.
5) In the process of electro-osmosis, a shear plate is used to test the soil strength once every 4 hours.
6) In the process of electro-osmosis, the current and voltage are measured by the multimeter and the final energy consumption is calculated.
7) The basic properties of the soil are measured once every 4 hours. The content of heavy metals in soil was measured once every 4 hours.

The experimental layout and equipment drawings are as follows

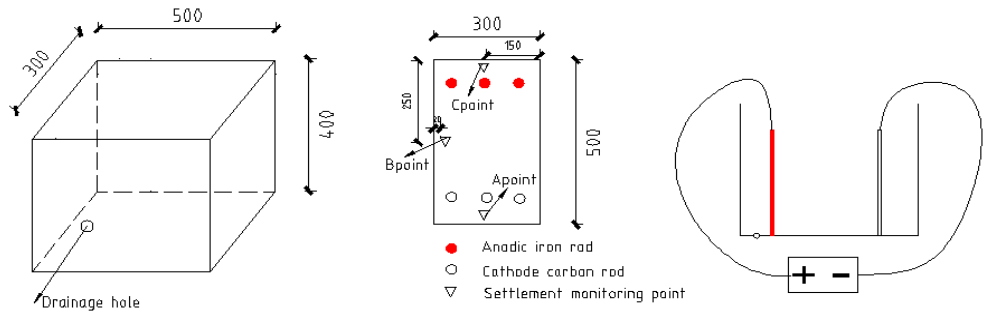

FIGURE 1: EXPERIMENTAL LAYOUT

FIGURE 2: YOUTAI ACQUISITION

FIGURE 3: GUWEI DC POWER SUPPLY

2.3 Basic parameters before electro-osmosis

According to the Standard for test method of geotechnical engineering GB-T50123-1999, the basic mechanical indexes for the determination and calculation of soil include three measured indexes: moisture content; specific gravity of solid particles; density. Six conversion indices: porosity ratio; porosity; saturation; dry density; saturated density; buoyant density. The

moisture content; density; dry density; porosity ratio; void ratio and saturation of soil are measured and calculated according to the test.

Basic mechanical parameters of soil before electro-osmosis:

TABLE 1
BASIC PARAMETERS OF SOIL BEFORE ELECTRO-OSMOSIS

Density g/cm3	Dry density g/cm3	Specific gravity of solid Gs	Moisture content %	Porosity ratio	Porosity	Saturation %
1.50	1.06	2.7	40.72%	1.54	0.606	71.42%

The plastic limit value of the soil is ω_P=15.19 and the liquid limit is ω_L =33.02。 The permeability coefficient of soil is 1.7068×10-6 by the method of variable water head penetration test.

III. EXPERIMENTAL DATA ANALYSIS

3.1 Change of moisture content

In the process of electro-osmosis, water will be discharged, the water content of the soil will be reduced, and the water content varies with time, as shown in Figure 4.The result of curve fitting curve is $w = 0.39651 - 0.0028t$.

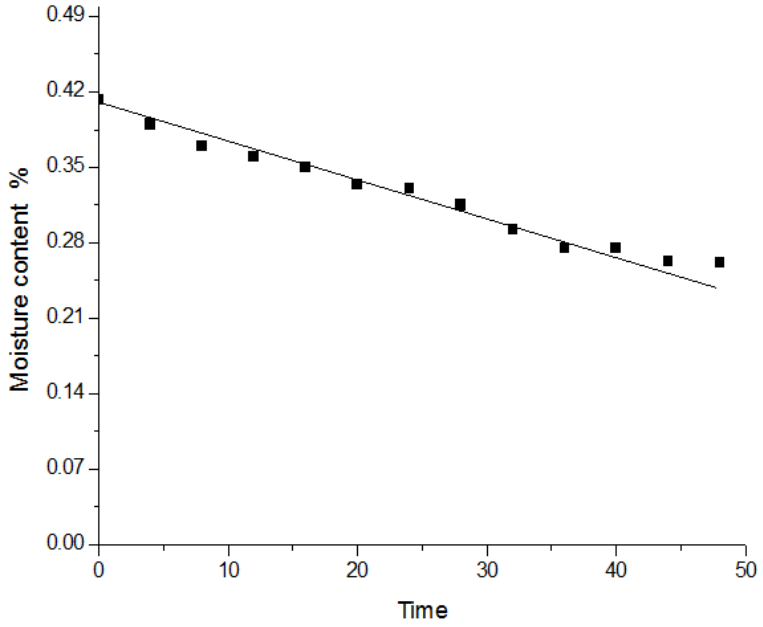

FIGURE 4: WATER FITTING CHANGE FITTING

The original soil moisture content of 40.72%, after the electro-osmosis test, the soil moisture content dropped to 27.76%.At the same time, it can be seen from Figure 4 that the slope of the curve is getting smaller and smaller. This shows that the electro-osmosis experiment at the beginning of the moisture content changes rapidly, the effect of electro-osmosis more obvious. After the test, the soil near the electrode was compared. It was found that the water content of the soil near the anode was 26.68%, and the water content near the cathode was 37.49%.It can be seen that the soil moisture content near the anode is the lowest, lower than the average level, and the water content near the cathode is the highest. In the process of electro-osmosis, the water in the soil is permeated from the anode to the cathode, which leads to the high water content of the cathode.

3.2 Density and dry density

The fitting curves of density and dry density are respectively

$\rho = 1.50346 + 0.00382t$, $\rho_d = 1.00846 + 0.00471t$

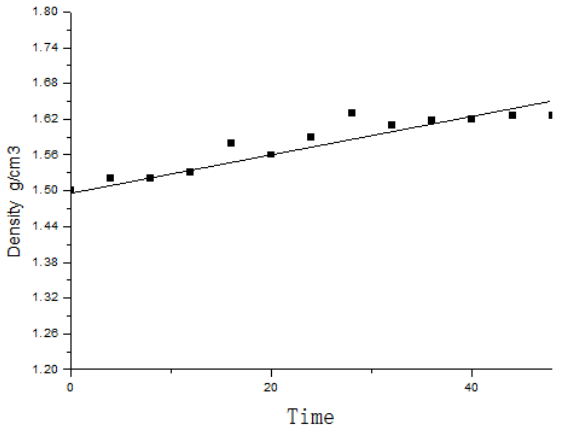

FIGURE 5: DENSITY VARIATION FITTING

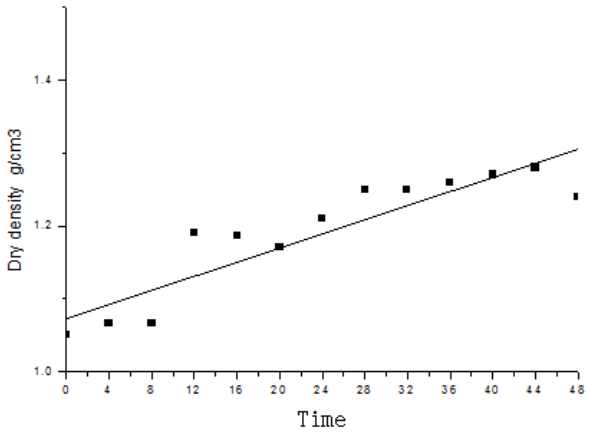

FIGURE 6: DRY DENSITY VARIATION FITTING

The original soil density of 1.50g / cm3 dry density of 1.06g / cm3.After the electro-osmosis test, the density of soil is 1.65g/cm3, the dry density is 1.29g/cm3, and the density increases 0.23g/cm3 for the density of 0.15g/cm3.Due to the consolidation and settlement of soil in the process of electro-osmosis, the porosity in the soil decreases, and the density and dry density of the soil increases.

Analysis of soil sampling near the cathode and anode after the test. The density of soil mass near the anode is 1.69g/cm3 dry density 1.34g/cm3, and the density of soil mass near the cathode is 1.54g/cm3 dry density of 1.12g/cm3.The density and dry density of the anode are greater than that of the cathode, which shows that the anodic electro-osmotic effect is better than that of the cathode.

3.3 Change of porosity ratio and porosity

The consolidation and settlement of soil occurred during the electro-osmosis process. The void in the soil will change to influence the porosity ratio and porosity. The changes in porosity ratio and porosity are fitted as the following

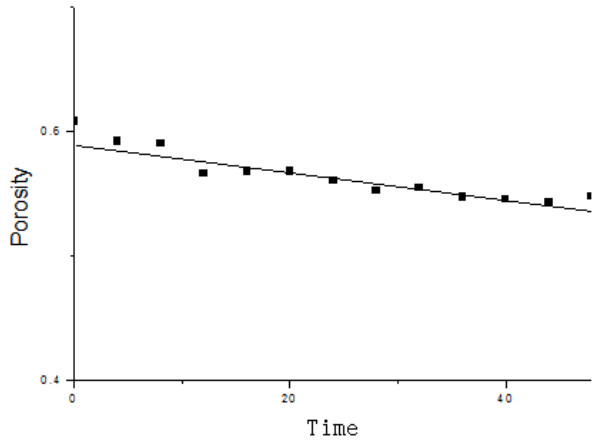

FIGURE 7: FITTING OF POROSITY RATIO VARIATION

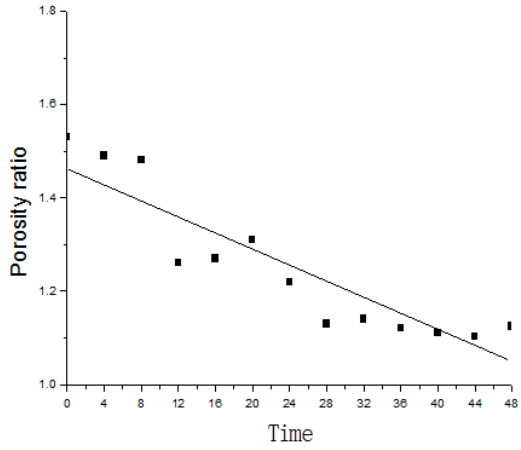

FIGURE 8: POROSITY FITTING CURVE

Analysis of soil sampling near the cathode and anode after the test. The comparison results show that the porosity ratio of the soil near the anode is 1.02, the porosity is 0.505, and the porosity ratio of the soil near the cathode is 1.41 porosity 0.585.The porosity ratio and porosity of the anode and cathode are lower than the porosity ratio and porosity of the original soil. This shows that during the process of electro-osmosis, the consolidation and settlement of soil occur, the porosity of soil decreases. The electro-osmotic effect near the anode is better than that of the cathode.

3.4 Saturation curve

The Moisture content and porosity change during the experiment and the specific gravity of the soil is constant. Calculation of soil saturation based on the basic parameters of the sample. The maximum value of saturation is 75.68%, and the minimum value is 66.37%.

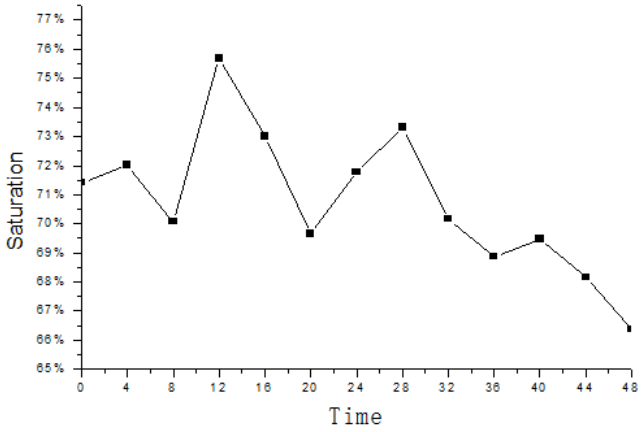

FIGURE 9: SATURATION CURVE

3.5 Change of permeability coefficient

Determination of permeability coefficient by variable head permeability test method.

Determination of permeability coefficient by variable head test method. The permeability coefficient before electro-osmosis was 1.7068 ×10-6 after electro-osmosis, 1.0381×10-6.Data analysis shows that the permeability coefficient of soil becomes smaller after the electro-osmosis experiment is completed.

3.6 The change of shear strength

The strength of the soil will change during the electro-osmosis process. The shear test of the electro-osmotic soil is carried out every eight hours. The shear strength is calculated by formula $\tau_f = \frac{2M}{\pi D^2\left(H+\frac{D}{3}\right)}$.

M - torque (Kn· m)

D - the width of the shear plate(m)

H - the height of the shear plate (m)

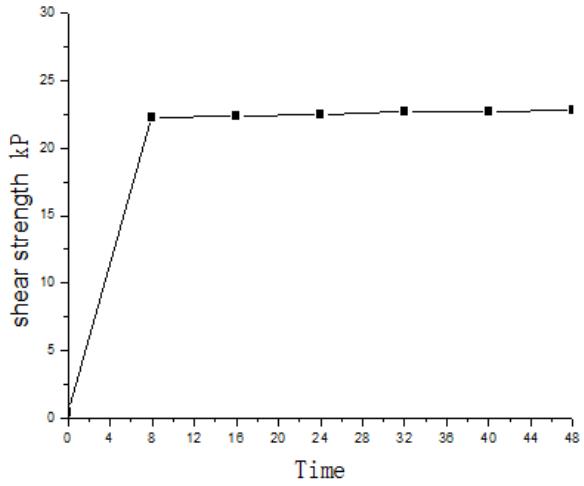

FIGURE 10: SHEAR STRENGTH CHANGE CURVE

It can be found that the shear strength of the original soil is very low, and the shear strength of the soil increases a lot after the electro-osmosis experiment is completed. After 48 hours, the shear strength reached 22.8Kpa.The shear strength increased rapidly in the first eight hours, and the rising speed of shear strength became slower after eight hours. It is found that the shear strength of the anode soil is 26.9Kpa, and the shear strength of the anode soil is greater than that of the cathode soil. The water of the anode permeated the cathode by the electro-osmotic effect, which increased the strength of the anode more.

3.7 Soil settlement detection

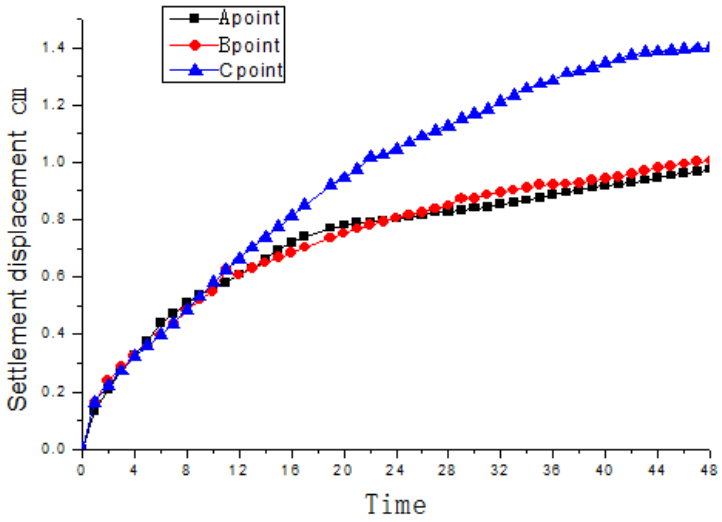

FIGURE 11: REAL-TIME DETECTION OF SETTLEMENT

The final settlement of A point near the cathode is 0.972cm, and the final settlement of B point near the anode is 1.004cm.The settlement of the C point in the middle is 1.399cm.Compared with the settlement of A, B and C, the settlement of C point is relatively large, which may be caused by the disturbance to the C point during the sampling and shear test.

3.8 Measurement of electric energy consumption

TABLE 2
ELECTRO-OSMOSIS ENERGY CONSUMPTION METER

Electro-osmosis energy consumption meter					
Time/h	**Voltage/v**	**Electric current/A**	**Power/W**	**Energy consumption/kw·h**	**Total energy consumption/kw·h**
0	65	0.70	45.50	0.128	2.1294
4	65	0.68	44.20	0.177	
8	65	0.68	44.20	0.177	
12	65	0.66	42.90	0.172	
16	65	0.65	42.25	0.169	
20	65	0.63	40.95	0.164	
24	65	0.62	40.30	0.161	
28	65	0.61	39.65	0.159	
32	65	0.61	39.65	0.159	
36	65	0.60	39.00	0.156	
40	65	0.59	38.35	0.153	
44	65	0.58	37.70	0.151	
48	65	0.58	37.70	0.151	

Energy consumption is 2.1294Kw·h in the process of continuous electro-osmosis per kilowatt hour of 1.025 yuan per kilowatt hour at the peak of current industrial power consumption in 2017.According to the above data, it is estimated that this test will cost 2.19 yuan. The area of this experiment is 0.15m2. The calculated electro-osmosis method takes 14.6 yuan per square meter for sludge treatment. Heavy tamping treatment of sludge foundation requires 30-40 yuan per square meter. It can be seen that the electro-osmosis method can reduce the cost of 2.05-2.74 times.

Notes: Post-graduate's Innovation Fund Project of Hebei University

3.9 Changes in heavy metals

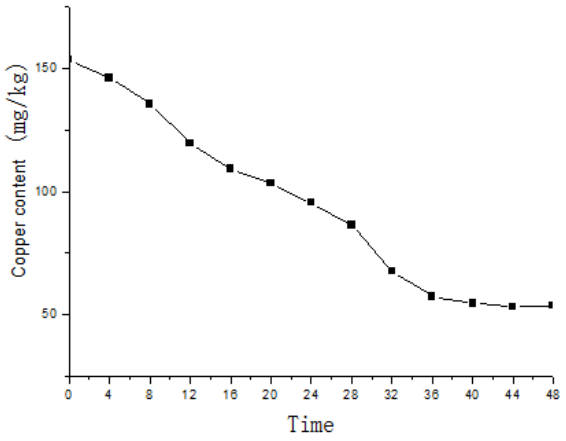

FIGURE 12: CHANGE CURVE OF ZINC CONTENT

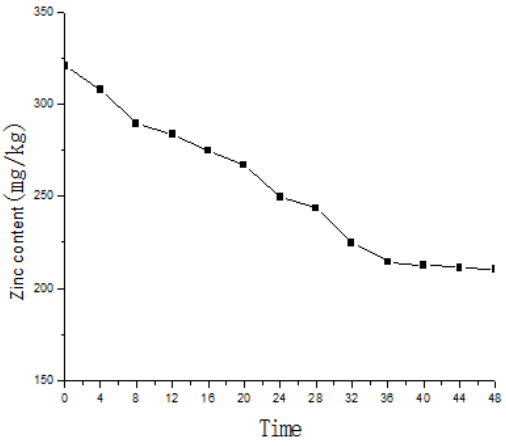

FIGURE 13: CURVE OF COPPER CONTENT CHANGE

Before the electro-osmosis experiment, the content of copper is 153.62mg/kg zinc 320.53mg/kg. After the electro-osmosis experiment, the content of copper is 53.68mg/kg zinc is 210.27mg/kg. According to the standard of soil environmental quality standard (GB15618) for the standard value of soil environmental quality, the content of copper and zinc is basically up to second levels.(the content of two grade copper is <=50mg/kg, the content of two grade zinc is <=200mg/kg).

IV. CONCLUSION

1) After the completion of electro-osmosis, the density increased from 1.50g/cm3 to 1.65g/cm3, and the moisture content decreased from 40.72% to 27.76%, and the shear strength increased from almost zero to the maximum intensity 26.9Kpa.The above changes occur only within 24 hours. From the above data, it is found that the visible electro-osmosis method has a good effect on the treatment of sludge strength.

2) For this two day experiment, from the energy consumption and economic benefits, the treatment of sludge by electro-osmosis method needs 14.6 yuan per square meter, compared with the dynamic consolidation of sludge foundation, the cost is reduced by 2.05-2.74 times.

3) The content of copper in the sludge decreased from 153.62mg/kg to 53.68mg/kg, and the content of zinc decreased from 320.53mg/kg to 210.27mg/kg.The final treatment result is close to the second level standard in the soil environmental quality standard GB15618.

REFERENCES

[1] Qingchen Cheng, Yongjun Sun,et al Application of electro-osmosis technology in consolidation of dredging dams [J]. Northeast Water Conservancy and Hydroelectric Power, 2001, (09): 14-16 + 55.

[2] Yanli Tao,Jian Zhou,Yiwen Li.Electro-osmotic experimental research on three arrangements of electrodes [J] .Building Structure, 2013,43 (S2): 214-218.

[3] Dongqing Pan, Jianzhong Zhang,Chiyu Zhang. Theoretical and Experimental Research on the reduction of electro-osmotic energy consumption [J]. low temperature construction technology, 2014,36 (03): 123-126

[4] Zhuo Chen. Experimental Research on the Effect of Electricity Design to Electro-osmotic Consolidation of Soft Clay[D]., Zhejiang University, 2013.

[5] Pingchuan Hu.Experimental study on the influential factors and improving method of electro-osmotic permeability of soft clay [D]., Zhejiang University, 2015.

[6] Ying Li,Xiaonan Gong.Experimental research on effect of electrode spacing on electro-osmotic dewatering under same voltage gradient [J]. geotechnical mechanics, 2012,33 (01): 89-95.

[7] Jianwei Lu. Experimental Study on Electrochemistry Phenomenon during Electro-osmotic Process [D]. Wuhan University of Technology, 2011.

[8] Yonghua Cao,Zhiyi Gao,Aimin Liu. Characteristics and Development of Electro-osmotic Treatment for Ground Improvement [J]. water transport project, 2008, (04): 92-95+116.

[9] Environmental quality standards for soils[S],GB15618.

Experimental Investigation of Thermal Performance of Photovoltaic Thermal (PVT) Systems

Ahmet Numan ÖZAKIN[1], Muhammet Kaan YEŞİLYURT[2], Kenan YAKUT[3]

Atatürk University, Erzurum, 25040, Turkey

Abstract— *The phenomenon of photovoltaic systems is based on the principals of semiconductor physics and they operate with a semiconductor element, such as silicon. Photovoltaic cells can generate electricity only when they receive a certain amount of photon energy and thus they convert only a fraction of the solar irradiance, which is received from the sun in the form of electromagnetic radiation in the electromagnetic spectrum, into electrical energy. The remaining radiation is stored as heat in photovoltaic systems, causing some irreversibilities in the system.*

In general, the experimental setup, the accumulated heat, which reduces the efficiency of the photovoltaic systems, is aimed to be removed from the system and turned it into useful energy. By employing some heat transfer enhancement systems, the photovoltaic cell temperature decreased to the range of 40-60 °C, the temperature range at which a photovoltaic system runs optimal, whereby an approximate improvement of 20% in electrical efficiency of the PV system achieved. Aluminum and copper cylindrical fins or some refrigerant fluids used as heat transfer enhancement elements in the systems.

In this operating conditions, the electrical efficiency of the system decreases to around 6.5% down from the nominal electrical efficiency of 12% under optimal operating temperature. The fin surface temperature and ambient temperature of the control volume decreased in direct proportion to the air velocity. At about 5 m/s air velocity, the fins bodies and ambient air were cooled down by about 50%, accordingly, the electrical efficiency decreased from 12% to only 9.5%.

Keywords— Thermal efficiency of PV cells; electrical efficiency; copper fins; aluminum fins; pv/t systems.

I. INTRODUCTION

In parallel with the developing and increasingly diversified industry, as well as the seek for comfort, the need for energy is increasing rapidly. This need can no longer be met by relying on fossil fuels even if conventional energy producing systems are used effectively and environmental pollution is disregarded. Due to increased energy load and the adverse effects of fossil fuels on environment, a quest for new and renewable clean energy sources are sought [1,2]. Renewable energy sources have been seen as a solution to the disadvantages caused by fossil fuels and solar energy has made its first place with its high potential and large geographical availability.

Surveying the literature, one can easily see that there is an abundance of experimental study on the thermal analysis of the photovoltaic system. Most of these studies focus on removing the radiation-induced heat accumulation, which decreases the yield from the photovoltaic system, with appropriate cooling systems in order to maintain the electrical output at fair levels as well as obtaining a utilizable thermal energy source.

In the literature, there are many complex and detailed mathematical models for thermal performance analysis. However, in order for the performance analysis of such systems should easily be calculated and be compared to similar systems; generally, a performance analysis based on the first law of Thermodynamics is sufficient. In thermodynamic analysis of the Photovoltaic thermal (PVT) systems, the system is regarded to be a continuous flow control volume (open system). Mass and energy transfers from the boundaries of the control volume are calculated using conservation equations. Atypical control volume set for the experimental systems studied in the literature is given in Fig. 1.

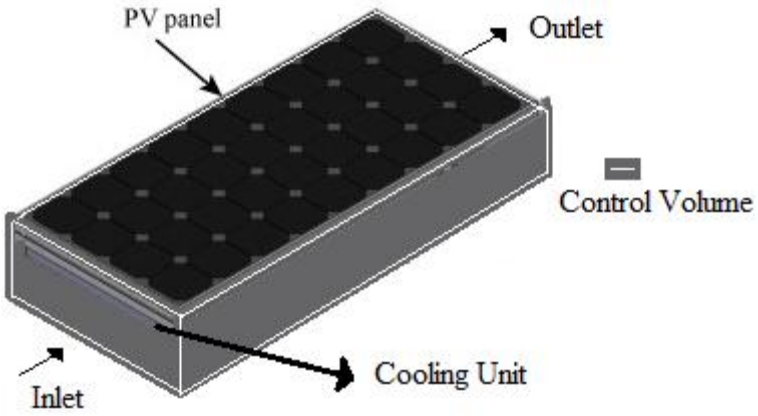

FIGURE 1. A TYPICAL CONTROL VOLUME FOR EXPERIMENTAL STUDIES IN THE LITERATURE

The mass transfer from system to control volume or from control volume to system at any given time interval of Δt is equal to the change in mass in the control volume in the same time interval.

$$\dot{m}_i - \dot{m}_o = \Delta \dot{m}_{kh} \quad [kg/s] \tag{1}$$

The changes in the control volume has to be equal to zero for it is a continuous flow system, and therefore;

$$\sum \dot{m}_i = \sum \dot{m}_o [kg/s] \tag{2}$$

The energy equation for continuous flow systems with necessary simplifications made is;

$$\dot{Q}_{thermal} = \dot{m}(h_o - h_i) \quad [kW] \tag{3}$$

$$\dot{Q}_{thermal} = \dot{m}.c_p(T_o - T_i) \quad [kW] \tag{4}$$

And the total solar power gained from the sun can be expressed as follows, as the sum of the thermal power gain and the generated electrical power ($\dot{Q}_e$ = V.I).

$$\dot{Q}_g = \dot{m}\left[(h_o - h_i) + \left(\frac{{V_o}^2 - {V_i}^2}{2}\right)\right] + \dot{Q}_e \quad [kW] \tag{5}$$

$$\dot{Q}_g = \dot{m}\left[c_p(T_o - T_i) + \left(\frac{{V_o}^2 - {V_i}^2}{2}\right)\right] + I.V \quad [kW] \tag{6}$$

The First Law efficiency is expressed as;

$$\eta_I = \frac{\dot{Q}_g}{\dot{Q}_{solar}} \tag{7}$$

which is a commonly used expression for efficiency calculations in the literature.

II. LITERATURE REVIEW

The use of energy is increasingly diversifying and the difference between the amount of energy produced and the energy load that has to be met is increasing each day. Fossil fuels were preferred to be the primary energy source to meet energy needs. Fossil fuels, which do not require use of high technology in neither accessing nor making use of, have brought in a number of problems. These problems, which showed off as simply environmental pollution in early times, have brought about the major global warming and the greenhouse effect issue, which is truly a catastrophe forerunner. Greenhouse gases which are emitted as a result of inefficient and excessive use of fossil fuels have caused serious damages to the atmosphere. Therefore, different types of environmental friendly sources are sought.

Energy sources referred to as renewable energy sources in the literature have almost no environmental impacts. The best renewable source of energy that can be used as an alternative to fossil fuels is solar energy [3]. Also the highest capacity renewable energy source among all renewable is solar [4]. Different applications are available in utilization of solar energy. The first application is solar collector systems while the latest and most technologically developed one is the photovoltaic systems which generate electricity from solar irradiation.

The greatest problem in photovoltaic systems is the increased cell temperature under in solution [5].A number of methods have been developed to prevent cell temperature from rising [6].This excess heat accumulated in photovoltaic systems can be converted into useful thermal energy [7].Such Photovoltaic systems can be combined with thermal systems (which is then called a PVT) and both reduction in the system efficiency can be avoided by drawing heat and the drawn heat can be transferred to a fluid which can serve as a thermal agent and hence increase the total yield from the system. PV/T systems were first implemented in 1970s by Martin Wolf [8]. Michel et al. used nano-fluids in PV/T system as heat transfer agent [9]. Numerical simulation studies are also being made on PV/T systems such as those referred to in a detailed review by Tchen et al. [10]. Ion the other hand, many numerical simulation studies focused on thermal and electrical efficiencies of PVT systems are available in the literature, too [11-15].

PV/T systems can be designed in different ways to optimize efficiency for different climate zones. Conventional PV systems are more efficient in cold climate regions because of the low ambient temperature [16].Among examples for integration of PV/T systems to cold climate regions are those of Chow et al. and Athientis et al. [17,18].

III. MATERIAL AND METHOD

The photovoltaic system reaches a steady state temperature of about 120 °C at under800 W/m2 solar irradiation. This temperature is far too higher than the optimum operating temperature of 40 °C for the photovoltaic system. At this operating conditions, the electrical efficiency of the system decreases to around 6.5% down from the nominal electrical efficiency of 12% under optimal operating temperature. The conversion of the photovoltaic system to the photovoltaic thermal (PV/T) system helped avoid this yield reduction.

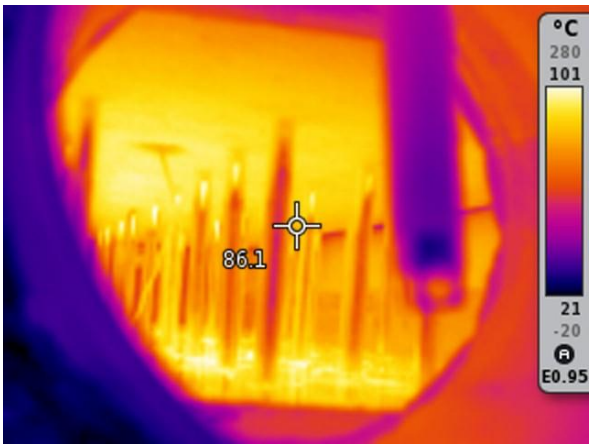

FIGURE 2.ALUMINUM FINS WITHIN THE CONTROL VOLUME WITH NATURAL CONVECTION

The PV / T is designed to create a control volume within the experimental rig. As can be seen from Fig. 2, in the absence of air flow in the control volume, the surface temperature of about 120 °C could be reduced to 86 °C by adding aluminum fins under natural convection conditions thanks to the increase in the total heat transfer surface area.

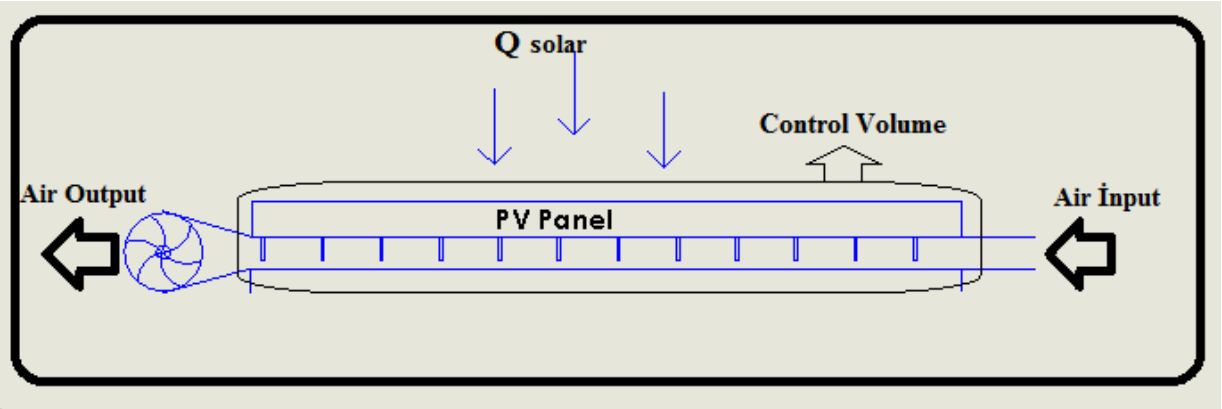

FIGURE 3.DESIGNED CONTROL VOLUME.

Additionally, in the next step, the PV/T experimental rig has been equipped with a fan at the outlet port of the control volume in order to draw air through the control volume. Why the fan has been installed on the outlet end is that this prevents the heat transfer to the feed air from the fan body, which is heated during the working regime.

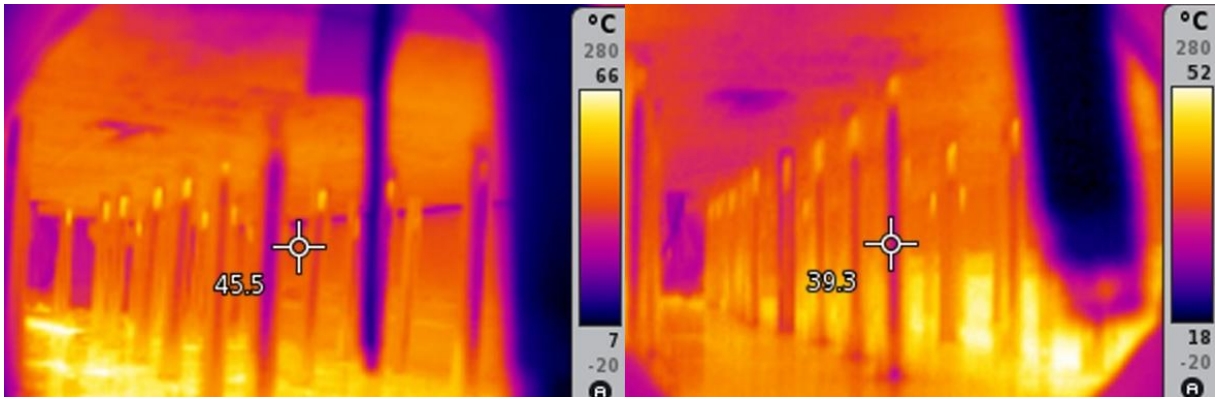

FIGURE 4.FIN BODY TEMPERATURE AND AMBIENT TEMPERATURE WITH SUCTION PUMP AT 5 m/s AIR VELOCITY

In the photovoltaic thermal experimental rig, air suction with forced convection is provided at different air velocities, the fin surface temperature and ambient temperature of the control volume decreased in direct proportion to the air velocity. At about 5 m/s air velocity, the fins bodies and ambient air were cooled down by about 50%, as shown in Fig. 4. Accordingly, the electrical efficiency decreased from 12% to only 9.5%. The efficiency calculation is made by considering the net yield, and the net electrical power drawn by the fan is subtracted.

IV. RESULTS AND DISCUSSION

Researchers conducted on thermal examination of photovoltaic systems (cooling) can be collected under several headings as follows;

- Using microchannel technology and nano-fluids.
- Liquid spray cooling.
- Thermoelectric modules.
- Forced convection cooling using the fins with air or water.
- Removing heat from the photovoltaic surface by employing phase change materials.

TABLE 1
COMPARISON OF DIFFERENT TECHNOLOGIES

Technology Used	Benefits	Drawbacks
Studies using microchannel technology nano-fluids	• Thermal efficiency • High heat transfer coefficient	• High cost and difficulty of applicability.
Cooling operation with water sprays.	• Increased energy efficiency. • It is more efficient than air cooling.	• The entire surface area of the PV panel is only partially cooled. • Removed heat is wasted.
Studies with thermoelectric modules.	• Electrical efficiency is increased. • It reduces hot spotting.	• Heat loss due to conduction between the hot and cold parts through semi-conductors • Heat cannot be transferred well enough.
Forced convection cooling using fins with air or water	• Overall efficiency is increased. • Economically feasible. • Heated air or water used to heat buildings.	• Air-cooling efficiency is lower than cooling with water. • More effective than cooling with air cooling with water in hot climates.
Removing heat from the photovoltaic surface by employing phase change materials.	• It can store large amount of heat with a small temperature changes. • The phase change takes place at a constant temperature. • The captured heat used to heat buildings.	• Paraffin solid which has a low thermal conductivity. • You need more capacity for heat storage. • In colder areas it is less efficient.

In this study, different types of PV / T systems were compared by examining the analysis of thermal performance. Efficiency of thermal systems integrated with photovoltaic system is high, and it also increases the overall system efficiency. The total yield from the system is about 55% greater than the yield of the photovoltaic electrical system alone.

The combination of thermal collectors and photovoltaic systems is very important in terms of energy efficiency. Using Photovoltaic systems in combination with thermal systems (which is simply called a PV/T system) will become general in the industry. Developing material technologies and increased energy demand will force increase researches on renewable energy sources which in turn will increase yields from renewable energy systems.

REFERENCES

[1] Othman, M.Y., et al., Performance analysis of PV/T Combi with water and air heating system: An experimental study. Renewable Energy, 2016. 86: p. 716-722.
[2] Wolf, M., Performance Analyses of Combined Heating and Photovoltaic Power-Systems for Residences. Energy Conversion, 1976. 16(1-2): p. 79-90.
[3] Sargunanathan, S., A. Elango, and S. TharvesMohideen. "Performance enhancement of solar photovoltaic cells using effective cooling methods: A review." Renewable and Sustainable Energy Reviews 64 (2016): 382-393.
[4] Özakın, A. N. 2016. The heat recovery with heat transfer methods from solar photovoltaic systems- Journal of Physics: Conference Series
[5] Ebrahimi, Morteza, MasoudRahimi, and AlirezaRahimi. "An experimental study on using natural vaporization for cooling of a photovoltaic solar cell." International Communications in Heat and Mass Transfer 65 (2015): 22-30.
[6] Skoplaki, E., and J. A. Palyvos. "On the temperature dependence of photovoltaic module electrical performance: A review of efficiency/power correlations." Solar energy 83.5 (2009): 614-624.
[7] Du, B. 2012. Performance analysis of water cooled concentrated photovoltaic (CPV) system. Renewable & Sustainable Energy Reviews 16: 6732-6736.
[8] Kolhe, M. 2012. Water Cooled Photovoltaic System. International Journal of Smart Grid and Clean Energy 2.
[9] Micheli, Leonardo, et al. "Opportunities and challenges in micro-and nano-technologies for concentrating photovoltaic cooling: A review." Renewable and Sustainable Energy Reviews 20 (2013): 595-610.
[10] Tchinda, Réné. "A review of the mathematical models for predicting solar air heaters systems." Renewable and sustainable energy reviews 13.8 (2009): 1734-1759.
[11] Tonui, J. K., and Y. Tripanagnostopoulos. "Air-cooled PV/T solar collectors with low cost performance improvements." Solar energy 81.4 (2007): 498-511.
[12] Garg, H. P., and R. K. Agarwal. "Some aspects of a PV/T collector/forced circulation flat plate solar water heater with solar cells." Energy Conversion and Management 36.2 (1995): 87-99.
[13] Sopian, Kamaruzzaman, et al. "Performance of a double pass photovoltaic thermal solar collector suitable for solar drying systems." Energy Conversion and Management 41.4 (2000): 353-365.
[14] Bambrook, S. M., and A. B. Sproul. "Maximising the energy output of a PVT air system." Solar Energy 86.6 (2012): 1857-1871.
[15] Schnieders, Jürgen. "Comparison of the energy yield predictions of stationary and dynamic solar collector models and the models' accuracy in the description of a vacuum tube collector." Solar Energy 61.3 (1997): 179-190.
[16] Yang, Tingting, and Andreas K. Athienitis. "Experimental investigation of a two-inlet air-based building integrated photovoltaic/thermal (BIPV/T) system." Applied Energy 159 (2015): 70-79.
[17] Chow, Tin Tai. "A review on photovoltaic/thermal hybrid solar technology." Applied energy 87.2 (2010): 365-379.
[18] Athienitis, Andreas K., et al. "A prototype photovoltaic/thermal system integrated with transpired collector." Solar Energy 85.1 (2011): 139-153.

Material structure particularity of polyethylene-terephtalate (PET) and poly-lactic (PLA)

Tibor Horvath[1], Kalman Marossy[2], Tamas Szabo[3], Krisztina Roman[4], Gabriella Zsoldos[5], Mariann Szabone Kollar[6]

Institute of Ceramic and Polymer Engineering, University of Miskolc, Miskolc- Egyetemvaros, 3515, HUNGARY

Abstract - The huge amount of synthetic plastics are used in the packaging area, especially in food packaging, because there have great effects in the environmental and alternative, more ecologic materials are being required. Poly-lactic acid (PLA) is one of the most significant biodegradable thermoplastic polymers. It is compostable and made it from renewable sources. The mechanical and optical property of PLA is very similar to the Polyethylene, but is more fragile, less heat-resistant and offer low resistance to oxygen permeation. In this work, two commercial PLA foils and one commercial PET foil properties were examined. The correlations between the mechanical, thermal and barrier properties were analyzed. From these measurements we can understand the PLA is a usable for packing applications, especially in the sweet manufacturing. Films were studied by tensile testing, differential scanning calorimetry and thermally simulated discharge analysis.

Keywords— PET, PLA, stretching, mechanical properties, TSD, DSC, crystal structure.

I. INTRODUCTION

The last few decades in the European Union, the environment protection is the most important, especially must be protected from the industrial and human contaminated. In the past years the depletion of the natural resources and environmental degradation threatens to the world. As a consequence, research efforts have been introduced at different levels to find alternative solutions. A specific concern is the field of packaging, which was producing huge amounts of non-degradable plastic in some critical areas. The non-degradable products can affect Europe's and the planet's natural resources. These problems caused further problems and the recycling costs of the products will be higher [1,2]. In Hungary the plastic industry is using only 36 percent from the PLA and PET foils such a packaging materials. Some industries worked on new biodegradable products. This material can become the part of nature, such microorganisms. There are already existing materials but their use is less prevalent because of their poor mechanical properties.

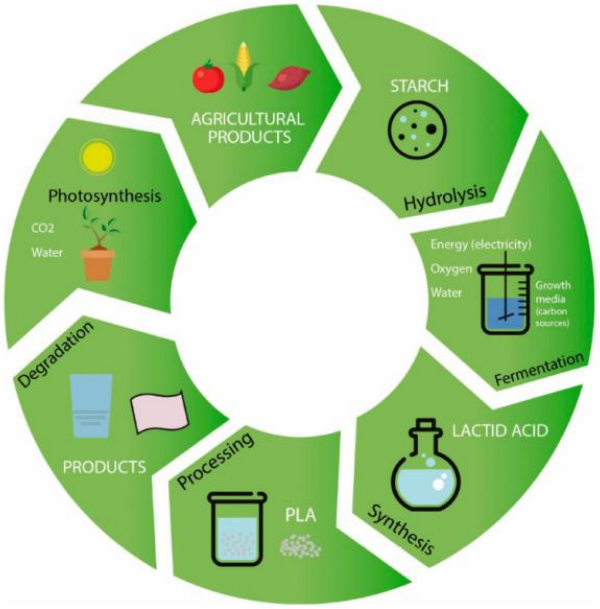

FIGURE I. PLA ROTATION IN THE NATURE [2]

Plastic materials can be found in the sweet industries to the most widely used plastic foil is the polyethylene-terephtalate (PET). The manufacture has special requirements; therefore the PET is a suitable material. A new material needs to be suitable for the seller, producer and consumer requirements and comply with the recent EU regulations. Alternative materials

have to have similar set of properties. However, they need to be biodegradable following "environment friendly" approach. PLA is a renewable sustainable option to the packaging industry. It has high molecular weight. The PLA foils are colorless, glossy and rigid which is similar to the properties of PS materials.

The two isomers of LA can produce three distinct materials: poly (D-lactic acid) (PDLA), a crystalline material with a regular chain structure; poly (L-lactic acid) (PLLA), it is a semi crystalline, it has same regular chain structure as the amorphous of poly (D, L-lactic acid) (PDLLA).Three different stereo chemical forms exist for lactide: L-, D- or both L-, D- Lactide (meso-lactide), each one having their own melting properties. PLA has a degradation half-life in the environment ranging from 6 months to 2 years, depends on the size-, shape- and the isomers of the materials and the production temperature.

TABLE 1

PHYSICAL AND CHEMICAL PROPERTIES OF THE USED PLA AND PET FOIL [3].

Properties	PDLA	PLLA	PDLLA	PET
Solubility	All are soluble in benzene, chloroform, acetonitrile, tetrahydrofuran (THF), dioxane etc., but insoluble in ethanol, methanol, and aliphatic hydrocarbons			phenol, o-chlorophenol DMSO, nitrobenzene,
Crystalline structure	Crystalline	Hemicrystalline	Amorphous	Amorphous and semi-crist.
Melting temperature (T_m)/ °C	180	180	variable	260
Glass transition temperature (T_g)/ °C	50-60	50-60	variable	67-81
Decomposition temperature/°C	200	200	180-200	293-306
Elongation at break/ (%)	20-30	20-30	variable	230
Breaking strength/ (g/d)	4-5	5-6	variable	5,3
Half-life in 37°C normal saline	4-6 month	4-6 month	2-3 month	700 year

II. EXPERIMENTAL

2.1 Materials and methods

PET and PDLLA samples were obtained by Pro-Form Kft. and the PLLA sample was purchased from Good fellow Cambridge Ltd. the thickness of the PDLLA and PET film were 300µm, and the sample thickness of the PLLA foil was of 50 µm. In case of PET and PDLLA preformed films were used. The PET film surface was screen printed with a 1 mm splitting lattice and a 10 mm splitting lattice was used for the PDLLA film samples to follow the deformation ranges. The forming temperature of PET was 100°C. The forming temperature of PDLLA was 70 °C. The preheating time both of samples was 2 minutes.

The mechanical properties can be determined with tensile test. The test was performed on INSTRON 5566 testing machine. The measurements procedure followed the ASTM D389 standard. The test speed was 100 mm/min at room temperature (23±1°C). During the tests the 150%, 200% and 250% stretching was determined.

The DSC measurements were carried out by DSC131 EVo machine to determine the polymer structure. The heating/cooling rate was: 10 °C/min.

The structural differences were measured by SETARAM-TSC II TSD equipment. The measurement cooling and heating rate was 5°C / min.

2.2 Results and discussion

During the PET mechanical test, founded that the fluidized PET samples were initially formatted in a relatively high power range. At this stage, the weak secondary bonds connected the molecular chains are disrupted. In the amorphous material the increased kinetic energy of the collapsed molecular chains due to heating. It means that they were able to orient themselves

in the direction of force in the direction of a sufficient degree of shaping force. This orientation process is also indicated by the fact that at a later stage of formatting, much smaller force was sufficient to further shape the sample. At higher forming (deformation between 200% and 250%) the molecular chains reached the maximum of orientation. The sample reached the threshold values, because the elongated molecular chains were smaller than the deformation. The center of gravity of shorter and smaller molecular chains moved, the material was been subjected to permanent flow.

From the mechanical test, the curves of poly-lactic acid (PDLLA) were significantly higher than the other samples. This can be explained by the forming force range is difference for different materials. From the result of tensile test of PET, forming was partially coupled with the long-running flow of molecular chains. In the case of PDLLA, the material was capable of absorbing even more loads without partial flow. This referred to longer molecular chains as well as stronger intramolecular interactions is in amorphous parts, but also caused by the partially crystalline structure. Larger amorphous molecules and highly folded crystalline parts need greater forces to form orientation.

In the process as a whole, it is very similar to that experienced for PET, because the PDLLA also required a higher rate of effort in the initial phase to initiate orientation. The process also started with the weak secondary cross linking of the chains, and the orientation of the amorphous and crystalline molecules happened.

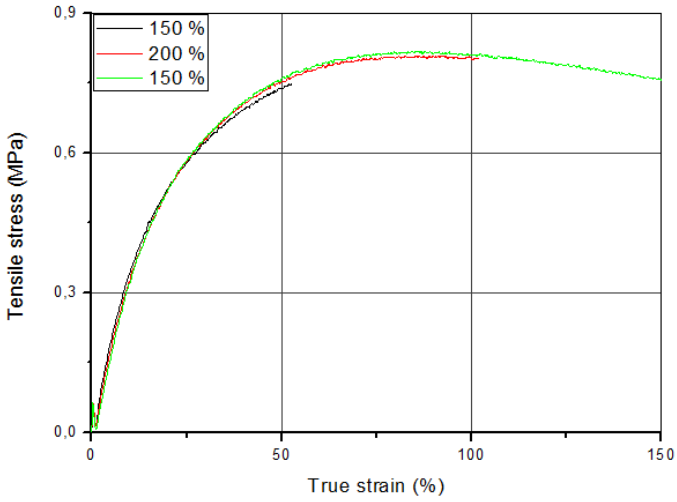

FIG. 2: RESULTS OF TENSILE TEST OF PET FOIL INN CASE OF DIFFERENT DEFORMATION RANGE

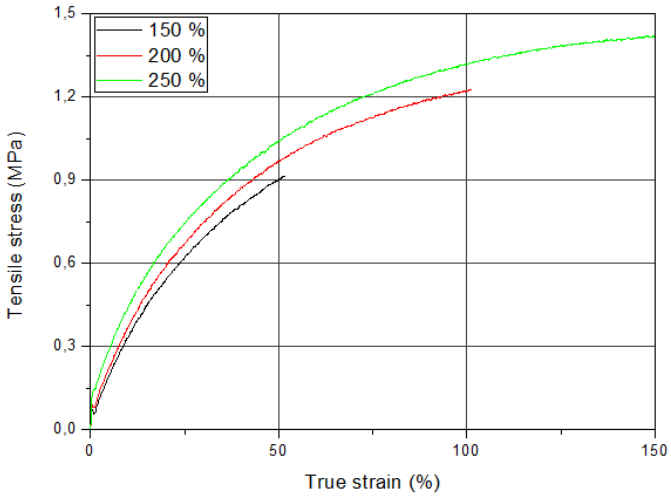

FIG. 3: RESULTS OF TENSILE TEST OF PDLLA FOIL IN CASE OF DIFFERENT DEFORMATION RANGE

During the function analysis, it became clear that both of L and D isomers of poly-lactic acid samples were tested. It formed crystalline structure under appropriate conditions. However, this dual crystal structure is also a disadvantage of the material, as the different isomers cannot build a homogeneous crystalline structure. It slows down and makes crystallization difficult. The measurements showed that the material contained two distinct crystalline fractions of heterogeneous crystal structure. This is supported by the two sub-functions obtained as a result of the resolution of the decomposition curve. During the DSC analysis, we also found that the crystalline fraction of the material is constantly changing in proportion to the degree of deformation and the purity of the material (including virgin / recycled material) also significantly influences the crystal structure of the material [4]. The former relates to the definition of the forming parameters (heating rate, forming force range, rate of decay, cooling rate). In the initial phase of deformation (0-150%), due to the one-axial stretching, the collapsed molecules are oriented towards the force.

This orientation favors the formation of crystalline structures. Above a boundary, the crystalline structure also breaks down, and like folded molecules, the folded molecular chains are partially oriented in the axis of the forming force, thus breaking down the polymer crystals. Of course, this is only true for deformations at temperatures above T_g, since only then is high enough the energy state of the molecule, which allows this deformation to be followed without structural damage and structural modification.

The required internal energy state is achieved by the surplus of energy input during the heat transfer. Of course, the rate of cooling also greatly influences the degree of crystallization because high speed cooling prevents crystallization, so the lower the cooling speed, the higher the ratio of the crystalline fraction. Thus, by heating the material, orientation can be applied to the material, which favors the formation of the crystalline structure during crystallization due to the cooling.

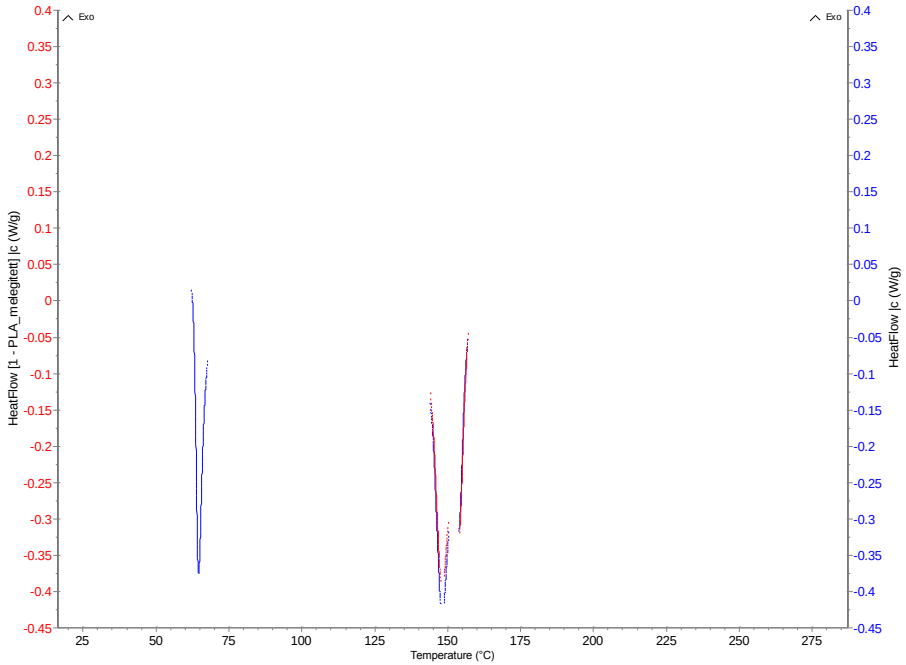

FIG. 4: DSC CURVES OF PDLLA FOIL (SECTION I. FIRST HEATING RUN; SECTION II SECOND HEATING RUN)

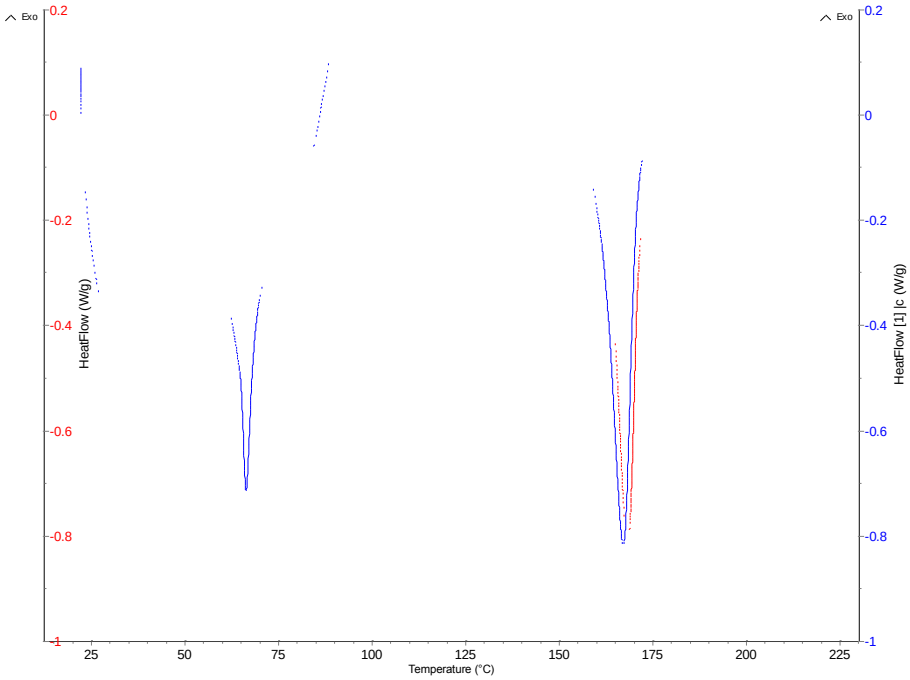

FIG. 5: DSC CURVES OF PLLA FOIL (SECTION I. FIRST HEATING RUN; SECTION II SECOND HEATING RUN).

The structural properties of PDLLA and PLLA were also investigated by TSD method. The measurements performed by SETARAM-TSC II. The polar groups of the diluted material were orientated by electrical field and then frozen in. Subsequently, with the slow rise of the temperature, we investigated the extent of the released current, which referred to the conformational movements that occurred, thus referring to the characteristics of the material structure.

The TSD test curve of PDLLA shows the relaxation process of the frozen polarization orientation. The range of temperature was about -100 to -50 ° C, the energy supplied by increased the temperature is sufficient to trigger the conformational rebounds. The mobile segments were already able to retard. These segments were usually located at the end of the chain, and may be more mobile side groups. The experienced phenomena could be split into three sub-processes, with segments of the same length and side groups for each sub process. The activation energy of which is almost the same.

If the temperature was raised more the Brownian-motion increased and appearances the greatest proportion of the glass transition. As at this stage enough energy is available for the polar groups in the main chain to recover.

TABLE 2
THE RESULTS OF PDLLA TSD MEASUREMENTS

Number of Peak	ϑ_{max} (°C)	I_{max} (pA)	A_e (kJ/mol)	Relax strength
1	-96.8	4.8	25	0.052
2	-73.6	5.5	25	0.079
3	-51	2.5	63	0.019
4	54	154	180	0.91
5	83.6	404	140	3.6
6	94.3	173	192	1.20

TABLE 3
THE RESULTS OF TSD ANALYSIS OF PLLA

Number of Peak	ϑ_{max} (°C)	I_{max} (pA)	A_e (kJ/mol)	Relax strength
1	-99	2.5	25	0.026
2	-73.6	4.2	30	0.052
3	-52	7.6	56	0.064
4	59.8	150	85	1.88
5	84.4	675	118	7.12
6	94.3	177	192	1.23

PLLA specimen TSD was also tested at low temperatures. The initial phase of the measurement - just in the case of PDLLA- was characterized by conformational rebounds. However, here we have also encountered an irregular process, which requires further measurements and tests to be identified.

Further temperature rising, also experienced a higher rearrangement near the T_g. The study was completed above the T_g, as no further relaxation process was expected.

During the examination, the generated orientation polarized part of molecular chains with an electronic field. This orientation has been fixed with cooling of the specimen. In the following step, slowly heated up the sample and measured the electron electricity. In this phase, the molecular disorientation was started to appear. This was correlated to the conformation movements and depends on the temperature [5].

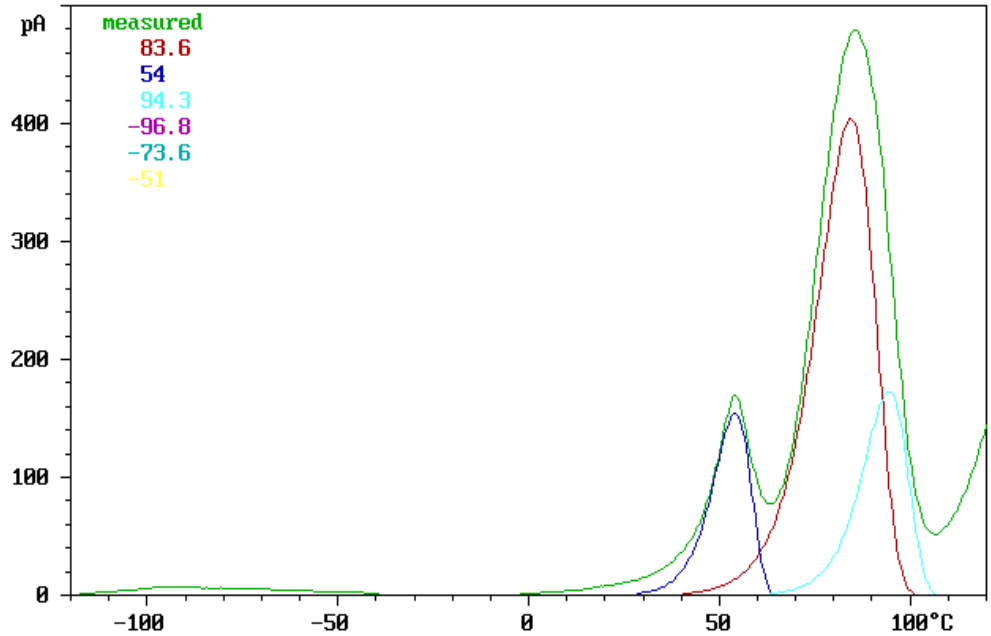

FIG. 6: TSD CURVES OF PDLLA FOIL (5K/MIN↓; 5K/MIN ↑)

In case of both materials (PDLLA and PLLA) the heat generated the molecule conformation movements. It has been started on relative low temperatures.

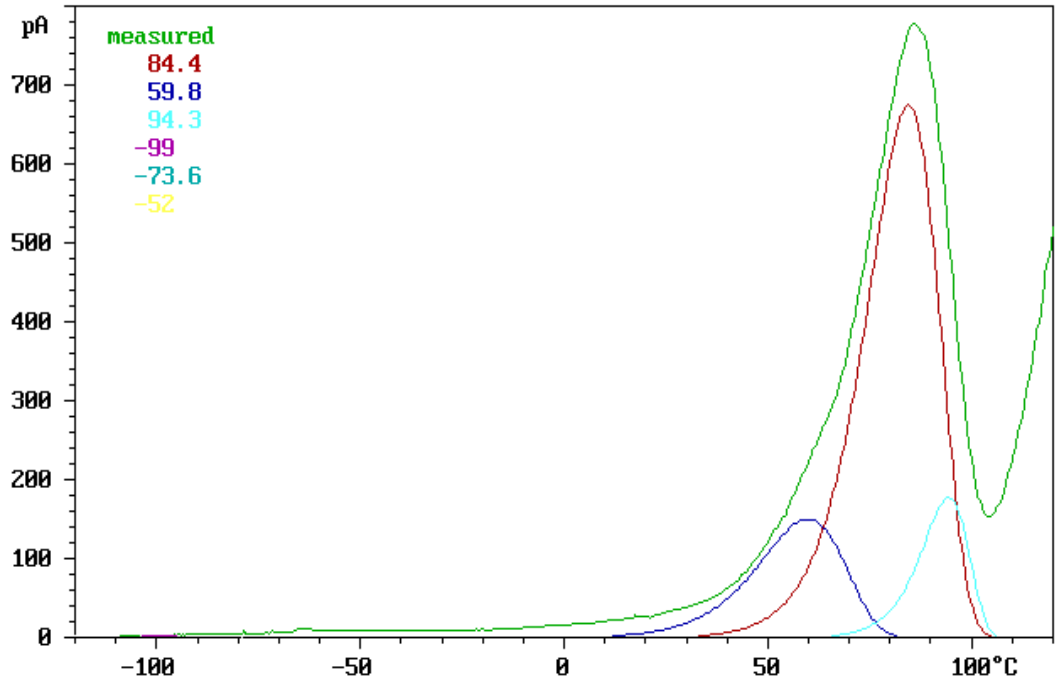

FIG. 7: TSD CURVES OF PLLA FOIL (5K/MIN↓; 5K/MIN ↑)

The temperature further changing causes the conformation movements. The rising heat was generated this movement. It means that the glass transition range was near the measurement result that the largest strength of the electricity's was determined. In this phase it was a quite available energy for polar parts of main chains to disorientate [5].

III. RESULTS

Mechanical- and structural's properties of the PET and PLA foils can be determined by mechanical-, TSD- and DSC analysis. The result of the TSD and DSC analysis is that the PLA (poly-lactic-acid) has special material structure, that ensuring better mechanical properties to forming it in higher load range compared to the PET properties. From the DSC and TSD analysis the PLLA and PLA have stabile materials structures, than the PDLLA. During the measurements of PDLLA contains L and D isomers, which is cause irregularity of molecular chains. This irregularity can be affected in the final structure. In case of PLLA the crystallization process is easier to control. As a result to the physical cross-linking between the molecular chains was more stable in the structure of final material. Finally, from the results can be confirmed that the PLLA can be used for as a packaging products in the sweet industrials, because this materials is compliance to the complex requirements.

ACKNOWLEDGEMENTS

This work has been carried out as part of the TÁMOP-4.2.1.B-10/2/KONV-2010-0001 project within the framework of the New Hungarian Development Plan. The realization of this project is supported by the European Union, co-financed by the European Social Fund.

REFERENCES

[1] Buzási Lajosné : A műanyag csomagolószer gyártás helyzete Magyarországon, Polimerek, 2. évf, 9 szám, 2016.

[2] Justine Muller, Chelo González-Martínez and Amparo Chiral: Combination of Poly(lactic) Acid and Starch for Biodegradable Food Packaging, Materials 2017, 10, 952

[3] Lin Xiao, Bo Wang, Guang Yang, Mario Gauthier: Poly(Lactic Acid)-Based Biomaterials: Synthesis, Modification and Applications, Biomedical Science, Engineering and Technology

[4] Gottfried W. Ehrenstein, Gabriela Riedel, Pia Trawiel: Thermal Analysis Of Plastics – Carl Hansen Verlag, Munich 2004. pp 236-275.

[5] K. Marossy, Depolarizációs spektroszkópia alkalmazása poláris polimerek vizsgálatára, Budapesti Műszaki Egyetem, Budapest, 1997.

[6] Dr. Czél György – Kollár Mariann: Anyagvizsgálati Praktikum – SUNPLANT 2008.

[7] Bodnár Ildikó: Potenciálisan biodegradábilis, politejsav bázisú polimerek szintézise és vizsgálata - Doktori (Ph. D.) értekezés – Debreceni Egyetem, Alkalmazott Kémiai Tanszék. Debrecen, 2002..

[8] Pukánszky Béla: Műanyagok – Budapesti Műszaki Egyetem Vegyészmérnöki Kar – Műegyetemi Kiadó, 1995.

[9] Zsoldos Gabriella: UHMWPE - Biopolimer Felületének módosítása polimerizációs technológiákkal – PhD értekezés – Miskolci Egyetem 2012.

Role of the Cluster Analysis in Logfacies and Depositional Environments Recognition from Well Log Response for Mishrif Formation in Southeast Iraq.

Jawad K. Radhy AlBahadily[1*], Medhat E. Nasser[2]

Department of geology, college of science, Baghdad University, Baghdad, Iraq.
*Corresponding Author Email: jawadkzm@gmail.com

Abstract*—The recognition of depositional environments from well logs is based on the principle that well log responses are related to changes in thickness, texture, grain size and lithology along the well path. The variations in sedimentary rock response are due to reservoir heterogeneity. A similar set of log responses that characterizes a specific rock type and allows it to be distinguished from others, have defined an electrofacies.Cluster analysis includes a broad suite of techniques designed to find groups of similar items within a data set. Partitioning methods divide the data set into a number of groups predesignated by the user. Hierarchical cluster methods produce a hierarchy of clusters from small clusters of very similar items to large clusters that include more dissimilar items. Hierarchical methods usually produce a graphical output known as a dendrogram or tree that shows this hierarchical clustering structure.The method has tested on a 398.5 m thick interval of Carbonate deposits in a vertical well from Amara field, located in southeast Iraq. Modal data have collected from both core and cutting samples. Cluster analysis and electrofacies classification have performed using advance interpretation in Interactive Petrophysics software version 3.6.Carbonate microfacies and marine depositional environments studied for Mishrif Formation depended on the available thin sections though they were not enough to cover all the depositional environments of Mishrif Formation. Therefore, previous studies and well logs were also depended in this study.Correlation of determined logfacies with those defined from cores and cuttings is fundamental to check the reliability of used methods and to define a meaningful cut off level for wells from which no cores or cuttings are available.*

***Keywords*—Cluster analysis, Mishrif Formation, Logfacies, Well Logs response,**

I. INTRODUCTION

The identification of depositional environments from well logs is based on the principle that well log responses are related to changes in thickness, texture, grain size and lithology along the well path. The variations in sedimentary rock response are due to reservoir heterogeneity. The description of a rock in terms of its type, origin, and depositional environment is called a Lithofacies description. This can be done by direct observation of the rocks or inferred from analysis and interpretation of well log data. Determining lithofacies from well logs requires calibration to known rocks (cores, samples, or outcrops). Understanding the rock facies is the only way to reconstruct the paleogeography of a lithologic succession, rock sequence, which in turn provides clues as to a potential reservoir quality and lateral extent(Crain, d. g.).

The purpose of well log cluster analysis is to look for similarities/dissimilarities between data points in the multivariate space of logs, in order to group them into classes also called electrofacies(Euzen, T., Delamaide, E., Feuchtwanger, T., & Kingsmith, 2010).

An electrofacies is defined by a similar set of log responses that characterizes a specific rock type and allows it to be distinguished from others. Electrofacies are obviously influenced by geology and often can be assigned to one or another lithofacies, although the correspondence is not universal(Doveton, J. H., & Prensky, 1992).

Electrofacies are primarily observational in nature, and the classification procedure is based on three steps: principal component analysis, cluster analysis, and discriminant analysis. Principal component analysis is used to summarize the data and to reduce the dimensionality of the data without any significant loss of information. The method displays the data as a function of new variables, called principal components, that are simple linear combination of the well logs. The aim of cluster analysis is to classify the well-log data into groups that are internally homogeneous and externally isolated on the basis of a measure of similarity or dissimilarity between the groups. The clusters define electrofacies on the basis of the unique characteristics of well-log measurements reflecting minerals and lithofacies within the loggedinterval.Once the electrofacies are identified, we can use discrimi- nant analysis, a multivariate statistical method, to assign an individual observation vector to one of the predefined electrofacies(Perez, Datta-Gupta, & Mishra, 2005).

II. BASIC CONCEPTS

Cluster analysis includes a broad suite of techniques designed to find groups of similar items within a data set. Partitioning methods divide the data set into a number of groups predesignated by the user. Hierarchical cluster methods produce a hierarchy of clusters from small clusters of very similar items to large clusters that include more dissimilar items. Hierarchical methods usually produce a graphical output known as a dendrogram or tree that shows this hierarchical clustering structure. Some hierarchical methods are divisive, that progressively divide the one large cluster comprising all of the data into two smaller clusters and repeat this process until all clusters have been divided. Other hierarchical methods are agglomerative and work in the opposite direction by first finding the clusters of the most similar items and progressively adding less similar items until all items have been included into a single large cluster. Cluster analysis can be run in the Q-mode in which clusters of samples are sought or in the R-mode, where clusters of variables are desired(Holland, 2006)

The clusters define electrofacies on the basis of the unique characteristics of well-log measurements reflecting minerals and lithofacies within the logged interval. Once the electrofacies are identified, we can use discriminant analysis, a multivariate statistical method, to assign an individual observation vector to one of the predefined electrofacies (Perez et al., 2005).

The Cluster Analysis module uses standard statistical routines to allow the user to cluster the data into groups to produce an electrical facies log. This log can then hopefully be used to correlate to geological facies (Senergy, 2008) .

III. METHODOLOGY

The theory of Cluster Analysis is the module works in two stages. Firstly, the data is divided up into manageable data clusters. The number of clusters should be enough to cover all the different data ranges seen on the logs.15 to 20 clusters would appear to be a reasonable number for most data sets. The second step, which is more manual, is to take these 15 to 20 clusters and group them into a manageable number of geological facies. This may involve reducing the data to 4 to 5 clusters.

(Stage-1 K-mean clustering) The first stage of Facies Clustering uses the K-mean statistical technique to cluster the data into a known entered number of clusters. For this to work an initial guess has to be made of the mean value of each cluster for each input log. The initial guess can affect the results and in order to get good results the initial values should cover the total range of the logs. K-mean clustering works by assigning each input data point to a cluster. The routine tries to minimize the within-cluster sums of squares of the difference between the data point and the cluster mean value. The routine works by calculating the sum of the squares difference for a data point and each cluster mean and assigning the point to the cluster with the minimum difference. Once all the data points have been assigned to the clusters the new mean values in each cluster are calculated. Using the new mean values the routines starts again re-assigning the data to the clusters. This loop continues until the mean values do not change between loops. These then become the results.

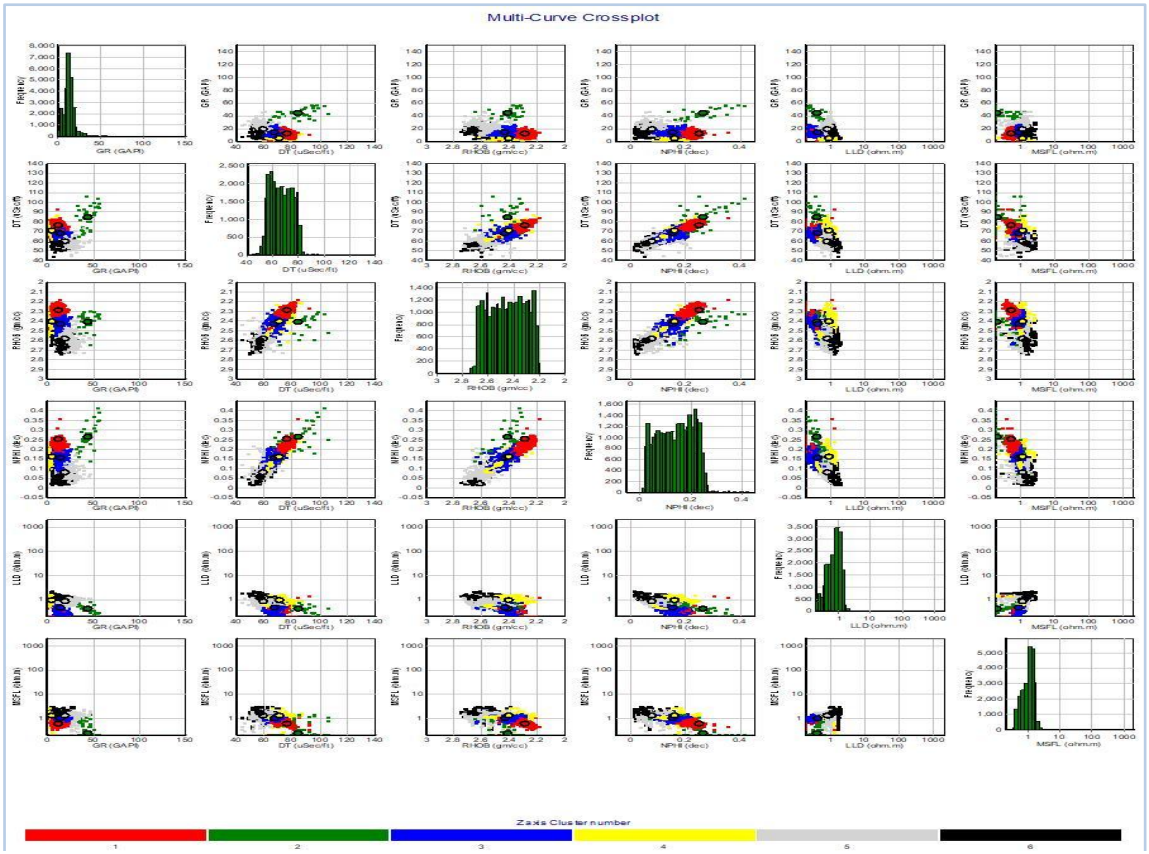

FIGURE (1): CROSSPLOTS AND HISTOGRAMS BETWEEN (RHOB, NPHI, DT, GR, LLD AND MSFL)AS GENERATED BY K-MEANS CLUSTER ANALYSIS FOR GROUPS OF MISHRIF FORMATION

(Stage-2 Cluster Consolidation) Cluster consolidation can be done completely manually by using the crossplot and log plot output to group data, or a hierarchical cluster technique can be used to group the data. Hierarchical clustering works by computing the distances between all clusters and then merging the two clusters closest together. The new cluster distance to all other clusters is then recomputed and the two closest clusters merged again. This process continues until you have only one cluster. The results can be plotted as a dendrogram, which IP displays. The dendrogram shows how the clusters were merged and the order they were merged (Senergy, 2010).

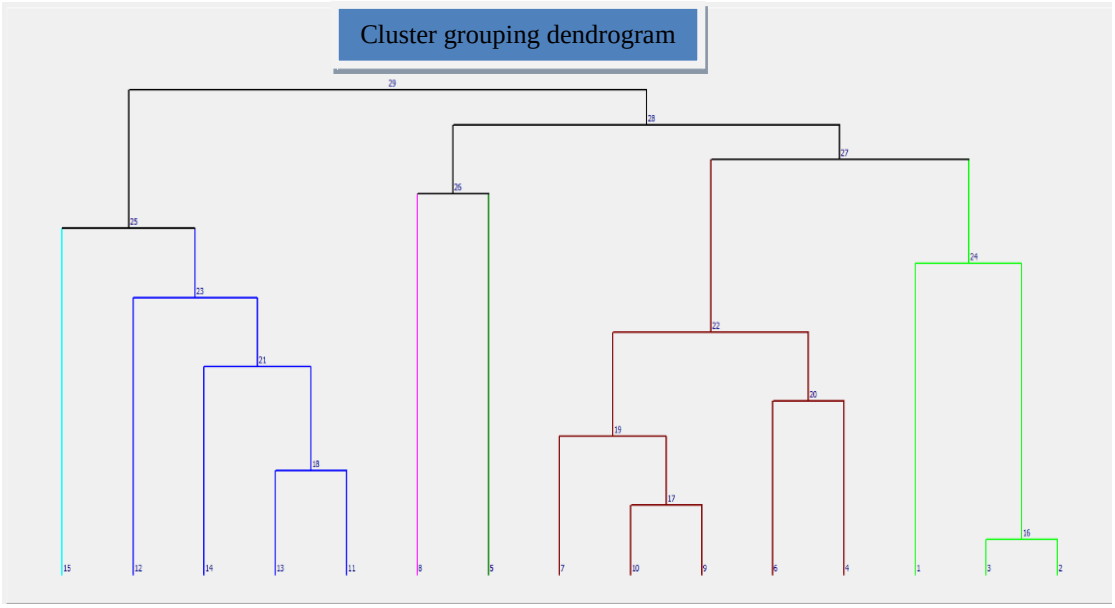

FIGURE (2): CLUSTER GROUPING DENDROGRAM OF MISHRIF FORMATION

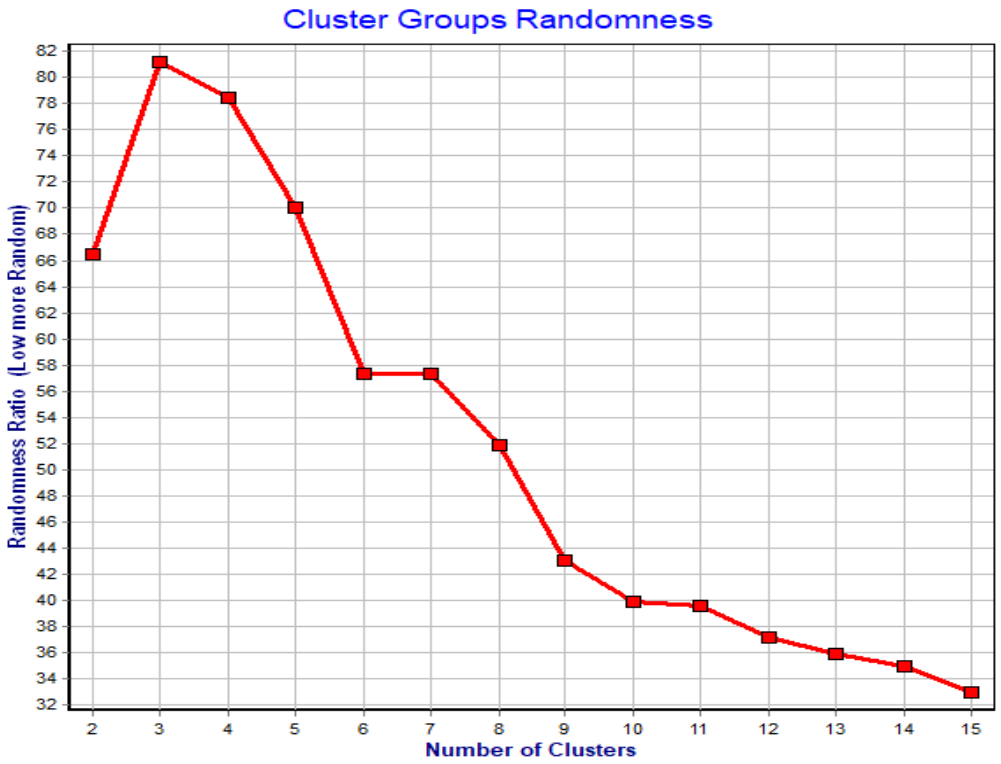

FIGURE (3): CLUSTER GROUPS RANDOMNESS OF MISHRIF FORMATION

TABLE 1
THE PROPERTIES FOR GROUPS OF CLUSTERS AND ENVIRONMENT

Zones	Clusters of group	Environment
MISHRIF	6	Lagoon
MA	4	Rudist Biostrome+ Shoal
BAR-2	3	Lagoon
MB11	2.3	Rudist Biostrome+ Shoal
BAR-3	3.4	Lagoon
MB12	3.2	Rudist Biostrome
BAR-4	4.2.3	Lagoon
MB13	2.3	Back Shoal
BAR-5	6	Basin
MB21	1.2	Slope
BAR-6	6.5.3	Basin
MC1	2.1.3	Slope
BAR-7	3.2	Basin
MC2	3.2.	Slope

IV. RESULTS AND DISCUSSIONS

The method has tested on a 398.5 m thick interval of Carbonate deposits in a vertical well from Amara field, located in southeast Iraq. Modal data have collected from both core and cutting samples. Cluster analysis and electrofacies classification have performed using advance interpretation in Interactive Petrophysics software version 3.6.

Recognition of Logfacies is a common practice in drilled wells where suitable well logs and core samples are available. Cluster analysis techniques such as hierarchical and k-means cluster analysis can be used for classifying well log data into discrete classes.

However , studying this part was made through two trends. The first trend includes the petrography and microfacies analysis of Mishrif Formation have been studied on the basis more than (120) thin sections of core samples and the previous microfacies studies for Mishrif Formation. The second trend includes the Mishrif depositional environments in studied wells depending on the available well logs utilizing cluster analysis technique.

4.1 Carbonate Microfacies and Depositional Environments

Carbonate microfacies and marine depositional environments studied for Mishrif Formation depended on the available thin sections though they were not enough to cover all the depositional environments of Mishrif Formation. Therefore, previous studies and well logs were also depended in this study.

4.2 Mishrif Facies Associations

The Mishrif Formation carbonates were classified following Dunham's (1962) classification (modified by Embry and Klovan, 1971) into mud- or grain-supported textural types. Each type consists of three principal microfacies,(Aqrawi, Thehni, Sherwani, & Kareem, 1998) as follows:

4.2.1 Mud-supported microfacies

4.2.1.1 Pelagic mudstone/wackestone

This microfacies occurs at various levels in Mishrif Formation , but was existing in the lower parts. Micrite is the main component, but planktonic foraminifera also occur . in various proportions usually less than 5O%. This microfacies dominates the underlying Rumaila Formation (Aqrawi, 1983: Aqrawi and Khaiwka, 1986 and 1989). Pelagic lime mudstone/wackestones are usually interpreted as outer- shelf or basinal deposits (Wilson, 1975).

4.2.1.2 Bioclastic wackestone

Bioclastic wackestones comprise one of the most common microfacies in the Mishrif Formation carbonates. Bioclasts (such as Praealveolinids, algae and echinoderms) comprise between 10 and 40% of the lithology, and limited pelagic foraminifera also occur. The microfacies is characteristic of shallow, open-marine environments (Flugel, 1982).

4.2.1.3 Wackestone/packstone

Wackestones/packstones are quite common in Mshrif formation. Benthic foraminifera (such as Miliolids and Textularia), sponge spicules, algae, small mollusc fragments and echinoderms occur in this microfacies in proportions up to about 50%. The microfacies is typical of lagoons (Flugel, 1982) or restricted subtidal zones with warm shallow waters and moderate circulation (Tucker, 1985).

4.2.2 Grain-supported microfacies

4.2.2.1 Peloidal packstone

This microfacies is principally composed of peloids of various sizes, many of which have an uncertain internal structure.In addition, benthic foraminifera, rudist fragments and ostracods also occur. The microfacies is common in the upper parts of the Mishrif Formation, and is interpreted to indicate shoals and subtidal zones .

4.2.2.2 Rudistid packstone/grainstone

This microfacies is characterised by a high content of rudist fragments, which are associated with other bioclasts such as algal debris, benthic foraminifera and peloids (in smaller proportions). It is one of the two principal reservoir facies of the Mishrif Formation. Rudist grainstones are interpreted to be a reef-bank or shoal deposit, and rudist packstones to be a back-reef deposit.

4.2.2.3 Rudstone

Rudstones are composed of rudist fragments, most of which are larger than sand-grade, in addition to coral fragments of a similar size. This microfacies is interpreted to be a fore-reef slope deposit (Wilson, 1975) . The rudstones and rudistid packstone/grainstones are generally over- and underlain by subtidal and outer-shelf facies, respectively, in the boreholes studied. These two microfacies are characterised by high primary and secondary porosities and permeabilities; together, they form the most important reservoir units in the Mishrif Formation throughout the Mesopotamian Basin (Aqrawi et al., 1998).

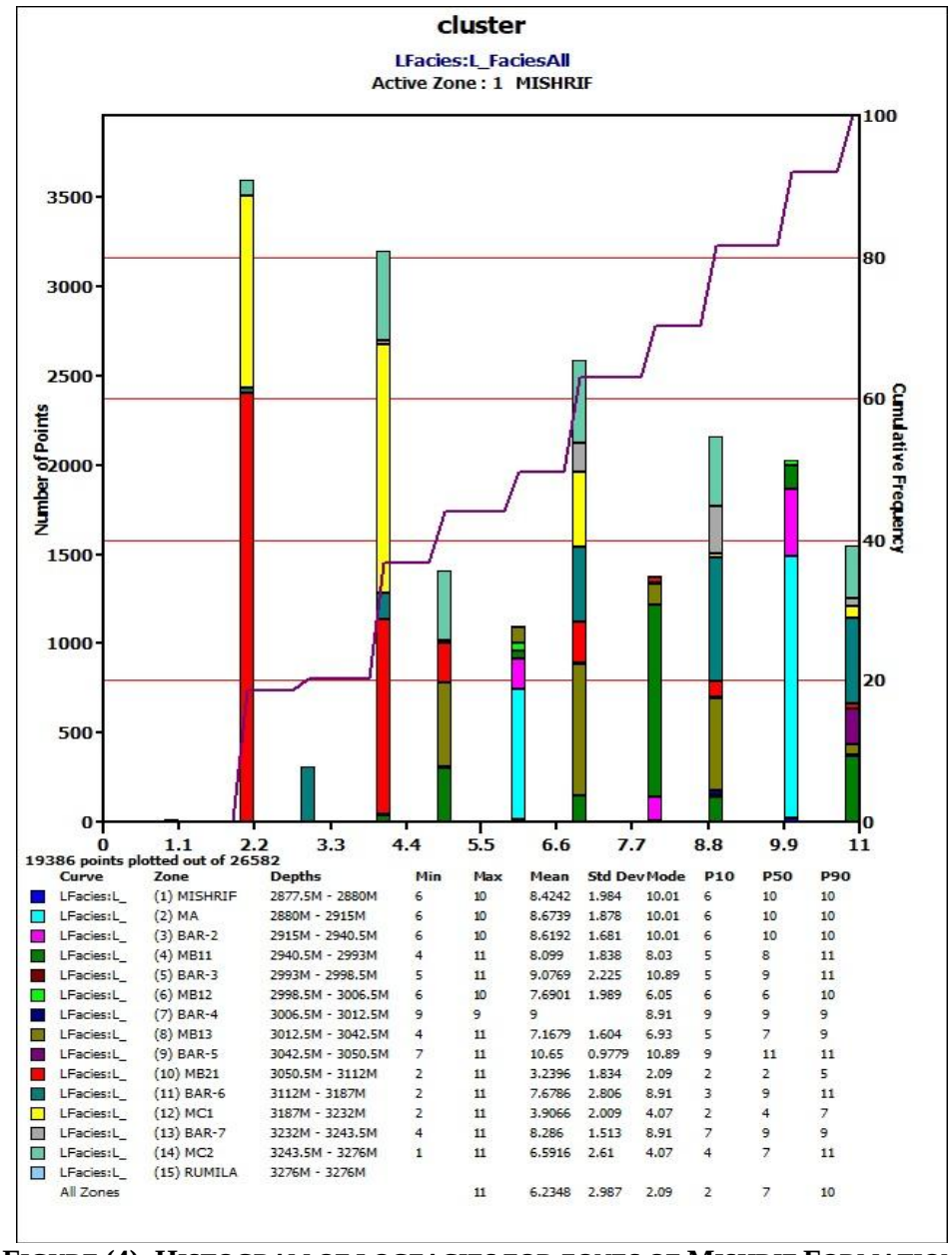

Curve	Zone	Depths	Min	Max	Mean	Std Dev	Mode	P10	P50	P90
LFacies:L_	(1) MISHRIF	2877.5M - 2880M	6	10	8.4242	1.984	10.01	6	10	10
LFacies:L_	(2) MA	2880M - 2915M	6	10	8.6739	1.878	10.01	6	10	10
LFacies:L_	(3) BAR-2	2915M - 2940.5M	6	10	8.6192	1.681	10.01	6	10	10
LFacies:L_	(4) MB11	2940.5M - 2993M	4	11	8.099	1.838	8.03	5	8	11
LFacies:L_	(5) BAR-3	2993M - 2998.5M	5	11	9.0769	2.225	10.89	5	9	11
LFacies:L_	(6) MB12	2998.5M - 3006.5M	6	10	7.6901	1.989	6.05	6	6	10
LFacies:L_	(7) BAR-4	3006.5M - 3012.5M	9	9	9		8.91	9	9	9
LFacies:L_	(8) MB13	3012.5M - 3042.5M	4	11	7.1679	1.604	6.93	5	7	9
LFacies:L_	(9) BAR-5	3042.5M - 3050.5M	7	11	10.65	0.9779	10.89	9	11	11
LFacies:L_	(10) MB21	3050.5M - 3112M	2	11	3.2396	1.834	2.09	2	2	5
LFacies:L_	(11) BAR-6	3112M - 3187M	2	11	7.6786	2.806	8.91	3	9	11
LFacies:L_	(12) MC1	3187M - 3232M	2	11	3.9066	2.009	4.07	2	4	7
LFacies:L_	(13) BAR-7	3232M - 3243.5M	4	11	8.286	1.513	8.91	7	9	9
LFacies:L_	(14) MC2	3243.5M - 3276M	1	11	6.5916	2.61	4.07	4	7	11
LFacies:L_	(15) RUMILA	3276M - 3276M								
All Zones				11	6.2348	2.987	2.09	2	7	10

FIGURE (4): HISTOGRAM OF LOGFACIES FOR ZONES OF MISHRIF FORMATION

Mishrif platform carbonates throughout the southern Iraq and especially in southeast Iraq can be divided into the following facies associations (Figure 4):

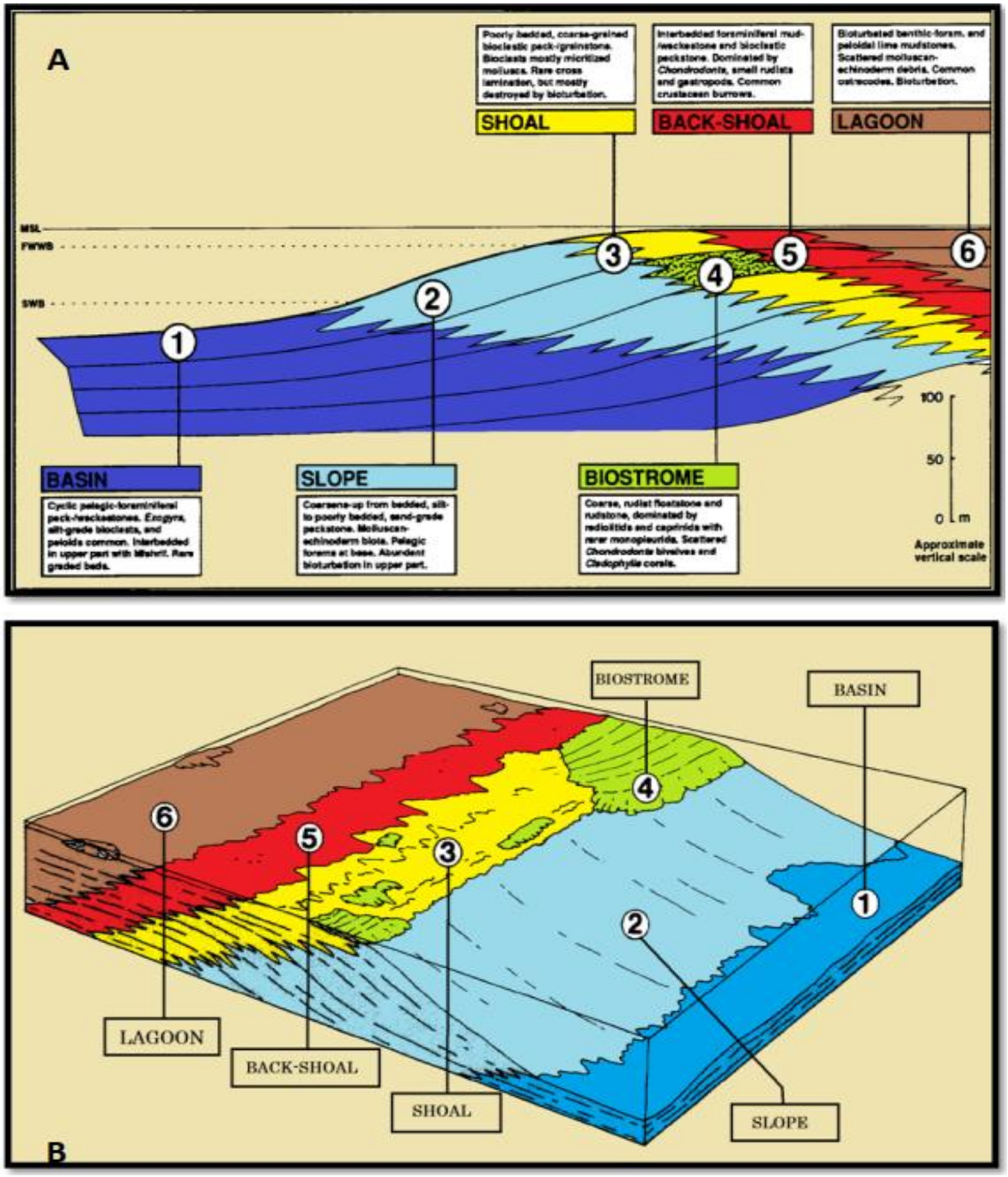

FIGURE (5): A-SCHEMATIC CROSS SECTION OF MISHRIF PLATFORM SHOWING THE ENVIRONMENTS OF DEPOSITION OF MICROFACIES ASSOCIATION. B-BLOCK DIAGRAM SHOWING DEPOSITIONAL ENVIRONMENTS OF MISHRIF FORMATION AND THE DISTRIBUTION OF MICROFACIES ASSOCIATIONS (CIRCLED NUMBERS). (FIGURES A & B ARE MODIFIED AFTER(BURCHETTE, 1993).

4.3 Mishrif Depositional Environments

4.3.1 Basin Environment

Basinal environment is simply the end of the marine environmental spectrum that began at the strandline and ended at the deepest part of that particular sedimentary basin (Figure 4). There is not even a rigid definition of basinal environment or

basinal facies. In fact, the greatest depth that exists in one basin may be the same measured depth as the shallow subtidal regime in another basin (Ahr, 2008).

4.3.2 Slope Environment

Slopes are commonly sites for upwelling, initiation of density or turbidity currents, and initiation of slumps, rock falls, and debris flows triggered by slope failures (Figure 4). Environmental processes on slopes are dominated by gravitational forces and pounding from waves. Upper slope zones in relatively shallow water may be subject to wind or storm waves, oceanic currents, and tides. Middle slope and base of slope zones are typically below fair - weather wave base, below the influence of surface currents, and relatively less influenced by tidal currents than the upper slope zone. Deeper parts of slope zones are sites where rocks and sediments swept off the slope by shallow - water processes come to rest (Ahr, 2008).

The succession, coarsening upward from basinal limestone to shallow marine packstone, reflects shallowing of the depositional environment in response to progradation of carbonate slope (Burchette, 1993).

4.3.3 Shoal Environment

Shoal forms a barrier that absorbs most of the wave energy from the open ocean (Nichols, 2009). This is the most widespread coarse-grained facies association of Mishrif Formation. The shoal association is composed of off-white, poorly sorted bioclastic packstone, grainstone, and rudstone. Bioclasts are predominantly molluscan, mostly rudistid. It represents the deposits of low energy shoals and banks along the platform margin (Burchette, 1993).

4.3.4 Rudist Biostrome Environment

This facies association represents the most important reservoir rock in Mishrif Formation. The diverse fauna, distribution, and context of this facies at the top of a coarsening upward succession all indicate an origin as biostromes within the prograding margin (Burchette, 1993).

4.3.5 Back Shoal Environment

Thin to medium-bedded, fine to very coarse-grained bioclastic packstone, wackestone, and grainstone characterize this association. The sediments are more varied, indurated, and stylolitized than other coarse facies. These deposits represent a zone of sediment mixing between shoal and interior lagoon. They overlie the coarsening upward succession and are interbedded in several-meter-thick intervals with lagoonal sediments (Burchette, 1993).

4.3.6 Lagoon Environment

Shallow elongate body of water between the mainland and a barrier island where circulation is commonly restricted and access to marine waters is only through inlets (Hughes, 1999). The lagoon association is characterized by indistinctly bedded benthonic foraminiferal and peloidal lime mudstone and wackestone. Molluscan (including rudist) debris, echinoderm, and ostracodes are locally important (Burchette, 1993).

The figure (1) shows Crossplots and histograms between (RHOB,NPHI,DT,GR,LLD and MSFL)as generated by k-means cluster analysis for groups of Mishrif Formation. The properties of these groups of logfacies have presented in Table 1.The figure(2) of dendrogram shows the Mishrif Formation has divided into 15 clusters and then created six groups of Logfacies, based on input data (RHOB,NPHI,DT,GR,LLD and MSFL) that utilized to build clusters. The results of "Cluster Means" have presented in Table (2) that shows the mean values plus other statistics of used data for each cluster (15 clusters). After classification of used data into 15 clusters, the groups of logfacies have created from these clusters. The Mishrif Formation has divided into six groups. Each group of logfacies has characterized to determine reservoir properties and each group may be containing one cluster or more than one cluster. Depending cluster groups have recognition environments own Mishrif formation that shows in figure (6).

TABLE 2

THE RESULTS OF "CLUSTER MEANS" PLUS OTHER STATISTICS OF USED DATA FOR EACH CLUSTER

K-Mean Clustering Results														
Cluster	#	Cluster	RHOB		NPHI		DT		GR		LLD		MSFL	
#	Points	Spread	Mean	Std. Dev.	Mean	Std. Dev.	Mean	Std. Dev.	Mean	Std. Dev.	Mean	Std. Dev.	Mean	Std. Dev.
0	863	0.5285	0.35413	0.00535	-0.64666	0.02324	1.8958	0.01248	0.79103	0.08191	-0.06746	0.07126	0.50984	0.08867
1	2841	0.7332	0.35496	0.00849	-0.61898	0.04001	1.8975	0.02257	1.193	0.1611	-0.01268	0.1367	0.48738	0.1577
2	3006	0.5053	0.36542	0.00508	-0.69029	0.03384	1.8691	0.01151	1.1211	0.0746	0.09248	0.08215	0.67196	0.07628
3	1392	0.8542	0.37293	0.00863	-0.71496	0.05205	1.861	0.02549	0.9327	0.08081	0.56225	0.2242	0.94635	0.1842
4	868	0.9621	0.36789	0.01118	-0.71437	0.0496	1.8778	0.02252	0.58838	0.09861	0.89645	0.202	1.1223	0.244
5	2540	0.6502	0.38125	0.0071	-0.77627	0.0497	1.8411	0.01493	1.1551	0.08541	0.33415	0.113	0.85991	0.1148
6	1369	0.8896	0.38716	0.00909	-0.8296	0.05832	1.8286	0.022	1.1391	0.1034	0.77388	0.1888	1.2675	0.1886
7	1505	1.054	0.3881	0.00961	-0.84366	0.07606	1.8279	0.02742	0.68786	0.09804	1.2183	0.1988	1.5468	0.273
8	2085	0.7369	0.40306	0.00845	-0.94258	0.1017	1.7939	0.01734	1.1063	0.06373	0.56012	0.1152	1.1127	0.132
9	1121	0.9448	0.39313	0.00906	-0.88176	0.08404	1.8032	0.03249	1.3128	0.09857	0.55189	0.1346	0.97268	0.253
10	1902	0.8349	0.40623	0.00781	-1.0181	0.07272	1.7834	0.02132	1.2926	0.09426	0.82135	0.1637	1.3836	0.1577
11	1282	1.069	0.40772	0.00669	-1.1102	0.1122	1.7706	0.025	1.0659	0.1332	1.1813	0.1651	1.7578	0.279
12	2050	0.7118	0.41812	0.00546	-1.2165	0.09504	1.7649	0.0154	1.1552	0.07663	0.87929	0.1545	1.2424	0.148
13	1280	0.9076	0.42119	0.00678	-1.3004	0.1209	1.7503	0.02054	1.3899	0.09345	1.0236	0.1413	1.3301	0.2084
14	2061	0.8811	0.42384	0.00513	-1.5124	0.1085	1.7413	0.01735	1.1805	0.1283	1.2795	0.1933	1.549	0.2124

Output Curves Cluster Values		
All Cluster		User set 1
Crv Name	L_FaciesAll	L_Facies
Cluster	Value	Value
0	1	1
1	2	1
2	3	1
3	4	2
4	5	3
5	6	2
6	7	2
7	8	4
8	9	2
9	10	2
10	11	5
11	12	5
12	13	5
13	14	5
14	15	6

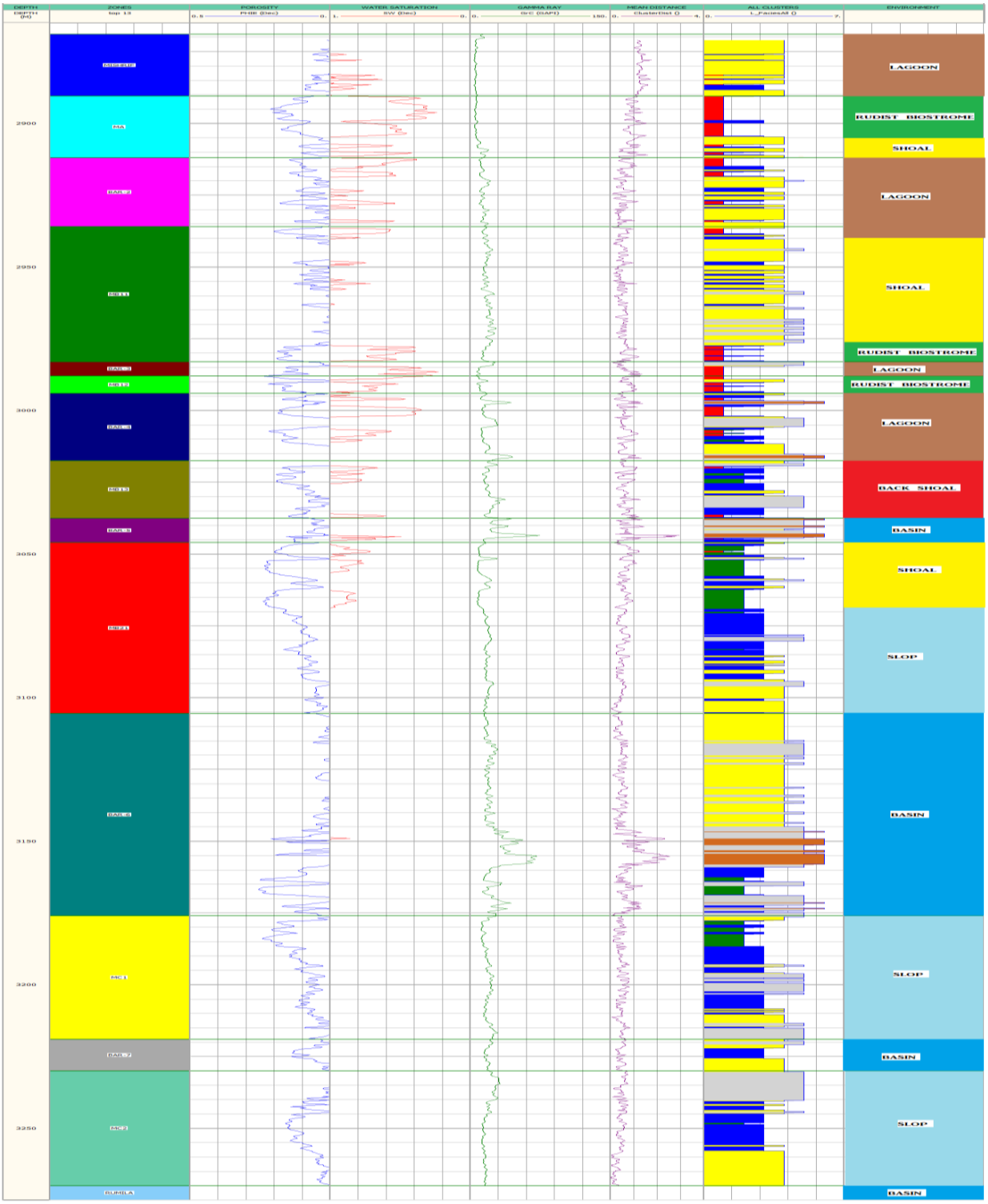

FIGURE (6): DEPOSITIONAL ENVIRONMENTS COLUMN OF MISHRIF FORMATION

V. CONCLUSION AND RECOMMENDATION

The function of multivariate cluster analysis based on response well logs determination has documented in this study by comparing with thin section examination. Based on different cutoff levels, a desirable number of logfacies for any given formation has achieved. Correlation of determined logfacies with those defined from cores and cuttings is fundamental to check the reliability of used methods and to define a meaningful cut off level for wells from which no cores or cuttings are available. The pliability of this technique in using the different combination of logs effective in the recognize logfacies and environment.

REFERENCES

[1] Ahr, W. M. (2008). *Geology of Carbonate Reservoirs: The Identification, Description, and Characterization of Hydrocarbon Reservoirs in Carbonate Rocks*. *Geology of Carbonate Reservoirs: The Identification, Description, and Characterization of Hydrocarbon Reservoirs in Carbonate Rocks*. https://doi.org/10.1002/9780470370650

[2] Aqrawi, A. A. M., Thehni, G. A., Sherwani, G. H., & Kareem, B. M. A. (1998). Mid-cretaceous rudist-bearing carbonates of the Mishrif formation: An important reservoir sequence in the Mesopotamian Basin, Iraq. *Journal of Petroleum Geology*, *21*(1), 57–82. https://doi.org/10.1111/j.1747-5457.1998.tb00646.x

[3] Burchette, T. P. (1993). Mishrif Formation (Cenomanian-Turonian), Southern Arabian Gulf: Carbonate Platform Growth Along a Cratonic Basin Margin, *2*.

[4] Crain, E. R. (Ross). (d. g.). Crain Petrophysics Handbook. Berreskuratua -(e)tik https://www.spec2000.net/21-strat1.htm

[5] Doveton, J. H., & Prensky, S. E. (1992). Geological applications of wireline logs: a synopsis of developments and trends. *The Log Analyst*, 286–303.

[6] Euzen, T., Delamaide, E., Feuchtwanger, T., & Kingsmith, K. D. (2010). Well Log Cluster Analysis: An Innovative Tool for Unconventional Exploration. *Society of Petroleum Engineers*. https://doi.org/10.2118/137822-MS

[7] Holland, S. M. (2006). Cluster analysis, (January), 7. https://doi.org/http://dx.doi.org/10.4135/9781412983648

[8] Hughes, B. (1999). *Petroleum Geology.Science (New York, N.Y.)*.

[9] Nichols, G. (2009). *Sedimentology and Stratigraphy*. Blackwell.

[10] Perez, H., Datta-Gupta, A., & Mishra, S. (2005). The Role of Electrofacies, Lithofacies, and Hydraulic Flow Units in Permeability Predictions From Well Logs: A Comparative Analysis Using Classification Trees. *SPE Reservoir Evaluation & Engineering*, *8*(2), 5–8. https://doi.org/10.2118/84301-PA

[11] Senergy. (2008). *Interactive Petrophysics Users Manual*.

[12] Senergy. (2010). *Interactive Petrophysics V3.6 Online Help Interactive*.

[13] Wilson, J. L. (1975). *Carbonate facies in geologic history*. Springer Science & Business Media.

The Impact of Different Electric Connection Types in Thermoelectric Generator Modules on Power

Abdullah Cem Ağaçayak[1], Süleyman Neşeli[2], Gökhan Yalçın[3], Hakan Terzioğlu[4]

[1,3,4]Vocational School of Technical Science, Department of Electrical, Selçuk University, TURKEY
[2]Faculty of Technology, Mechanical Engineering, Selçuk University, TURKEY

Abstract— *Recently, there is a need for increase in energy efficiency and more energy due to increase in the human population and increased production with the development of technology. This pushes scientists to search for alternative energy. In this respect, interest in renewable energy sources is increasing day by day due to the fact that it is clean energy. Thermal sources have some advantages when compared to other sources, which is why they are at the forefront of renewable energy sources. Today we make use of thermal sources in many fields ranging from greenhouse, fish breeding, thermal facilities, city heating and electricity production. When generating electricity from geothermal electricity conventional methods such as steam turbine-generator cycle are used as well as innovative methods such as semiconductor thermoelectric modules. In the light of developing technologies and researches, we know that we can produce electricity using the heat that the thermal energy gives out while it is being transmitted from one place to another. In this study, in order to shed light on the technological developments in electricity generation using thermal sources, Thermoelectric Coolers (TEC) which convert heat energy into electricity have been used. Two different TEC1-12706 and TEC1-12710 materials from the market were used. The effects of the serial and parallel connections of these materials on the generated power have been observed. Following the experimental studies, the reactions of the different connection types of the TECs to the load were examined. It was observed that the power values obtained from different TECs used varied according to the connection types, both loaded and unloaded.*

Keywords— Electricity generation, Output power and efficiency, Renewable energy sources, Thermoelectric generator, Thermoelectric modules.

I. INTRODUCTION

Energy is one of the main factors that reflect the economic and social development potential of a country because it has an important place in production. In order to meet the increasing need for electricity energy with the developing technology, efforts are being made to obtain energy from alternative energy sources all over the world. These studies aim to achieve clean, cheap and efficient energy. Fossil sources such as coal, oil, natural gas, LPG, wood, which we use widely today, both cause harm to the environment as well as are expected to be consumed in the near future. Nuclear energy, which has started to be used as an alternative to these, has a dangerous production method that requires attention in production and recycling. Due to these reasons, the use of renewable energy sources such as biogas, hydrolic, wind, sun, tidal wave energy, thermal, geothermal has become inevitable in today and in the future. Renewable energy sources differ in terms of efficiency, cheapness, damage to the environment and advanced technologies. Among these energy sources, geothermal energy is more advantageous in that it is efficient, cheap, does not cause damage to the environment and can be utilized at any time of the year, and recently attracts more attention from scientists.

Although today it does not have the potential to be used as the major source of energy production, geothermal energy stands out as a non-polluting, renewable, sustainable and environmentally friendly energy when appropriate technologies are used. Several studies have been carried out on generating electricity with TEC from various waste heat [1-5]. In this study, in order to shed light on the technological developments in electricity generation using thermal sources, Thermoelectric Coolers (TEC) which convert heat energy into electricity have been used. Two different TEC1-12706 and TEC1-12710 materials from the market were used. The effects of the serial and parallel connections of these materials on the generated power have been observed. Following the experimental studies, the reactions of the different connection types of the TECs to the load were examined. It was observed that the power values obtained from different TECs used varied according to the connection types, both loaded and unloaded.

II. THERMOELECTRIC GENERATOR (TEG)

As shown in Fig. 1, a load is attached to the +/- ends of the TEMs and if one of the two surfaces of the ceramic is subjected to high heat and the other low heat, the temperature difference (ΔT) between the two surfaces is formed and DC current is

generated by the movement of electrons along P and N type semiconductors as a result of heat flow. In the P type semiconductor part, the holes move to the cold surface of the part, while in the N type semiconductor parts, the electron flow moves to the cold surface of the part. As shown in Fig. 1, the module generates DC current and thus a thermoelectric power generator (TEG) is obtained. There are technologically advanced and commercially viable TEGs or TECs. TECs have maximum COP (Coefficient of Performance) and cooling efficiency in small temperature differences (ΔT) between two surfaces while TEGs have the maximum efficiency in great temperature differences (ΔT) [6-9]

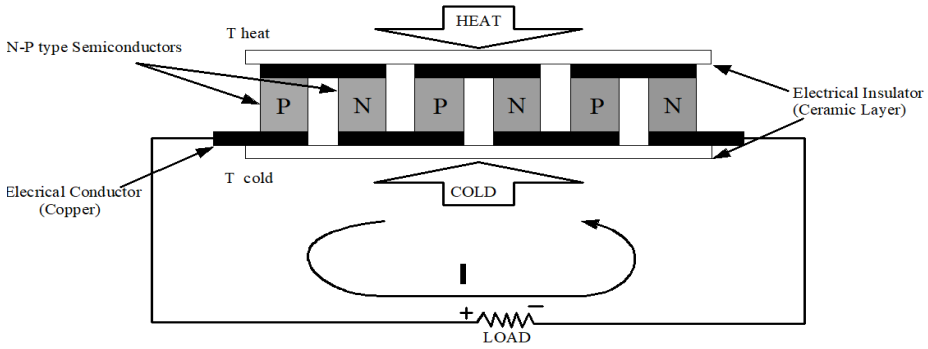

FIGURE 1. THERMOELECTRIC GENERATOR (TEG)

III. MATERIAL AND METHOD

A closed hot-cold water circulation system was designed and the TEMs were operated as TEG in the laboratory environment in this study. Electricity has been produced by making various electrical connections among 8 TECs in each. Hot-cold water was passed through plates with dimensions of 10x10x20 mm in the experimental setup designed as a closed system. In order to increase heat conduction, 4 TECs were placed on the surface of the plates using thermal paste. Thus, cold and hot water is passed through the two plates that formed the blocks designed to have 4 TECs between the two plates. Thus, the impacts of the temperature difference (ΔT) between the surfaces of the TEMs and the types of electrical connections of the TEMs on the power produced in the TEMs have been determined [10-12][10-12]. In addition, two different thermoelectric modules which were coded TEC1-12706 and TEC1-12710, were used during the experiment and their effects on different TECs were examined.

3.1 Thermoelectric Generator (TEG) Module

In the system, two different TECs with the sizes of 40 * 40 * 3.8 mm were used with the codes of TEC1-12706 ve TEC1-12710 in order to generate heat energy from temperature difference. The parameters of the TECs used are given in Table 1.

TABLE 1
TEC1-12706 AND TEC1-12710 CHARACTERISTICS

Performance characteristics	TEC1-12706			TEC1-12710	
Hot Side Temperature (℃)	25	50		25	50
Qmax (Watt)	50	57		85	96
ΔTmax (℃)	66	75		66	75
Imax (Ampere)	6,4	6,4		10,5	10,5
Vmax (Voltage)	14,4	16,4		15,2	17,4
Modul Resistance (Ohm)	1,98	2,30		1,08	1,24

3.2 Design of the plates on which TECs were placed and placement of TECs

In the design of the plates, the article "The plate design for obtaining maximum energy with thermoelectric generator" was utilized [13]. TEC1-12710 and TEC1-12706 were placed on the plates shown in Fig. 2 using thermal paste. In addition, a thermocouple temperature sensor was installed between the TECs to measure surface temperatures.

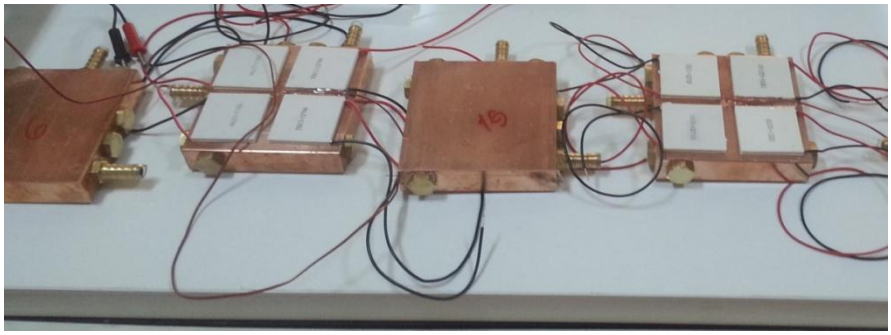

FIGURE 2. IMAGE OF TEC MODULES PLACED ON THE PLATE

IV. EXPERIMENTAL SETUP

The experimental setup used to pass the thermal water from the blocks is given in Fig. 3. In the design of this system, the article "Electrical Conduction with Thermoelectric Generator" from the previous work of the authors were utilized [14].

In the experimental setup shown in Fig. 3, two independent closed systems for hot and cold water circulation were designed. In the designed system, the temperature of hot / cold water entering and exiting the plates can be continuously measured with sensors.

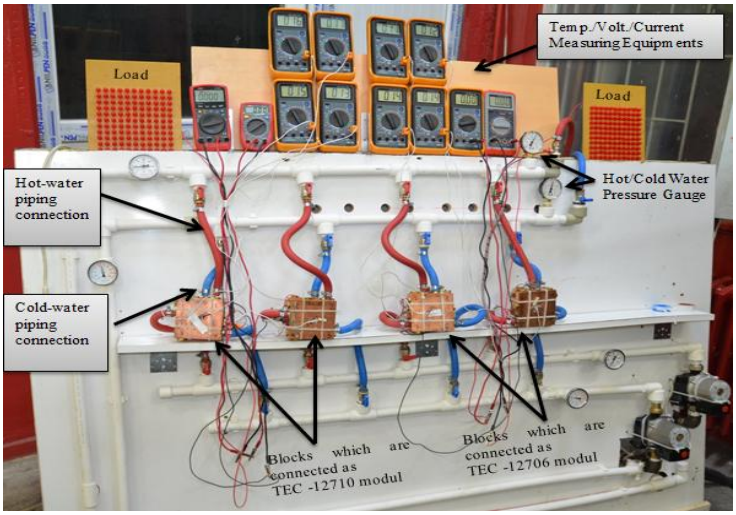

FIGURE 3. CONNECTION IMAGE OF THE DESIGNED SYSTEM

In the designed system, two heat sources were utilized by connecting two heat exchangers in series for hot water. This allowed the hot water in the system to reach the desired value more quickly. Because of the fineness of the thermoelectric modules and because the plates from which hot and cold water were conveyed were impacted, the fan heat exchanger was used to cool the cold water and the air temperature was kept at a certain temperature [15].

The temperature values on the plates, voltage generated by thermoelectric modules and current values were measured using measuring tools. T he load is also connected to the output of the system in order to measure the loaded and unloaded voltages of the system.

V. CONDUCTION THE EXPERIMENTS

Since the power produced by the thermoelectric modules (TEM) alone is often insufficient for the receivers, Thermoelectric generators (TEGs) were made in a variety of ways between the two blocks of the same block contents, as well as the connections between the same types of TECs, and their power and efficiency were noted. Thus, the most efficient connection method was tried to be determined. Fig. 4 to 11 show these connection methods and Tables 2 to 9 show the data from the connections.

In the type of connection shown in Fig. 4, although the voltage generated by TEC1-12706 at $\Delta T \sim 54\ ^\circ C$ when it is unloaded is higher than that of TEC1-12710, the current and voltage needed by the load were not provided when the load is connected to the output. The TEC1-12710 provided very low power when loaded.

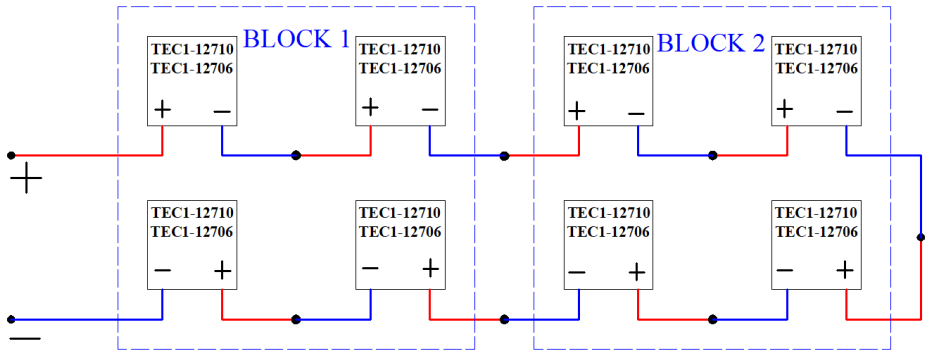

FIGURE 4. SERIAL CONNECTION IMAGE OF ALL TEC1-12706 AND TEC1-12710 THERMOELECTRIC MODULES

TABLE 2
THE DATA TABLE OF THE CONNECTION SCHEME IN FIG. 4

TEC1-12706							
1.BLOCK		**2. BLOCK**		**No-Load State**	**Loaded State**		
Heat	Cold	Heat	Cold	Voltage (V)	Voltage (V)	Current (A)	Power (W)
70	19	73	19	15,56	?	?	?
TEC1-12710							
1.BLOCK		**2. BLOCK**		**No-Load State**	**Loaded State**		
Heat	Cold	Heat	Cold	Voltage (V)	Voltage (V)	Current (A)	Power (W)
74	19	75	19	12,03	0,13	0,5	0,065

In the type of connection shown in Fig. 5, although the voltage generated by TEC1-12706 at $\Delta T \sim 53\ ^\circ C$ when it is unloaded is higher than that of TEC1-12710, TEC1-12710 thermoelectric module produced 14.8% more power when the load is connected to the outlet.

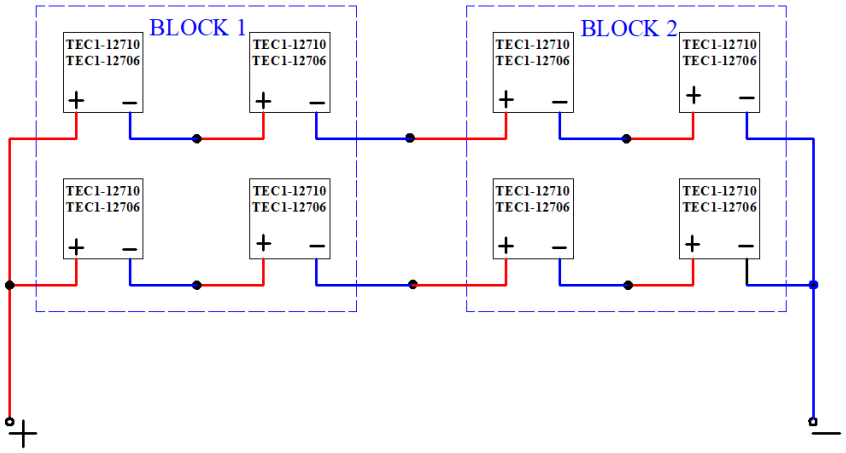

FIGURE 5. PARALLEL CONNECTION IMAGE OF 4 SERIAL SERIES OF TWO GROUPS TEC1-12706 AND TEC1-12710 THERMOELECTRIC MODULES

TABLE 3
THE DATA TABLE OF THE CONNECTION SCHEME IN FIG. 5

TEC1-12706							
1.BLOCK		**2. BLOCK**		**No-Load State**	**Loaded State**		
Heat	Cold	Heat	Cold	Voltage (V)	Voltage (V)	Current (A)	Power (W)
74	21	74	22	8,2	0,09	0,35	0,032
TEC1-12710							
1.BLOCK		**2. BLOCK**		**No-Load State**	**Loaded State**		
Heat	Cold	Heat	Cold	Voltage (V)	Voltage (V)	Current (A)	Power (W)
71	19	72	21	5,56	0,24	0,9	0,216

In the connection type of Fig. 6, TEC1-12710 at ΔT ~ 54°C produced close values to the connection type in Fig. 5. However, in this type of connection, while the unloaded TEC1-12706 produced voltage at values close to the connection type in Fig. 5, when the load is connected to its ends, it produced 20% more power.

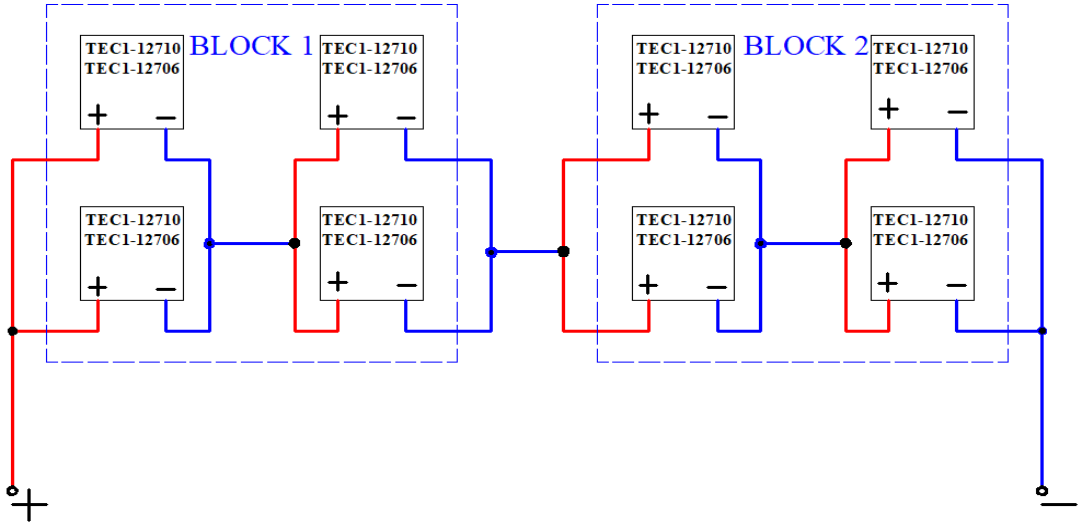

FIGURE 6. SERIAL CONNECTION IMAGE OF 2 PARALLEL SERIES OF GROUPS TEC1-12706 AND TEC1-12710 THERMOELECTRIC MODULES

TABLE 4
THE DATA TABLE OF THE CONNECTION SCHEME IN FIG. 6

TEC1-12706							
1.BLOCK		**2. BLOCK**		**No-Load State**	**Loaded State**		
Heat	Cold	Heat	Cold	Voltage (V)	Voltage (V)	Current (A)	Power (W)
73	19	71	19	8,96	0,22	0,72	0,158
TEC1-12710							
1.BLOCK		**2. BLOCK**		**No-Load State**	**Loaded State**		
Heat	Cold	Heat	Cold	Voltage (V)	Voltage (V)	Current (A)	Power (W)
71	19	71	19	5,79	0,27	0,97	0,262

In the type of connection in Fig. 7, both TEC types at ΔT ~ 57 ° C produced voltage, current and power at values close to the connection type in Fig. 6.

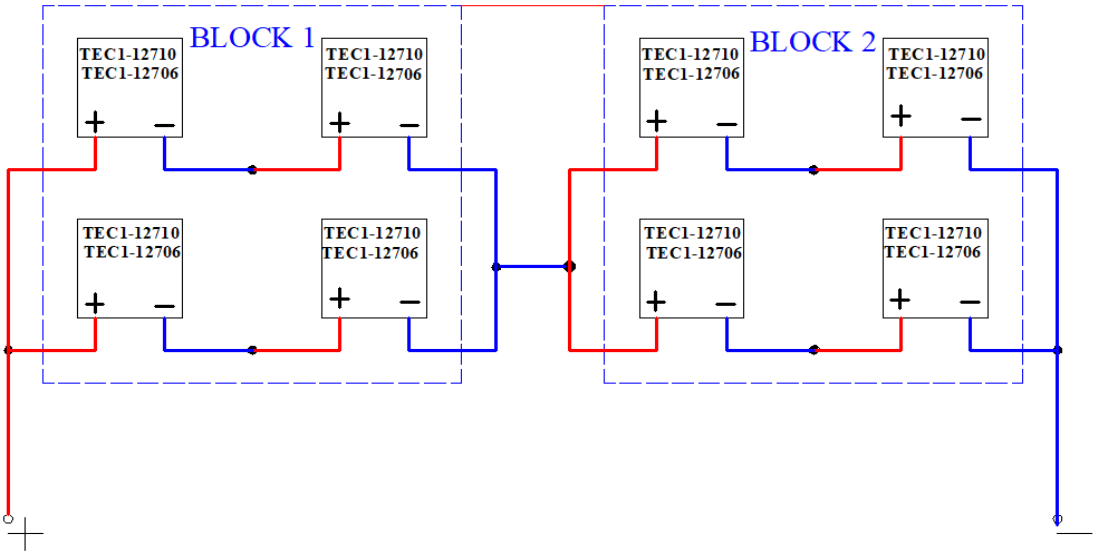

FIGURE 7. TWO SERIAL CONNECTIONS OF TEC1-12706 AND TEC1-12710 THERMOELECTRIC MODULES IN BLOCK AND THE PARALLELISM BETWEEN THEM AND THE SERIAL CONNECTION IMAGE OF THE TWO BLOCKS

TABLE 5
THE DATA TABLE OF THE CONNECTION SCHEME IN FIG. 7

TEC1-12706							
1.BLOCK		2. BLOCK		No-Load State	Loaded State		
Heat	Cold	Heat	Cold	Voltage (V)	Voltage (V)	Current (A)	Power (W)
72	15	73	16	9,24	0,2	0,78	0,156
TEC1-12710							
1.BLOCK		2. BLOCK		No-Load State	Loaded State		
Heat	Cold	Heat	Cold	Voltage (V)	Voltage (V)	Current (A)	Power (W)
71	18	73	16	6,4	0,28	1,05	0,294

In the type of connection in Fig. 8, although the voltage produced by both unloaded TEC types at ΔT ~ 52 ° C is less than the types of connections we mentioned earlier when loads are connected to their ends, they produced more power. Also, in this connection, the power produced by TEC1-12710 is 40% greater than the power produced by TEC1-12706.

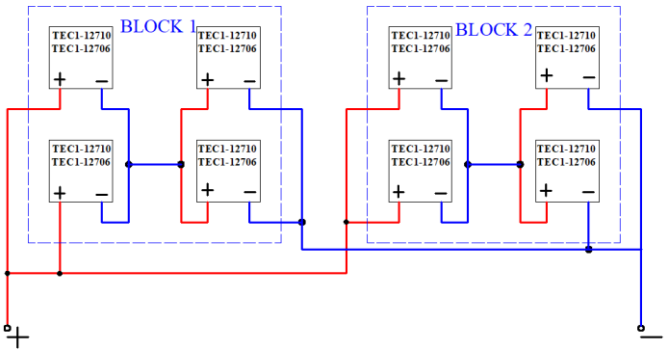

FIGURE 8. THE IMAGES OF SERIAL CONNECTION TO EACH OTHER AND PARALLEL CONNECTION TO THE OTHER BLOCKS OF PARALLEL GROUPS OF TWO IN TEC1-12706 AND TEC1-12710 THERMOELECTRIC MODULES IN THE SAME BLOCKS

TABLE 6
THE DATA TABLE OF THE CONNECTION SCHEME IN FIG. 8

TEC1-12706							
1.BLOCK		2. BLOCK		No-Load State	Loaded State		
Heat	Cold	Heat	Cold	Voltage (V)	Voltage (V)	Current (A)	Power (W)
71	19	74	19	4,11	0,29	1,08	0,313
TEC1-12710							
1.BLOCK		2. BLOCK		No-Load State	Loaded State		
Heat	Cold	Heat	Cold	Voltage (V)	Voltage (V)	Current (A)	Power (W)
70	19	71	21	2,67	0,41	1,55	0,636

In the type of connection of Fig. 9, at ΔT ~ 52 ° C, when the TECs were both loaded and unloaded, they produced values very close to the connection type in Fig. 8.

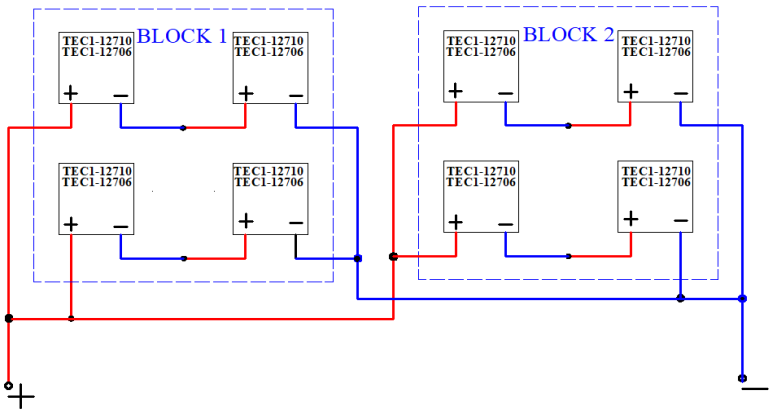

FIGURE 9. PARALLEL CONNECTION IMAGE OF 2 SERIAL SERIES OF TWO GROUPS TEC1-12706 AND TEC1-12710 THERMOELECTRIC MODULES

TABLE 7
THE DATA TABLE OF THE CONNECTION SCHEME IN FIG. 9

TEC1-12706							
1.BLOCK		2. BLOCK		No-Load State	Loaded State		
Heat	Cold	Heat	Cold	Voltage (V)	Voltage (V)	Current (A)	Power (W)
75	17	75	18	4,41	0,37	1,4	0,518
TEC1-12710							
1.BLOCK		2. BLOCK		No-Load State	Loaded State		
Heat	Cold	Heat	Cold	Voltage (V)	Voltage (V)	Current (A)	Power (W)
71	17	73	17	3,01	0,44	1,66	0,730

In the connection type of Fig. 10,at $\Delta T \sim 52$ ° C, the voltage produced by both unloaded TEC types is closer to the types of connections we mentioned earlier, while they produced more power when loads are connected to their ends. In addition, the power generated by TEC1-12710 in this connection is 51.6% more than the power generated by TEC1-12706

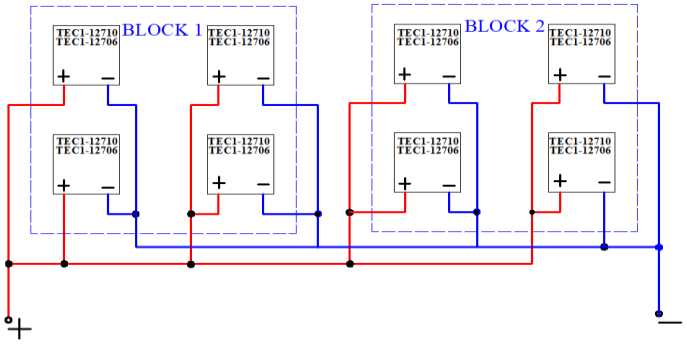

FIGURE 10. PARALLEL CONNECTION IMAGE OF ALL TEC1-12706 AND TEC1-12710 THERMOELECTRIC MODULES

TABLE 8
THE DATA TABLE OF THE CONNECTION SCHEME IN FIG. 10

TEC1-12706							
1.BLOCK		2. BLOCK		No-Load State	Loaded State		
Heat	Cold	Heat	Cold	Voltage (V)	Voltage (V)	Current (A)	Power (W)
71	19	72	19	4,29	0,36	1,34	0,482
TEC1-12710							
1.BLOCK		2. BLOCK		No-Load State	Loaded State		
Heat	Cold	Heat	Cold	Voltage (V)	Voltage (V)	Current (A)	Power (W)
78	18	80	18	3,1	0,51	1,83	0,933

In the connection type in Fig. 11, at $\Delta T \sim 55$ ° C, although both types of TEC produced voltage at the lowest value from the voltages that the connection types that we had tested up till then had produced, they produced the most power when the load was connected to their ends. In addition, the power produced by TEC1-12710 in this connection is 63% more than the power produced by TEC1-12706.

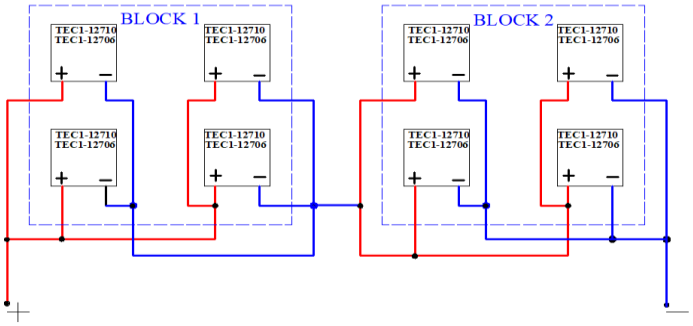

FIGURE 11. PARALLEL CONNECTION IMAGE OF TEC1-12706 AND TEC1-12710 THERMOELECTRIC MODULES IN THE SAME BLOCK AND THE SERIAL CONNECTION IMAGE OF THE THERMOELECTRIC MODULE GROUPS IN THE TWO BLOCKS

TABLE 9
THE DATA TABLE OF THE CONNECTION SCHEME IN FIG. 11

TEC1-12706							
1.BLOCK		2. BLOCK		No-Load State	Loaded State		
Heat	Cold	Heat	Cold	Voltage (V)	Voltage (V)	Current (A)	Power (W)
73	18	74	19	2,1	0,48	1,8	0,864
TEC1-12710							
1.BLOCK		2. BLOCK		No-Load State	Loaded State		
Heat	Cold	Heat	Cold	Voltage (V)	Voltage (V)	Current (A)	Power (W)
73	18	74	19	1,52	0,612	2,24	1,371

In the experiments, in the same hot and cold water circulation, 4 TECs were connected to 2 separate blocks and the voltage, current and power values they produced were compared. The connection type in Fig. 11 gave us the best values both in terms of current and voltage. Table 9 shows the data from this connection type. In this preliminary study, in the connection type in Fig. 11, TEC1-12706 thermoelectric module produces 2.1 V DC voltage at a temperature rise of $\Delta T = 55\ ^{\circ}C$ when unloaded and when it was loaded with 0,25 Ω load obtained by parallel connecting 4 resistors of 1 Ω, we could obtain 1.8 A current and 0.864 W power with 0,48 V DC voltage. Under the same conditions, TEC1-12710 thermoelectric module produced 1.52 V DC voltage when it was not loaded at $\Delta T = 55\ ^{0}C$ temperature difference while it produced 2,24 A current and 1,371 W of power with a voltage of 0,612 V DC when loaded.

VI. CONCLUSION

In the experimental setup prepared in this study, experiments were carried out with electrical connection between two types of TECs. According to these experiments, the type of electrical connection in Fig. 11 has been the type of connection that gave the best value for both TEC1-12706 and TEC1-12710 in terms of current and voltage ratio. Later, (T_H) module hot surface, (T_C) module cold surface, voltage (V), current (A) and power (W) values obtained from geothermal energy and time were measured starting from the operation of the system until the hot water reached 100 ◦ C at the third stage speed of the recirculation motor at 2.5 bar water pressure in this connection type closed system. When we look at the analysis graph of the voltage produced by TEC1-12706 and TEC12710 in Fig. 12, we can see that the values are very close to each other but TEC1-12706 produces more voltage at low temperature.

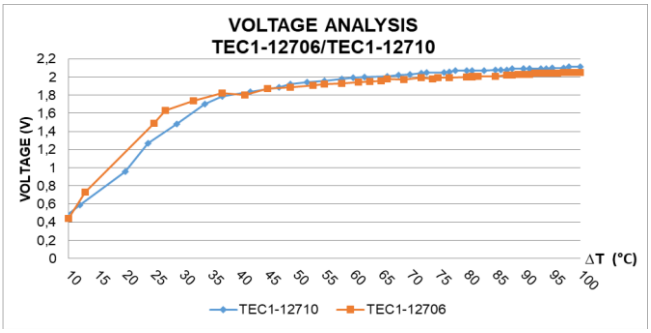

FIGURE 12. TEC1-12710 AND TEC1-12706 VOLTAGE (V) GRAPHIC

When we look at the graph of current analysis produced by TEC1-12706 and TEC12710 in Fig. 13, although TEC1-12706 provided current at lower temperature, at later temperatures, TEC1-12710 caught up and produced more current.

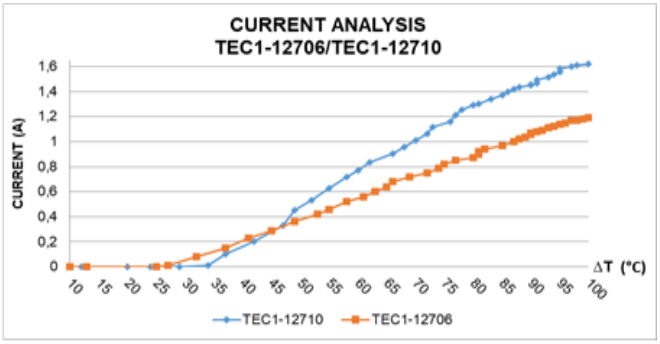

FIGURE 13. TEC1-12710 AND TEC1-12706 CURRENT (A) GRAPHIC

When we look at the graph of power analysis produced by TEC1-12706 and TEC12710 in Fig. 14, since the voltages produced by both TECs are very close to each other, the decisive element seems to be the current and although TEC1-12706 provided power for the current at lower temperature, at later temperatures, TEC1-12710 caught up and produced more power also.

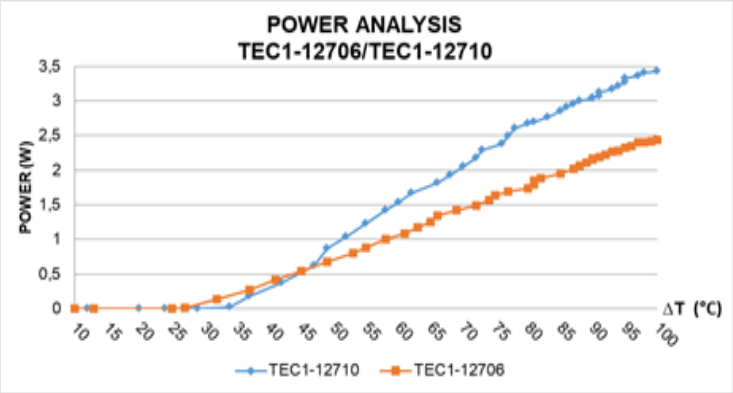

FIGURE 14. TEC1-12710 AND TEC1-12706 POWER (W) GRAPHIC

The graphs show that while TEC1-12706 thermoelectric modules provided system current and power at a temperature difference of about 27-28 °C, TEC1-12710 thermoelectric modules started to provide current and power at about 33-36 °C. However, when the surface temperature differences in both thermoelectric modules rose above 50 ^{0} C, TEC1-12710 thermoelectric module is more powerful than TEC1-12706 thermoelectric module due to the voltage-current it generates. At the end of the experiment, 71.2% difference between the power produced by the two modules emerged. In the direction of the experiment's purpose, it was determined that the TECs gave each other the highest current and voltage with the electrical connection shown in Fig. 11. Furthermore, comparisons between the two types of TEC have shown that TEC1-12706 was more efficient in places where the thermal temperature is below 50 ° C and TEC1-12710 was more efficient in places where the thermal temperature is above 50 ° C.

ACKNOWLEDGEMENTS

This study was carried out with the research project number 15401127 of Selcuk University Scientific Researches Coordination Office.

REFERENCES

[1] S. A. Atouei, A. A. Ranjbar, and A. Rezania, "Experimental investigation of two-stage thermoelectric generator system integrated with phase change materials," Applied Energy, 2017. 208: p. 332-343.

[2] D. Champier, "Thermoelectric generators: A review of applications," Energy Conversion and Management, 2017. 140: p. 167-181.

[3] H. A. Gabbar, et al., "Evaluation and optimization of thermoelectric generator network for waste heat utilization in nuclear power plants and non-nuclear energy applications," Annals of Nuclear Energy, 2017. 101: p. 454-464.

[4] F. Meng, et al., "Thermoelectric generator for industrial gas phase waste heat recovery," Energy, 2017. 135: p. 83-90.

[5] A. C. Ağaçayak, "Investigation of Factors Affecting the Electric Energy Production of Thermoelectric Generators by Using Geothermal Energy," in Electrical Education. 2017, Afyon Kocatepe University: Graduate School of Natural and Applied Sciences. p. 125.

[6] F. Suarez, et al., "Flexible thermoelectric generator using bulk legs and liquid metal interconnects for wearable electronics," Applied Energy, 2017. 202: p. 736-745.

[7] T. Wang, et al., "Performance Improvement of High-temperature Silicone Oil Based Thermoelectric Generator," Energy Procedia, 2017. 105: p. 1211-1218.

[8] E. Kanimba, et al., "A comprehensive model of a lead telluride thermoelectric generator," Energy, 2018. 142: p. 813-821.

[9] A. A. Angeline, et al., "Power generation enhancement with hybrid thermoelectric generator using biomass waste heat energy," Experimental Thermal and Fluid Science, 2017. 85: p. 1-12.

[10] R. Ahıska, H. Mamur, and M. Uliş, " Modeling and experimental study of thermoelectric module as generator," J. Fac. Eng. Arch. Gazi Univ. Cilt 26, No 4, 889-896, 2011 Vol 26, No 4, 889-896, 2011.

[11] T.Y. Kim, A. Negash, and G. Cho, "Direct contact thermoelectric generator (DCTEG): A concept for removing the contact resistance between thermoelectric modules and heat source," Energy Conversion and Management, 2017. 142: p. 20-27.

[12] A. Montecucco, J. Siviter, and A. Knox, "Combined heat and power system for stoves with thermoelectric generators," Applied Energy, 2015.

[13] G. Yalçın, M. Selek, and H. Terzioğlu. " Plate Design for Maximum Energy Acquisition with Thermoelectric Generator," in Paper presented at the UMYOS 5th INTERNATIONAL VOCATIONAL SCHOOL SYMPOSIUM. 2016. Prizen.

[14] A.C. Ağaçayak, et al., "Electricity generation by thermoelectric generator," in Paper presented at the UMYOS 6th INTERNATIONAL VOCATIONAL SCHOOL SYMPOSIUM. 2017: Saray Bosna.

[15] H. Çimen, et al., "Comparison of Two Different Peltiers Running as Thermoelectric Generator at Different Temperatures," in IRSEC17. 2017: Tangier, Morocco.

Categorizing software vulnerabilities using overlapping self-organizing map

Sima Hassanvand[1], Mohammad Ghasemzadeh[2*]

[1,2]Department of Computer Engineering, Yazd University, Yazd, Iran
*Corresponding Author's Email: m.ghasemzadeh@yazd.ac.ir

Abstract— *Software has always been vulnerable to various vulnerably issues. Increasing the number of vulnerabilities and their complexity in the software area has made it more important to categorize them. In this research work, by selecting the MoSCoW prioritization method and by combining it with the SOM self-organizing mapping algorithm, we present a new categorization for the frequent software vulnerabilities. We implemented the proposed method in MATLAB using the relevant tool boxes. The experimental results were evaluated using in-class and out-of-class distance measurements. Classification of software vulnerabilities using OSOM algorithms gives us better results than conventional clustering methods. It can be inferred that the classification of software vulnerabilities is of particular importance in improving the security of a software application. The proposed algorithm can provide an appropriate categorization by taking advantage from the existing overlapping feature.*

Keywords— Overlapping, Overlapping Self-Organizing Map, Software Vulnerability, Vulnerability Categorization.

I. INTRODUCTION

In many cases, programmers' faults during programming, which could easily be prevented, create vulnerabilities, providing an opportunity for hackers to misuse it. A proper classification for vulnerability could be sufficient to understand vulnerabilities and propose a solution to prevent them. By collected information from vulnerabilities, suitable classification is achievable, and new vulnerabilities could be easily classified into appropriate classes. Vulnerability classification is a substantial task due to weak software that could be easily manipulated. In the present study, a proper approach for vulnerabilities via MoSCoW method to select reliable database coupled with self-organizing map, is introduced, and the classification results are compared with the self-organizing map. The algorithm is generated from combination of SOM and K-means clustering, and by considering overlapping, a suitable classification is introduced. Overlapped self-organizing map is applied on different databases and is present in acceptable results compared to previous methods, and it is planned to examine the algorithm on software vulnerabilities, leading to appropriate standard classification. This paper is organized as follows: Section 2 describes the few works related to the study. Section 3 presents the applied approach, which in this section; database and extracting Eigen vectors are evaluated. Section 4 is dedicated to experiments and results, and Section 5 discusses the study conclusions.

II. RELATED WORKS

Primary researches were conducted in1976 by the United States making calculation centers to conduct studies on software vulnerability, specifically on operating systems[1].Bishop and Krsul could be introduced as pioneers on presenting vulnerability classification methods. Bishop [2], by studying vulnerabilities, explained their various types; for example, when vulnerability was introduced? What would occur after misuse? On what issues are affected by vulnerability? What are the minimum necessary components to use vulnerability and it's recognizing resources? Bishop investigated 11 failures in Unix and provided six classifications. Afterward, Krsul[3]studied the same subject and presented a vulnerability classification based on the decision tree. Decision trees are in accordance with prior assumptions. Krsul's purpose was to assign a specific classification for each relative vulnerability. Venter introduced a category range, including 13 homogeneous vulnerability portions, providing a complete scale for known vulnerabilities [4].

The classification consisted of ahead items: shapes in password, system and network information collection, backdoors, trojans and remote control, unauthorized accessibility to junctions and remote services, privileges and user accessibilities, spoofing or masquerading, misconfiguration, service rejection, buffer overflow, viruses and worms, absolute hardware, absolute software and updates, and security method bug. The mentioned items were classified based on knowledge and personal or general experiences. After Venter's research, Cisco[5], a known security corporation, in 2003 categorized

vulnerabilities in 5 different sections as design errors, protocol feeble, software vulnerabilities, misconfiguration, and bad codes.

The major vulnerability scanners have their own classification such as SAINT, which in 2004, vulnerabilities were classified in 12 divisions [6]: web, Email, FTP, shell, print, RPC, DNS, database, network, windows, password, and miscellaneous. Microsoft [7] proposed a warning model in 2002, including six vulnerability categories, namely spoofing identity, data manipulation, repudiation, information disclosure, service rejection and privilege elevation. SF-Protect [8] introduced seven groups for classification: user reports, audit policy, system logon, file system, registration, services, and shares. Missouri Research and Education Network classified vulnerabilities in 25 groups in 2014[9]. Venter, Ellof and Li [10] presented few articles for general categorization of vulnerabilities in CVE database by means of SOM. Their approach is effective to eliminate tiredness and fatigue of human classification and to decrease error due to tiredness. SOM advantage is to ease explanation and interpretation. SOM is useful as a device to visualize large amount of data in 2D dimension. In many practical programs such as classification, due to several reasons, overlapping always exists between different sections [11].

Ideally, different groups are pure distinct, nevertheless, having overlapping is unavoidable. Whenever different classes have overlapping in between, generally ´´winner-take-all´´ will be used to choose groups, but it is not effective in most cases. Classification overlapping is not a new issue and Sibson and Jardine investigated it and recommended an overlapping categorizing model in which performance was similar to present-day taxonomy [12]. Diday[13]extended K-Ultra-metric model by Jardin, and introduced a new model, but in the model, each class could have overlapping only with two other classes. PoBoc's model was introduced by Cleuziou[14]. Henceforth, Banerjee presented overlapping clustering [15]. The model is known MOC and is a generalization of EM. Cleuziou (2007), by using Banerjee's clustering model, recommended K-means overlapping model. Two major differences exist between Banerjee's model and K-means; the difference in determining one or several classes for each sample, and the difference in updating process of center classes [16].

III. THE PROPOSED METHOD

3.1 Research Database

After identification of vulnerabilities, they could be stored in a database. Generally, vulnerabilities database can be classified into two categories: general vulnerabilities database and software developer vulnerability database. General vulnerability database such as NVD, CVE, OSVDB. Software developer vulnerability database is like MFSA (Mozilla Foundation Security Advisories). National vulnerability database is a standard source developed by the United States. It provides automatic vulnerabilities management and security measurement and coincident. It also utilizes SCAP automation protocol for management and automatic categorization of known security bugs governed by the National Institute of Standards and Technology (NIST)[17]. NVD consists of CVE, vulnerability effect, standard code of vulnerability intensity, vulnerability description in a natural language, vulnerability type, and name of vulnerability software, published date, update date, and available references for vulnerabilities. Selecting a suitable database is one of the basic steps in data analysis. In some cases, selecting an inappropriate database leads to unreliable results. The employed data should be valid and reliable. There are various databases registering software vulnerability reports. Known databases are OVAL, NVD, OSVDB, and CVE. In other words, in most studies, combination and integration of different databases are not required, and researchers only need to choose a proper database according to the research aims [18]. In addition, vulnerability description on CVE and CWE is required to extract features from vulnerability explanation. The database is selected based on MoSCoW prioritization technique. The term MoSCoW itself is an acronym derived from the first letter of each of the four prioritization categories (Must have, Should have, Could have, and won't have), with the interstitial o's added to make the word pronounceable.

M – Must have:

This point describes requirements that must be met in the final solution. These requirements are non-negotiable, and the project will fail without them.

S – Should have:

A high-priority feature that is not critical to launch, but it is considered to be important and of a high value to users. Such requirements occupy the second place in the priority list.

C – Could have:

A requirement that is desirable, but not necessary. According to the method, this point will be removed first from the scope if the project's timescales are at risk.

W – Won't have:

A requirement that will not be implemented in a current release, but may be included in a future stage of development. Such requirements usually do not affect the project success. For priorities assessment with MoSCoW technique, a score should be considered for each level and score of each database is calculated by means of the following expression.

$$(\text{Must})\times 4 + (\text{Should})\times 3 + (\text{Could})\times 2 + (\text{Want})\times 1$$

3.2 Feature vectors extraction

Term Frequency–Inverse Document Frequency (TF-IDF) is a document. The TFIDF gives weight to each word based on its frequency in document. In fact, TFIDF shows how a word in a document is important. This is highly practical in information detection. Weight of a word increased via repetition in the document, but it is controlled by words quantity, while if the document is long, some words normally will be more repeated than others, even they had less importance[19]. The study objective is to present a new classification according to document information of vulnerability explanation. Therefore, features vector is generated from document tools and evaluation method through vulnerability explanation. Feature vector creation methods in the research are:

- Words extraction from documents
- Delete pause words
- Root recognition of words
- TF-IDF calculation for each feature

In this step, WVT (Word Vector Tool) tool is used, which generates two files as output, including words list and created vectors list. Feature vector is constructed from NUMBER and TF-IDF VALUE. For non-existing words in the document, no. 1 is used, and for existing words in the document, its equivalent value from TF-IDF is employed. The feature vector reached 2997 for each vulnerability. Figure 1 illustrates feature extraction steps.

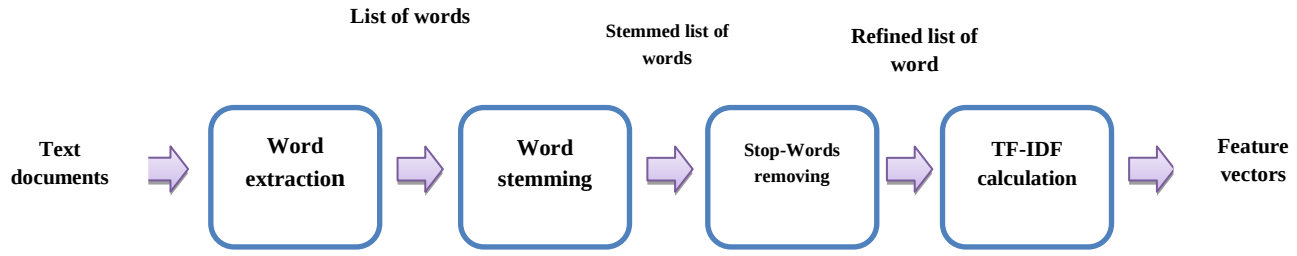

FIGURE 1: FEATURE EXTRACTION STEPS

3.3 Evaluation Method

Clustering evaluation is a boring process, which can be accomplished with two measurement approaches: external and internal measurement [20]. According to previous investigations, there is a general framework to apply on internal and external measurements. Inter-cluster interval is calculated by formula (1) and intra-cluster interval is computed by formula (2).

$$int-classif = \sum_{i \in 1:N} \sum_{j \in 1:N} d(x_i - x_j) \quad (1)$$

$$ext - classif = \sum_{i \in 1:N} d(x_i - c) \tag{2}$$

In the mentioned equations, N is quantity of data being placed in a clustering. To evaluate efficiency in the model, confusion matrix is used to determine correctness or imperfection amount of data recognition in each class. Moreover, precision and accuracy, sensitivity, and specificity could be achieved to have a proper estimation of algorithm quality. Other criteria for classification consist of inter-cluster and intra-cluster intervals [21].

TABLE 1
CONFUSION MATRIX

Actual \ Predicate	Positive	Negative
Positive	True Positives	False Negatives
Negative	False positives	True Negatives

Overlapped self-organizing map uses SOM, providing a structural algorithm with less sensitivity on quantity of clusters. Data are categorized on a matrix with specific number of neurons, and topology correctness is shown with a simple matrix method. Finally, it prepares a suitable clustering structure on data, causing to decrease complexity. Advantage of utilizing overlapping clusters is to have a datum belonging to different clusters. When a datum is sent to matrix, instead of a neuron, a set of neurons is needed for evaluation. Validity of overlapping topology could be evaluated by confining a set to a specific class ς in matrix [22]. OSOM algorithm is introduced by combination of K-means and type of SOM, which was proposed by Heskes [23]. A new model is demonstrated as (3) criteria.

$$E_{osom} = \frac{1}{N} \sum_{x_i \in X} \sum_{G_r \in W} h_{rg(W, x_i)} \| x_i - \bar{w}_r \|^2 \tag{3}$$

IV. EXPERIMENT AND RESULTS

To analyze clusters data, model recognition and model behavior prediction, first the data should be classified and then evaluated and predicted by the obtained model. For example, a classified model for vulnerability taxonomy may be categorized in two sections: low risk vulnerabilities sand high risk vulnerabilities, while in the recommended model, prediction is applied on vulnerability clusters based on vulnerability interpretation. Classification is a model detection along with cluster determination or data concepts, which could predict unknown clusters of other objects. Classification is a learning process assigning a cluster to a datum. Data are divided into two sections: training and test data. Training data are employed for system learning, and test data are used for the model accuracy evaluation. As it was discussed, after valid database selection of software vulnerabilities, proper fields are chosen as: CVE number, CWE and software vulnerabilities interpretation. Vulnerabilities interpretation is used to generate the feature vector. The field is textual and is employed for feature extraction by using WVT. The tool produces the feature involving TF-IDF pattern. Afterward, the vector is converted to a matrix, and if the pattern holds the feature amount in TFF-IDF, it is situated in matrix, otherwise, 1 is replaced instead. Up to now, there is a matrix with 2997 rows by 47295 columns filled by TF-IDF amounts and 1. Furthermore, the overlapped amount between the patterns is obtained 1.01. To process assurance, each pattern of CVE is correspondingly settled in addition to its CWE pattern. To develop the model, the selected algorithm is OSOM, being selected based on the experiment results from vulnerability issues. The obtained matrix from previous steps is brought forward to algorithm and output is achieved. There is no regular or specific process for number of clusters, but clustering correctness could be evaluated via assessment. In total, 80% of the utilized data is used in training step and 20% in test step, and the experiments are accomplished 10 times in average. Clustering by OSOM is made in three phases: competition phase, collaboration phase and accommodation phase. Overlapping self-organized map is utilized in competition phase that uses HESKES error criteria. In clusters centers selection step, it uses clusters average as clusters centers, and in collaboration phase, to select adjacency, it uses Hasdorf interval instead of Euclidean. Table 2 presents the obtained results from the proposed method via OSOM.

TABLE 2
RESULTS FROM THE PROPOSED METHOD VIA OSOM

		$Qext_{classif}$			$Qint_{classif}$	
	3x3	**5x5**	**10x10**	**3x3**	**5x5**	**10x10**
Scene	0.525	0.542	0.542	0.199	**0.146**	0.116
Emotion	**0.479**	**0.472**	0.484	**0.176**	0.150	**0.099**
CVE	0.561	0.496	**0.448**	0.597	0.412	0.284

As Table 2 illustrates, it is concluded that OSOM inter-cluster interval has greater improvement in smaller patterns. In contrary, software vulnerabilities are increased by pattern increment, and the improvement is increased, correspondingly. Classification evaluation is made for each cluster separately, and favorite criteria are obtained.

TABLE 3
SAMPLE CONFUSION MATRIX FOR A CLASS

	Positive	**Negative**	**Total**
Positive	860	496	1356
Negative	578	356	934
Total	1438	852	2290

Table 4 shows the results obtained from the proposed model and primary model as the prediction model on CVE. During the study, 10 times algorithm executing and 10x10 pattern with 100 times repeat were accomplished.

TABLE 4
ESTIMATION OF THE PREDICTOR MODEL

	Precision	**Sensitivity**	**F-measure**
SOM	0.33	**0.60**	0.42
OSOM	**0.37**	0.54	**0.43**

According to Table 4, OSOM accuracy is higher than the ordinary method, and its precision value is less, but eventually, F criterion of the proposed model is better than the ordinary method.

V. CONCLUSION

This article deals with software vulnerability clustering as an important and time-consuming issue for researchers. After selecting a valid database and required fields such as CVE, CWE and vulnerability interpretation, relevant features were extracted. By using WVT tool, TF-IDF of each pattern was obtained and 2997 features were achieved. According to the experiment results, high amount of vulnerability could belong to different patterns. Therefore, it was required to database be evaluated and value of vulnerability database overlapping is obtained 1.01. The proposed OSOM method was introduced as an extension from SOM algorithm by means of overlapped K-means. Classification accuracy increased through a new algorithm via combination of centers and a new definition for winner neuron. The accuracy was obtained from variations in the ordinary self-organized map. After applying experiments on vulnerabilities and evaluation on favorite criterions, it is concluded that overlapped self-organized map could be a suitable approach for software vulnerability classification. Performed activities on the research were only a step to present a standard classification on software vulnerabilities. To have an accurate model, complete date is required. In this research, the overlapped self-organized method has been utilized for prediction, and it is planned to use other unemployed methods for software vulnerabilities classification. Moreover, in future studies. We can use the ideas proposed in OSOM model, for clustering models in which the overlapping issue is not considered.

REFERENCES

[1] Ammala, DE. (2004). Derivation OF Metrics for Effective Evaluation of Vulnerability Assessment Technology. Mississippi State University.

[2] Bishop, M. (1995). A taxonomy of UNIX system and network vulnerabilities. Technical Report CSE-9510. Davis: Department of Computer Science, University of California.

[3] Krsul IV (1998) Software vulnerability analysis. Available at: http://www.krsul.org/ivan [Accessed 1 Sep. 2015].

[4] Venter, H. Elofe, J. (2002).Harmonizing Vulnerability Categories. Computer Society of South Africa South Africa, ISSN 1015-7999, pp. 24-31.

[5] Kujawski, P. (2003). Why Networks Must Be Secured. Cisco Systems, Incorporation.

[6] The SAINT Corporation. Available at: http://www.saintcorporation.com [Accessed 11 Feb. 2017].

[7] Microsoft Commerce Server (2002). The STRIDE threat model. Available at: http://msdn2.microsoft.com [Accessed 11 Feb. 2017].

[8] MOREnet, Missouri Research & Education Network Available at: http://www.more.net/services [Accessed 1 Sep. 2015].

[9] Venter, H. Eloff, J. Li, Y. Standardising vulnerability categories. Computers & Security.

[10] Tang, W. Mao, KZ. Mak, G. (2010). Classification for Overlapping Classes Using Optimized Overlapping Region Detection and Soft Decision. International Conference on Information Fusion.

[11] Jardine, N. Sibson, R. (1971). Mathematical Taxonomy. Statistical Data Analysis, pp. 405–416

[12] Diday, E. (1987). Orders and overlapping clusters by pyramids. Technical report, INRIA num.730, France.

[13] Cleuziou, G. Martin, L. Vrain, C. (2004). PoBOC: an Overlapping Clustering Algorithm. Application to Rule-Based Classication and Textual Data.

[14] R. L´opez de M´antaras and L. Saitta, IOS Press, editor, Proceedings of the 16th European Conf. on Articial Intelligence, pp. 440-444.

[15] Banerjee, A. Krumpelman, C. Ghosh, J. Basu, S. Mooney, R. (2005). Model-based overlapping clustering. Proceeding of the eleventh ACMSIGKDD, pp. 532–537.

[16] Cleuziou, G. (2007). OKM: une extension des k-moyennes pour la recherche de classes recouvrantes. EGC, 2.

[17] Last, D. (2011). Using Historical Software Vulnerability Data to Forecast Future Vulnerabilities. Air Force Research Laboratory information Directorate, RISB.

[18] Khazaei, A. Ghasemzadeh, M. (2016). Software Vulnerabilities Database Selection Using MoSCoW Prioritization Method. 3rd Int. Conference on Applied Research in Computer & Information, Tehran, pp. 1-7.

[19] The wikipedia (2017). Tfidf [online] Available at: https://en.wikipedia.org [Accessed 1 Sep. 2016].

[20] Jain, A. Dubes, R. (1988). Algorithms for Clustering Data. Prentice Hall Englewood Cliffs.

[21] T, Fawcett. (2006). An introduction to ROC analysis. Pattern Recognition, 27, 8, pp. 861–874.

[22] Cleuziou, G. (2013). A Method for building overlapping topological map. Pattern Recognition Letters, 34, 3, pp. 239–246.

[23] Heskes, T. (1999). Energy functions for self-organizing maps. University of Nijmegen Geert Grooteplein 21, 6252 EZ, Nijmegen, The Netherlands.

AD Publications
Sector-3, MP Nagar, Bikaner,
Rajasthan, India
www.adpublications.org, info@adpublications.org